Treatment of Domestic Wastewater with Natural Zeolites

By

Beyhan CANSEVER

**A Dissertation Submitted to the
Graduate School in partial Fulfillment of the
Requirement for the Degree of**

MASTER OF SCIENCE

Department: Chemical Engineering

Major: Chemical Engineering

İzmir Institute of Technology

İzmir, Turkey

July, 2004

ACKNOWLEDGEMENTS

I would like to acknowledge the people who have helped to make this work possible. My sincere gratitude is first for my thesis advisor Prof. Semra Ülkü for her consistent and thoughtful advice, continuous encouragement and help during the course of this work. I am also grateful to Prof. Devrim Balköse for her valuable comments and recommendations. I would like to give my special thanks to Dr. Mehmet Polat for his valuable suggestions during the study.

I also wish to thank to personnel of IZTECH Centre for Material Research for their help during my material characterization studies. Also, I acknowledge to Izmir Çiğli Domestic Wastewater Plant personnel for their valuable help during my studies.

I would like to appreciate deeply to my roommates, Yelda Akdeniz, Filiz Özmıhçı, Güler Narin and Ozge Can for their friendships, supports and encouragements

I am grateful to my friends for assisting me with my research and offering advice and discussion. Specifically I would like to thank Gökhan Erdoğan, Yelda Ergün and Emre Kuduğ.

Finally, I would like to express my heartfelt gratitude to my parents for their continuous support and encouragement, which enabled me to overcome difficulties.

ABSTRACT

In this study, the use of Gördes natural zeolite for removing NH_4^+ ion from wastewater effluent and from NH_4Cl solution was investigated under various conditions. The effect of the solid:solution ratio, initial concentration of the solution, presence of competing cation, particle size of the clinoptilolite sample on ammonium ion removal capacity were studied. **Highest amount of ammonium removal per gram zeolite was found in the solution having 1% solid: solution ratio. The experimental results indicate that the NH_4^+ exchange capacity is not dependent on the particle size of the clinoptilolite sample.** Increasing the initial concentration **increases the NH_4^+ uptake capacity. NH_4^+ removal decreases with increasing the initial ammonium concentration. For instance, the higher NH_4^+ ion concentrations show the 30.5-55 % removal and lower NH_4^+ ion concentrations lead to 87-95 % removal for pure ammonium chloride solution.** The presence of potassium ion had the most significant effect upon ammonium ion uptake, followed by calcium ion. Magnesium ion had the least effect.

Equilibrium data obtained have been found to fit both Langmuir and Freundlich models. The Langmuir model provided excellent equilibrium data fitting (R^2>0.995). From the plateau of the isotherms maximum exchange capacities were determined as 9.03, 8.76, 8.695 and 7.84 mg NH_4^+/gr for NH_4^+, NH_4^+-Mg^{+2}, NH_4^+-$Ca^{+2}$and NH_4^+-K^+, respectively. As a consequence of this result, the ammonium capacity of Gördes clinoptilolite was approximately 0.51meq/gr for pure ammonium chloride solution.

When comparing the removal of NH_4^+ ion from wastewater effluent and from NH_4Cl, the percent removal and the uptake capacity were lower for wastewater than for NH_4Cl for same solid: solution ratio and the same initial concentration. It is expected that in domestic wastewater, where the complexity of the system is high, several matter could influence the removal of specific target cations. The decreased ammonium removal for wastewater may be attributed to by the existence of several matters (suspended solid, organic matter) in the wastewater effluent samples, which reduce the ammonium exchange capacity.

The experimental results indicate a significant potential for the Gördes clinoptilolite rich mineral as an ion exchange material for wastewater treatment and water reuse application.

ÖZ

Bu çalışmada, Gördes doğal zeolitinin, atıksudan ve NH_4Cl çözeltisinden, değişik şartlarda NH_4^+ iyonu uzaklaştırılması araştırılmıştır. Katı:çözelti oranı, çözeltinin başlangıç konsantrasyonu, çözeltideki rakip iyonlarının varlığı ve zeolitin parçacık boyutunun amonyum iyonu uzaklaştırma kapasitesine etkisi çalışılmıştır. Birim gram zeolitin en yüksek NH_4^+ tutma kapasitesi, %1 katı:çözelti oranında bulunmuştur. Deneysel sonuçlar, NH_4^+ değişim kapasitesinin parçacık boyutundan bağımsız olduğunu göstermiştir. Başlangıç çözelti konsantrasyonunun artması NH_4^+ tutma kapasitesini arttırmıştır. Amonyum iyonunun uzaklaştırılma yüzdesi başlangıç amonyum konsantrasyonunun artmasıyla azalmıştır. Örneğin, saf amonyum klorür çözeltisi için yüksek NH_4^+ iyonu konsantrasyonları %30.5-55, NH_4^+ giderimi gösterirken, düşük konsantrasyonlar %87-95 NH_4^+ giderimi sağlamıştır. Amonyum tutma kapasitesi potasyum iyonunu varlığında en yüksek azalma göstermiş, bunu kalsiyum iyonu izlemiştir. En düşük etki magnezyum iyonu varlığında görülmüştür.

Elde edilen denge verilerinin, hem Langmuir hemde Freundlich modellerine uyduğu saptanmıştır. Langmuir modeli, mükemmel denge veri uyumu göstermiştir (R^2>0.995). İzotermlerin platolarından maksimum iyon değişim kapasiteleri, NH_4^+ , NH_4^+-Mg^{+2}, NH_4^+-Ca^{+2} ve NH_4^+-K^+ için sırasıyla 9.03, 8.76, 8.695 ve 7.84 mg NH_4^+/ gr olarak bulunmuştur. Sonuç olarak; Gördes klinoptilolitinin amonyum kapasitesi, saf amonyum klorür solüsyonu için yaklaşık 0.51 milieşdeğer/gr olarak hesaplanmıştır.

Aynı katı /çözelti oranı ve aynı başlangıç konsantrasyonu ele alındığında klinoptilolitin NH_4^+ iyonu tutma kapasitesi ve NH_4^+ iyonu uzaklaştırma yüzdesi atıksu için NH_4Cl çözeltisine göre daha düşük bulunmuştur. Evsel atıksuların kompleks sistemi, belirli hedef katyonların uzaklaştırılmasını etkileyebilir. Atıksulardan amonyum uzaklaştırılmasındaki azalma, askıda katı ve/veya organik maddeler gibi bazı faktörlerin varlığına bağlanabilir. Dolayısıyla bu amonyum değişim kapasitesinin düşmesine neden olur.

Deneysel sonuçlar, klinoptilolitçe zengin Gördes mineralinin atıksu arıtımı ve suyun tekrar kullanılmasında, önemli bir potansiyeli olduğunu göstermektedir.

TABLE OF CONTENTS

LIST OF FIGURES

LIST OF TABLES

CHAPTER 1

INTRODUCTION

The sources of domestic wastewater comes from the discharge of water closets, laundry tubs, washing machines, sinks, dishwashers, or other source of water-carried wastes of human origin. The composition of domestic wastewater changes depending on the location of the source, seasonal variation, climate, time of day, water consumption and population. The domestic wastewater is characterized in terms of its physical, chemical and biological constituents. Temperature, color, odor and total solid are the physical constituents; BOD, COD, total nitrogen, total phosphorous and alkalinity are the chemical constituents; and total coliform is the microbiological constituent of the domestic wastewater. These constituents cause permanent damage to the environment. Conventional treatment methods are applied to the domestic wastewater to reduce their concentrations to acceptable limits before discharging.

In the primary treatment, a portion of the suspended solid (30-60%) and organic matter (20-30 %) is removed from the wastewater. Secondary treatment removes more than 85% of both suspended solids and BOD. The aim of tertiary treatment process is to remove the nutrients in the wastewater effluent. Nutrients in untreated wastewater are principally in the form of organic nitrogen. Organic nitrogen is mainly in the form of urea and amino acids. Decomposition of the urea and amino acids by bacteria readily changes the form to ammonium. The detrimental effects of excessive ammonium concentrations in receiving waters are; the contribution to explosive algal growths, toxic effect on fish and aquatic life, reduction of dissolved oxygen in receiving waters, the corrosive effect of certain metals and materials of construction. The generally accepted limit for free ammonium for receiving water is between 0.5 to 1 mg /lt. (EC Drinking Water Directive, 1980). It is stated in Water Pollution Control Regulation in Turkey that the permissible ammonium nitrogen concentration for first and second class surface water sources should not exceed 0.2 and 1mg/lt, respectively.

The principal methods found feasible for the removal of ammonium are ion exchange, air stripping of ammonia at high pH, biological nitrification followed by denitrification and breakpoint chlorination. The ion exchange process has several advantages over other methods of ammonium removal. Since it is cost effective and it has higher ammonium removal efficiency. The ion exchange method usually employs

organic resins which are very selective but sometimes their cost is prohibitively high. An alternative material that could be used is clinoptilolite rich natural zeolite, which is a natural mineral of a very low cost.

Clinoptilolite is a member of the Heulandite group. The structure of zeolites consists of a three dimensional framework of SiO_4 and AlO_4 tetrahedra. The aluminum ion is small enough to occupy the position in the center of the tetrahedron of four oxygen atoms, and the isomorphous replacement of Al^{+3} and Si^{+4} raises a negative charge in the lattice. The negative charge is balanced by the exchangeable cation (sodium, magnesium, calcium and potassium). These cations are exchangeable with certain cations in the solution such as ammonium, copper, zinc and lead. The fact that clinoptilolite is suitable for removing undesirable heavy metals and ammonium ion in wastewater.

Considerable research has been conducted to characterize the mechanism of ammonium removal from wastewater and aqueous solution by clinoptilolite rich natural zeolite. Depending on the studies, it can be concluded that, ion exchange capacity of clinoptilolite mainly depends on the solution and ion exchanger properties. Ammonium exchange capacity of clinoptilolite vary widely depending on the particle size of the zeolite, solid:solution ratio, initial concentration of the solution, presence of competing cation, pH of the solution, temperature and physical and chemical properties of zeolite composition.

In this study, these effective parameters were changed and the effects on the ammonium exchange capacity were investigated. The objectives of the thesis were:

- To evaluate the ammonium ion exchange capacity of Gördes clinoptilolite in batch studies under varying processing conditions. (Solid: solution ratio, initial concentration of the solution, particle size of the zeolite, etc.)
- To evaluate the effect of competing cations present in the domestic wastewater on the exchange mechanism.
- To identify the ability of clinoptilolite in the removal of ammonium ion from synthetic and contaminated domestic wastewater solution.
- To investigate ammonium ion removal performance of original clinoptilolite.

CHAPTER 2

DOMESTIC WASTEWATER

2.1. Composition of Domestic Wastewater

Physically, domestic wastewater is usually characterized by a grey color and must odor. Chemically, wastewater is composed of organic and inorganic compounds as well as various gases. Biologically, wastewater contains various microorganisms but the ones that are of concern are those classified as protista, plants, and animals.

The sources of domestic wastewater come from the discharge of water closets, laundry tubs, washing machines, sinks, dishwashers, or other source of water-carried wastes of human origin. Figure 2.1 shows the typical sources of domestic wastewater.

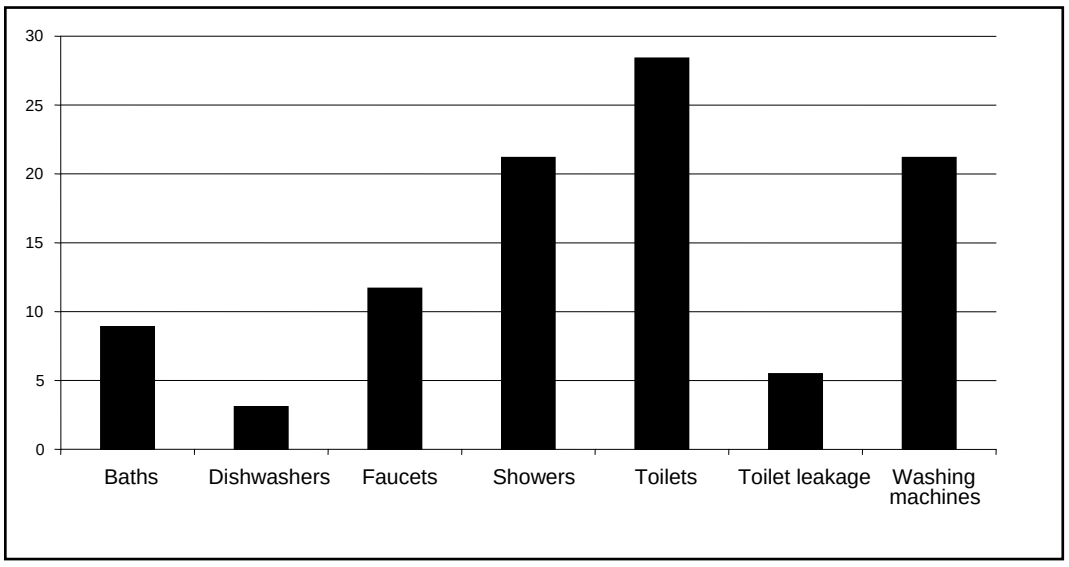

Figure 2.1. Typical Sources of Domestic Wastewater.

The domestic wastewater is characterized in terms of its physical, chemical and biological composition. The composition changes depending on the location of the source, seasonal variation, climate, time of day, water consumption and population. Composition refers to the actual amounts of physical, chemical and biological constituents present in wastewater. Typical data on the individual constituents found in domestic wastewater are reported in Table 2.1. These constituents cause permanent damage to the environment. For this reason, all of these constituents' values should be reduced acceptable levels before discharging.

Table 2.1. Typical Composition of Untreated Domestic Wastewater [Metcalf and Eddy, 1991].

	Concentration (mg/lt.)		
Contaminants	Weak	Medium	Strong
Total Solids (TS)	350	720	1200
Total Dissolved Solid (TDS)	250	500	850
Suspended Solid (SS)	100	220	350
Settleable Solid	5	10	20
Biological Oxygen Demand (BOD_5)	110	220	400
Total Organic Carbon (TOC)	80	160	290
Chemical Oxygen Demand (COD)	250	500	1000
Nitrogen (total as N)	20	40	85
Organic	8	15	35
Free ammonia	12	25	50
Nitrites	0	0	0
Nitrates	0	0	0
Phosphorous (total as P)	4	8	15
Chlorides	30	50	100
Sulfate	20	30	50
Alkalinity (as $CaCO_3$)	50	100	200
Grease	50	100	150
Total coliform (no/100 ml)	10^6-10^7	10^7-10^8	10^7-10^9

2.1.1 Physical Constituents

The physical constituents of wastewater include those items that can be detected using the physical senses. They are temperature, color, odor, and solids.

- Temperature: The temperature of wastewater varies greatly, depending upon the type of operations being conducted at your installation. Changes in wastewater temperatures affect the settling rates, dissolved oxygen levels, and biological action.
- Color and Odor: Domestic wastewater is usually characterized by gray color and musty odor. Odors in domestic wastewater usually are caused by gases produced by decomposition of organic matter. The age of the wastewater is determined qualitatively by its color and odor.
- Solids: The most important physical constituent of domestic wastewater is its total solid contents. If a wastewater sample is evaporated, the solids remaining are called total *solids*. Settleable solid are those solids that will settle to the bottom of a container. Total solid or residue upon evaporation can be classified as suspended or dissolved solid by passing a known volume of liquid through a filter.

2.1.2 Chemical Constituents

The chemical constituents of domestic wastewater include organic matter, inorganic matter, alkalinity, total phosphorus and nitrogen, chloride and sulphate.

- Organic Matter: Organic materials in wastewater originate from plants, animals, or synthetic organic compounds. Organic compounds normally are some combination of carbon, hydrogen, oxygen, nitrogen, and other elements. Many organics are biodegradable, which means they can be consumed and broken down by organisms. The concentration of organic matter is measured by the BOD_5, COD and TOC analyses. For typical untreated domestic wastewater, the BOD_5/ COD ratio varies from 0.4 to 0.8, and the BOD_5/TOC ratio varies from 1.0 to 1.6. [Metcalf and Eddy, 1991]
- Inorganic matter: The principal groups of inorganic substance found in wastewater are sodium, potassium, calcium, magnesium, cadmium, copper, lead, nickel, and zinc. Large amounts of many inorganic substances can contaminate soil and water. Some are toxic to animals and humans and may accumulate in the environment.
- Alkalinity: Alkalinity in wastewater results from the presence of hydroxides, carbonates and bicarbonates of elements such as calcium, magnesium, sodium and potassium. The concentration of alkalinity in wastewater is important where chemical treatment is to be used.
- Total phosphorous: Phosphorus occurs in natural waters and in wastewaters almost solely as phosphates. These phosphates include organic phosphate, polyphosphate (particulate P) and orthophosphate (inorganic P). With respect to domestic wastewater, there are two means by which phosphorous is removed: chemical precipitation and the use of various biological treatment processes.
- Total nitrogen: Total nitrogen is comprised of organic nitrogen, ammonia, nitrate (NO_3^-), nitrite (NO_2^-) and nitrogen gas (N_2).
  - ***Organic nitrogen*** is mainly in the form of the urea and amino acids. Decomposition of the urea and amino acids by bacteria readily changes the form of ammonium.
  - ***Nitrate nitrogen*** is the most highly oxidized form of nitrogen found in wastewaters. Where secondary effluent is to be reclaimed for groundwater

recharge, the nitrate concentration is important. Nitrate may vary in concentration from 0 to 20 mg/lt as N in wastewater.

- ***Nitrite*** is not usually observed in water sources because it is readily converted to nitrate by bacterial processes; however, it is extremely toxic to most fish and other aquatic species. Nitrites present in wastewater effluents are oxidized by chlorine and thus increase the chlorine dosage requirements and the cost of disinfection.
- ***Ammonia nitrogen*** exists in aqueous solution as either the non-ionized form (NH_3) or ionized form (NH_4^+), depending on the pH of the solution and the temperature, in accordance with the following equilibrium reaction. At the pH levels above 7, the equilibrium is displaced to left; ammonium exists in the non-ionized form. At the pH level below 7, the ionized form is predominant. Ammonium discharged with municipal or domestic wastewater effluent is responsible for different harmful effects, such as eutrophication, toxicity to aquatic life, increased corrosion rate of soil materials. As a consequence of these concerns it is usually desirable to reduce the ammonium concentrations in wastewaters to level less than 1 mg/lt.

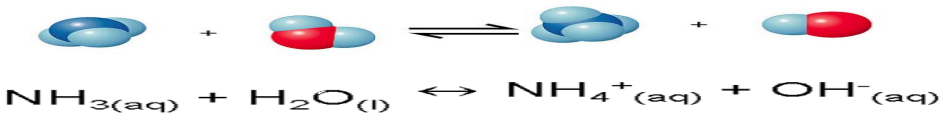

Figure 2.2. NH_3- NH_4^+ equilibrium reaction.

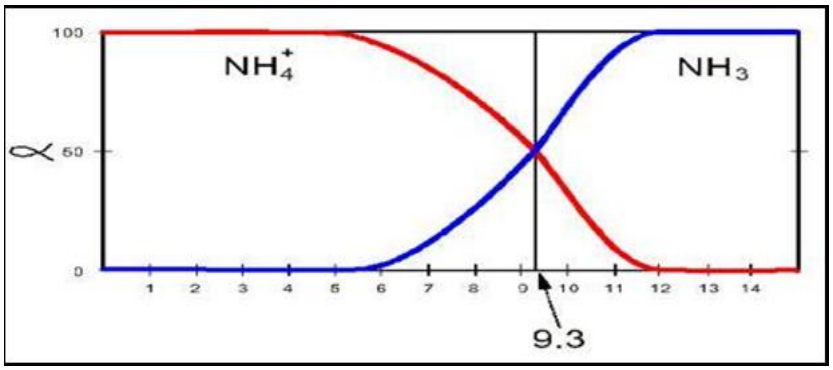

Figure 2.3. Ammonium percentage as a function of the pH of the solution.

- ***Chlorides*****:** Another quality parameter of significance is the chlorine concentration. Small amounts of chlorides are required for normal cell functions

in plant and animal life. High chloride levels can cause human illness and also can affect plant growth at levels in excess of 1000 mg/l.

- ***Sulphates:*** Sulphates are associated with gypsum formations and are common in several areas. Sulphate levels at 500 ppm or greater can have a laxative effect High sulphate levels can also have a corrosive effect on plumbing.

2.1.3. Microbiological Constituents

The principal groups of microorganisms found in wastewater classified as protista, plant and animals. The category of protista includes algae, fungi and protozoa. Giardia Intestinalis is an example for protozoa which causes diarrhea, nausea and indigestion. The general aspect of *Giardia Intestinalis* as revealed by scanning electron microscopy (SEM) is shown in Figure 2.4. This figure presents a view onto the ventral side of the protozoa with its adhesive disk and its ventral groove with the ventral pair of flagella. These pathogens often originate from people and animals that are infected with or are carriers of a disease. Important wastewater-related diseases include hepatitis A, typhoid, polio, cholera and dysentery. Outbreaks of these diseases can occur as a result of eating contaminated fish or recreational activities in polluted waters.

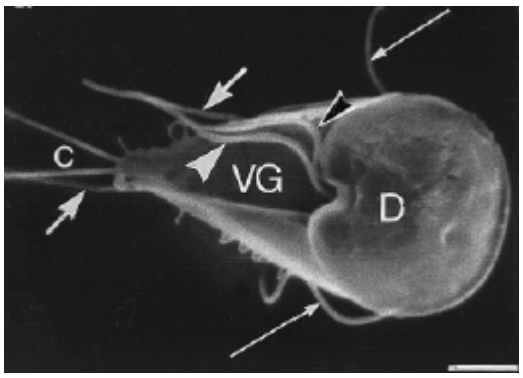

Figure 2.4. Scanning electron microscopy shows the general aspect of *Giardia Intestinalis*.

2.2. Domestic Wastewater Cation Analysis

Magnesium, calcium, potassium and sodium are known as competing cation. In domestic wastewater, competing cations concentration is important. Treated wastewater effluent may be used for the agricultural purpose. For this reason, the concentrations level of the competing cations should be acceptable level for irrigation. For example,

the high level of sodium concentration affects the salinity of soil. If the salinity of soil is much higher than the requirement, the plant growth and crop is reduced significantly. The domestic wastewater cations concentration before and after secondary treatment were given in Table 2.2. The concentration of the competing cations changes depending on the location of the source, water characteristic and treatment type.

Table 2.2. Domestic Wastewater Competing Cation Concentration (before and after secondary treatment) [Metcalf and Eddy, 1991].

Cation	Before Treatment (mg/lt)	After Secondary Treatment (mg/lt)
Calcium	7-166	34
Magnesium	2-19	8
Potassium	14-180	12
Sodium	26-318	58

The ion exchange mechanism is significantly influenced by the presence of these cations in wastewater effluent.(Discussed in Chapter 5.5) Ion exchange capacity is reduced with the presence of the competing cations. For this reason, the cation concentration and type should be identified before applying this process.

2.3. Domestic Wastewater Treatment Methods

Four types of treatment processes are applied to the domestic wastewater. These are classified as preliminary, primary, secondary and tertiary processes.

2.3.1. Preliminary Treatment

It is defined as the removal of wastewater constituents that may cause maintenance and operational problems with the treatment processes. Examples of preliminary operations are screening and grit removal for the elimination of coarse suspended matter that may cause wear or clogging of equipment.

2.3.2. Primary Treatment

In the primary treatment, a portion of the suspended solid and organic matter is removed from the wastewater. This removal is usually accomplished with physical operations such as sedimentation. After preliminary treatment, the wastewater flows into the primary settling tanks where the flow velocity is further reduced and the suspended material is allowed to settle to the bottom of the tanks. The settled material, referred to as primary sludge, is pushed by automatic sludge collection equipment into a hopper from which the sludge is pumped to the sludge thickeners. Approximately 60% of the suspended solids and 35% of the BOD are removed in this unit process.

2.3.3. Secondary Treatment

Secondary treatment removes more than 85% of both suspended solids and BOD. A minimum level of secondary treatment is usually required in most developed countries. Removal is usually accomplished by biological processes in which microbes consume the organic impurities as food, converting them into carbon dioxide, water, and energy for their own growth and reproduction. There are two basic biological treatment methods: (a) trickling filter, (b) activated sludge. The activated sludge process is very common in biological wastewater treatment. This method is more efficient than a trickle filter and less subject to temperature effects. The flowchart of the secondary treatment is given in Figure 2.5.

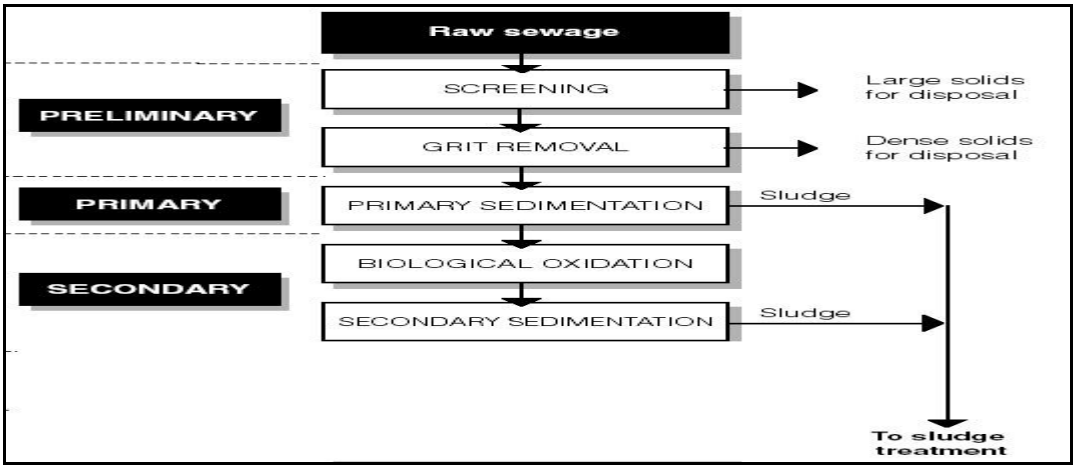

Figure 2.5. The flowchart of the Secondary Treatment.

2.3.4. Tertiary Treatment

Tertiary treatment is any additional treatment process designed to achieve higher standards of water quality. The aim of this process is to remove the nutrients in the wastewater effluent. The removal of nutrients in wastewater treatment is important for several reasons. Nutrients removal is generally required for (a) discharges to confined bodies of water where eutrophication may be caused, (b) discharges to flowing streams where rooted aquatic plants can flourish, (c) recharge of ground waters that may be used indirectly for public water supplies (Metcalf and Eddy, 1991). As a consequence of these concerns, four processing methods are applied to remove nutrient from wastewater. These are given as follows:

- Nitrification-Denitrification: Nitrification is a biological process that converts ammonia nitrogen to nitrate nitrogen. In this process, NH_4^+ ions are oxidized to NO_2^- with the help from nitrosomanas bacteria species and the activity of the other bacteria species (Nitrobacteria), nitrite is converted to nitrate. Denitrification is the process where nitrate is reduced to nitrogen gas in the absence of dissolved oxygen. The disadvantages of the biological methods are limited to a minimum of 5 ppm ammonium concentration due to the formation of the undesirable chemical compound.
- Breakpoint Chlorination: It involves the addition of chlorine to wastewater to oxidize the ammonia nitrogen in solution to nitrogen gas. The disadvantages of this process are to produce high chemical residuals and require the pH control to avoid the formation of undesirable compound.
- Air Stripping: Air stripping of ammonium is the term used to describe the loss of ammonium from wastewater when air passed through wastewater of high pH (>11). The disadvantages of this process are high operating cost and the cost of temperature controlling.

Ion exchange method (discussed in Chapter 5) is preferred over the other conventional methods. Since:

- This process can be achieved at a minimal cost.
- The ion exchange process has higher ammonium removal efficiency.
- Ion exchange material can be easily regenerated with suitable salt solution.

2.4. İzmir Çiğli Domestic Wastewater Plant

In the Çiğli Domestic Wastewater Plant, the sewage coming from the pumping station. It is received in an inlet chamber and is distributed into 3 parallel running screen channels. Each channel equipped with fine screen that works for removing fine particles in the wastewater. Primary treatment is performed by using screen, grit channels, Parshall flumes and sedimentation tank. In the sedimentation tank, % 24 BOD, % 64 SS, % 8 total phosphorous removals were observed.Secondary treatment is performed by using bio-phosphor tank, oxidation ditch tanks with aeration unit and final sedimentation tank. One line of aeration unit consists of two oxidation ditch tanks operating in series. Primary effluent will first be let into ditch type anaerobic tanks for biological phosphorus removal. The effluent was collected in the final sedimentation tank. The sludge treatment process was performed by using these following steps. Firstly, the primary sludge is collected in first sludge holding tank. The second sludge holding tank will be used as sludge mixing. The primary sludge holding tank will be equipped with two submersible mixers. One small mixing compartment of the second tank serves for the mixing and homogenizing of primary sludge. The second compartment is used for storing the mixed sludge for a short time. The mixing compartment of second holding tank is equipped with diffusers. The air is used for mixing and homogenizing the primary- and excess sludge and to keep the sludge under aerobic conditions to avoid biological phosphorus release. Homogenized sludge from the sludge tank will be pumped into mechanical sludge thickeners.

Water quality data for İzmir Çiğli Domestic Wastewater effluent are listed in Table 2.3.

Table 2.3. Water Quality Data for Izmir Çiğli Domestic Wastewater Effluent

Parameters	Inlet Domestic Wastewater Composition	Discharging Domestic Wastewater Composition
COD	300-500 mg/lt	30-70 mg/lt
BOD_5	150-250 mg/lt	10-25 mg/lt
SS	500-600 mg/lt	20-30 mg/lt
Total N	50-60 mg/lt	10-12 mg/lt
NH_4^+	30-40 mg/lt	1-3 mg/lt
Total P	9-12 mg/lt	3-4 mg/lt

Grit Channels

Parshall Flumes

Primary Sedimentation Tank

Bio-phosphor Tank

Oxidation Ditch Tank

Final Sedimentation Tank

Sludge Holding Tank

Figure 2.6. Çiğli Domestic Wastewater Treatment Plant

CHAPTER 3

ZEOLITES

3.1 Definition of the Zeolites

Zeolites have been recognized for more than 200 years, but only during the middle of the 20th century have attracted the attention of scientists and engineers who demonstrated their technological importance in several fields. The main reason of the interest for natural zeolite-bearing materials is the increasing demand of low-cost ion exchange and adsorbent materials in fields such as wastewater treatment, gas separation and heavy metal removal as well as their wide availability on the earth.

Zeolites are a group of naturally occurring framework alumino-silicates with high cation exchange capacities, high adsorption and hydration-dehydration properties. About fifty different species of this mineral group have been identified, but only eight zeolite minerals make up the major part of volcano sedimentary deposits: analcime, chabazite, clinoptilolite-heulandite, erionite, ferrierite, laumontite, mordenite and phillipsite. The structure of each of these minerals is different but they all have large open 'channels' in the crystal structure that provide a large void space for the adsorption and exchange of cations. The internal surface area of these channels can reach as much as several hundred square meters per gram of zeolite, making zeolites extremely effective ion exchangers (Mumpton, 1984).

Zeolites are crystalline, hydrated aluminosilicates of alkaline or alkaline earth metals, especially, sodium, potassium, calcium, magnesium, strontium and barium. Structurally, zeolite is the "framework" aluminosilicate which is based on an infinitely extending three dimensional network of AlO_4 and SiO_4 tetrahedra linked to each other by sharing all of the oxygens. (Mumpton, Flanigen, 1983) This framework contains channels and interconnected voids which are occupied by the cation and water molecules. The cations are quite mobile and can usually be exchanged, to varying degrees, by other cations. These cations play a very important role in determining the adsorption and gas-separation properties of zeolites. These properties depend heavily on the size, charge density, and distribution of cations in the porous structure.

Zeolites may be represented by the two different formulas; oxide formula and idealized formula as follows:

- Oxide formula: $M_{2/n}O.Al_2O_3.xSiO_2.yH_2O$
- Idealized formula: $M_{x/n}[(AlO_3)_x(SiO_2)_y].wH_2O$

In the oxide formula; x is generally equal or greater than 2 since AlO_4 tetrahedra are joined only to SiO_4 tetrahedra, n is the cation valence. The structural formula of a zeolite is best expressed by the idealized formula for the crystallographic unit cell where M is the cation of valence n, w is the number of water molecules and the ratio y/x varies between 1 and 5 depending on the structure.

Synthetic zeolites are manufactured on a large scale for industrial use, but natural zeolites have not yet found extensive application as commercial molecular sieves, even though a few, particularly clinoptilolite are abundant in volcanogenic sedimentary rocks.

3.2 Structure of the Zeolites

Zeolites structure consists of two types of building units namely, primary and secondary. The primary building unit of the zeolite framework is the tetrahedron in which the center is occupied by a silicon or aluminum atom with four oxygen atoms at the corners as shown in Figure 3.1. Each oxygen atom is shared between two tetrahedra. Substitution of Si^{+4} by Al^{+3} defines negative charge of framework, which compensated by monovalent or divalent cations located together with water molecules in the channels. Cations in the channels can be substituted easily and therefore they are termed exchange or extra framework cation while Si and Al, which are not exchanged under ordinary conditions, are called tetrahedral (T) or framework cations (Tsisthivilli et al., 1992).

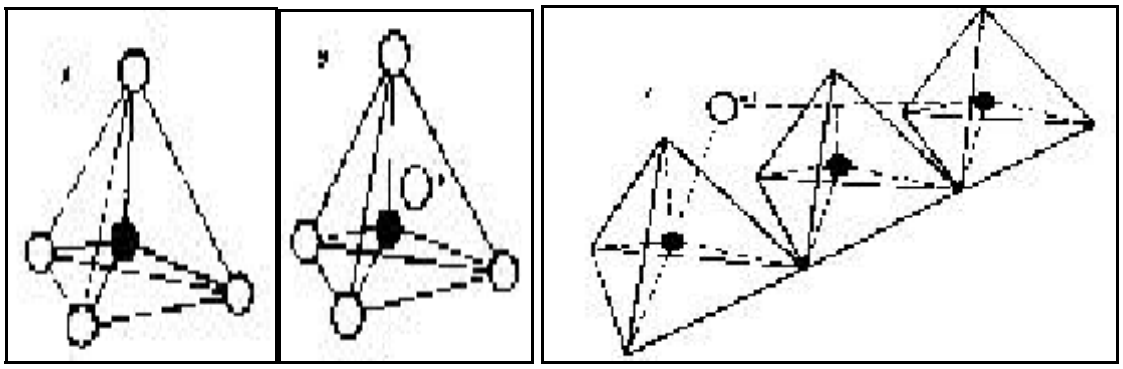

(a) (b)

Figure 3.1 Primary Building Units (PBU) in zeolite structure (a) $(SiO_4)^{-4}$, (b) $(AlO_4)^{-5}$

Zeolites structure also contains secondary building units, which are formed by the linking of the primary building tetrahedral. They consist of double and single rings of tetrahedra, forming the three dimensional structure of the zeolite. In the SBU Si-Al distribution is neglected, only the positions of the tetrahedral silicons or aluminums are shown. Oxygen atoms lie near the connecting the solid lines.

3.3 Properties of Zeolites

The following are some of the important properties of zeolites that make them an important material compared to other crystalline inorganic oxide materials. [Breck, 1974]

1. High degree of hydration,
2. Low density and large void volume when dehydrated,
3. Stability of the crystal structure of many zeolites when dehydrated,
4. Cation exchange properties,
5. Uniform molecular-sized channels in the dehydrated crystals,
6. Ability to adsorb gases and vapors,
7. Catalytic properties.

Commercial applications of natural zeolites make use of one or more of several physical or chemical properties.

3.4 Natural Zeolites

Natural zeolites are aluminum silicate minerals with high cation exchange capacities (CECs) and high ammonium selective properties (Kithome et al. 1998). More than 50 different species of this mineral group have been identified (Tsitsishvili et al. 1992). Different kinds of zeolites are clinoptilolite (Kithome et al. 1998), ferrierite and mordenite (Townsend et al., 1984), erionite (Mondale et al. 1995), and chabazite (Green et al. 1996). It has been stressed that the characteristics of a zeolite mineral depend on its origin because of variations in natural processes during the genesis (Townsend et al., 1984; Mondale et al. 1995). Mondale et al. (1995) mentioned that, for example, structural imperfections, a variety of exchangeable cations, and the presence of clay may lead to pore blockage and slow diffusion rates. Another relevant aspect is that the

zeolite mineral concentration of an ore sample depends on the deposit from which the zeolite originates. Mondale et al. (1995) used zeolite samples with 80–100% zeolite and other occurring minerals such as volcanic glass, quartz, and feldspars. However, Curkovic et al. (1997) used a clinoptilolite that was 40–50% pure and Jørgensen et al. (1979) used clinoptilolites with 50–90% purity.

The Si/Al ratio can vary considerably within the limits of one structural type, depending upon the composition of original solutions and conditions of crystallization. The Si/Al ratio in natural zeolites lies within the limits of 1 to 6. The upper limit of the Si/Al ratio in the natural zeolites reaches 5 to 6 (clinoptilolite, mordenite and ferrierite)

The channels in natural zeolites contain water that make up the 10-25% of their weight. The water content varies within the certain limits depending upon the character of the exchange cations and conditions of crystallization.

3.5 Clinoptilolite-Rich Natural Zeolite

Clinoptilolite is the most abundant of the natural zeolites (Mumpton et al., 1976), but composition and purity vary widely among the deposits found throughout the world. It is a member of the Heulandite group of natural zeolites. Clinoptilolite is isostructural with the zeolite Heulandite, which it differs in having higher Si/Al ratio and monovalent/divalent cation ratios. The higher thermal stability of clinoptilolite compared with heulandite was obtained in terms of an elevated Si/Al ratio. The Si/Al ratio is between 4.25-5.25 for clinoptilolite and 2.7-4 for heulandite. Heulandite transforms into two phases at about 230°C and becomes non-crystalline at about 350°C. Clinoptilolite survives its crystal structure up to about 700°C. (Tsitsishvili et al., 1992).The general formula for clinoptilolite-rich natural zeolite is:

$$(Li, Na, K)_a\ (Mg, Ca, Sr, Ba)_d\ [Al_{(a+2d)}Si_{n-(a+2d)}O_{2n}].mH_2O$$

The unit cell is monoclinic C-centered and is usually characterized on the basis of 72 O atoms (n = 36) and m = 24 water molecules with Na^+, K^+, Ca^{2+}, and Mg^{2+} as the most common charge balancing cations. Its characteristic properties are summarized by Breck (1974).

Table 3.1 Summary of clinoptilolite characteristic properties (Breck, 1974)

Structure Group:	7		
Chemical Composition			
Typical Oxide Formula:	$(Na_2, K_2)O \cdot Al_2O_3 \cdot 10SiO_2 \cdot 8H_2O$		
Typical Unit Cell Contents:	$Na_6[(AlO_2)_6(SiO_2)_{30}] \cdot 24H_2O$		
Variations:	Ca, K, Mg also present; Na, K>>Ca Si/Al, 4.25 to 5.25		
Crystallographic Data			
Symmetry:	Monoclinic	Density:	2.16g/cc
Space Group:	I 2/m	Unit Cell Volume:	$2100A^3$
Unit Cell Constants:	a = 7.41 A b = 17.89 A c = 15.85 A β = 91°29'		
Structural Properties			
Framework:	Possibly related to heulandite but not determined.		
Void Volume:	0.34 cc/cc	Framework density:	1.71 g/cc
Dehydrated -			
Effect of Dehydration:	Very stable – in air to 700°C		
Largest Molecule Adsorbed:	O_2		
Kinetic Diameter, σ, A:	3.5		

It has HEU topology, whose secondary building unit can be described by 4-4-1 type (Breck, 1974). According to the literature, the structure of clinoptilolite consists of a three dimensional system of three types channels, A (10-member ring) and B (8-member ring) ring) are parallel to each other while C channel (8-member ring) intersects both the A and B channels as shown in Figure 3.2. Channel characteristics and cation sites of clinoptilolites are summarized in Table 3.2.

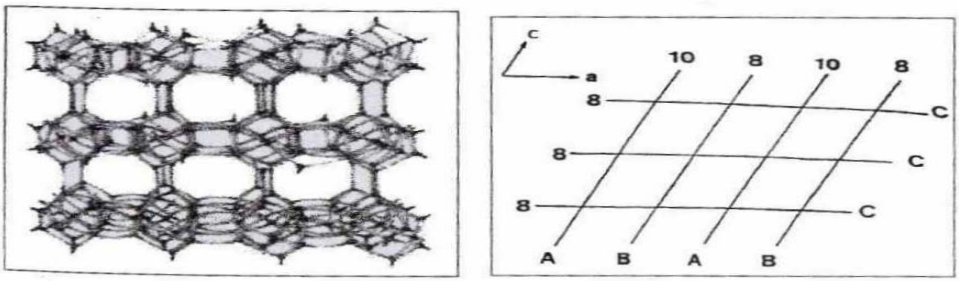

(a) (b)

Figure 3.2. (a) Model framework for structure of clinoptilolite. (b) Orientation of clinoptilolite structure of clinoptilolite (Ackley et al., 1991)

Table 3.2. Channel Characteristics and Cation Sites in Clinoptilolite (Ackley et al., 1991)

Channel	Tetrahedral ring size/channel axis	Cation site	Major cations	Approximate channel dimensions, nm×nm
A	10/c	M(1)	Na, Ca	0.72×0.44
B	8/c	M(2)	Ca, Na	0.47×0.41
C	8/a	M(3)	K	0.55×0.40
A	10/c	M(4)	Mg	0.72×0.44

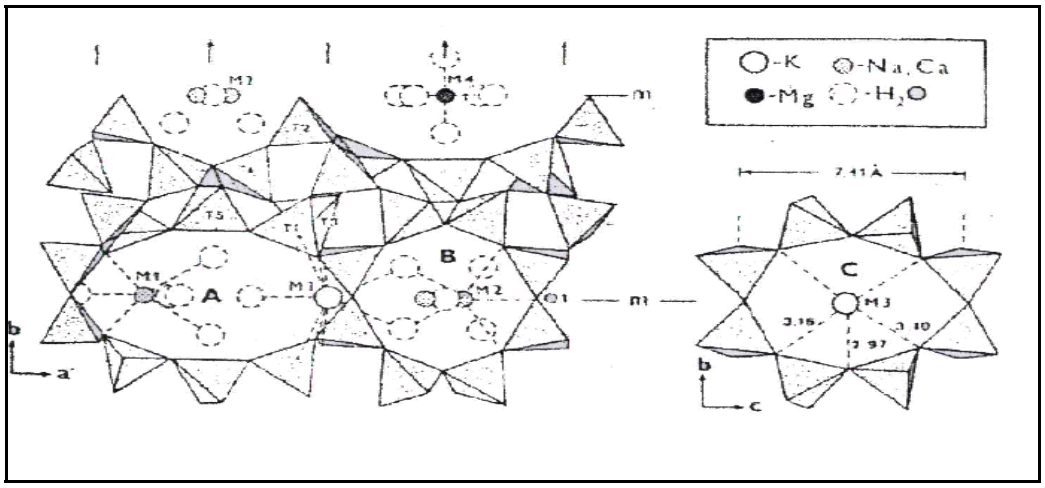

Figure 3.3. The main cation positions in the clinoptilolite structure

Cation exchange, catalytic, adsorption properties are heavily influenced by the type, number and location of the charge balancing in the A, B and C channels. A view of clinoptilolite structure, including the cation sites is represented in Figure 3.3. The main cation positions in this structure are: M (1), in channel A, is coordinated with two framework oxygen and five water molecules. This site is occupied by Ca^{+2} and preferably by Na^{+} .M (2), located in channel B coordinated by three framework oxygen and five water molecules. M (2) is occupied by Na^{+} and preferably Ca^{+2}. M (3) is situated in channel C and coordinated by six framework oxygen atoms and three water molecule. It is occupied by K^{+} and probably, Ba^{+2}. M (4) is located in the center of channel A different from M (1).It is coordinated by six water molecules. This site is occupied by the Mg^{+2} ions.

3.6 Uses and Application of Zeolites

Due to their unique properties, zeolites can be used in a wide variety of applications such as in wastewater treatment, aquaculture, odour control, animal feed, gas purification, construction (lightweight aggregates), paper production (as filler), health application. Pavelic and Hadzija (2002) studied that a novel use of finely ground clinoptilolite as a potential adjuvant in anticancer therapy. Clinoptilolite treatment of mice and dogs suffering from a variety of tumor types led to improvement in the overall health status, prolongation of life-span, and decrease in tumors size. Local application of clinoptilolite to skin cancers of dogs effectively reduced tumor formation and growth. In addition, toxicology studies on mice and rats demonstrated that the treatment does not have negative effects. The most important recent uses of zeolites are tabulated in Table 3.3.

Table 3.3. Application Fields of Zeolites

Application Areas		References
Wastewater Treatment	*Ammonium removal*	Ülkü(1984), Yücel(1990), Alsoy(1993), Şenatalar(1995), Demir et al.(2002), Cincotti et al. (2001), Hlavay et al. (1982), Jorgensen and Weatherley (2003), Klieve and Semmens(1980).
	Heavy metals removal	Çelenli (1996) ,Türkman (2001), Inglezakis et al., 2001, Kesraoui-Ouki et al., 1994, Mondela et al.(1995)
	Organic compound removal	Şimşek (1998), Garcia et al.(1993), Li et al.(2000)
	Radioactive elements removal	Yücel (2002), Dyer and Zubair(1998)
Purification and Gas Separation		Sirkecioğlu (1995, 1997), Tıhmınlıoğlu and Ülkü (1996),Yaşyerli(2002)
Heat Storage		Ülkü (1989, 1991), Özkan (1991, 1997).
Animal Nutrition		Çoşkun (1998), Oğuz (2000), Öztürk (1998).

CHAPTER 4

ION EXCHANGE PROCESS

4.1 Definition of Ion Exchange Process

Ion exchange is defined as the reversible exchange of ions between a solid and a liquid in which there is no substantial change in the structure of the solid. Today, the applications of ion exchange range from water purification to separation of various antibiotics from fermentation broth.

Ion exchange phenomenon can be simply explained by “sponge model”. In this model, ion exchanger is thought as a sponge with counter ions (exchangeable ions) floating in the pores. When the sponge is immersed in a solution, counter ions can leave the pores and float out. However, to preserve electroneutrality another counter ion from the solution enters the sponge and takes it place in compensating of the framework charge (Helfferich, 1962).

Ion exchangers are materials that can exchange ion for another, hold it temporarily, and release it to a regenerant solution. When an ion exchanger, loaded with ions “A” comes into contact with a solution containing counter ions “B” Ions “A” will diffuse into the solution and an equivalent amount of ions “B” diffuses into the resin phase. This exchange is accompanied by changes of the water content and develops until a state of equilibrium has adjusted. The state of equilibrium does not depend on the original system. In the state of equilibrium phases, solution and exchanger contain both types of ions.

4.2 Ion Exchange Reactions in Zeolites

The cation exchange property of zeolite minerals was first observed 130 years ago. Among the different alternative ion exchangers, zeolites have some advantages compared with the conventional organic resin types. The key features of the zeolites are as follows:

1. Their well defined framework structure leads to a uniformity of molecular sized channels and cavities through which cations diffuse in order to undergo exchange in sites within the crystals. The nature of these intracrystalline

penetrations is important in ion sieving and diffusion control, and depends mainly upon the framework topology.

2. Because of their three dimensional framework structure most zeolites do not undergo any appreciable dimensional change with ion exchange.
3. The aluminum content, that is the number of tetrahedrally oriented aluminum atoms per unit cell of framework, defines the maximum number of negative charges available to cations. The ion exchange capacity is directly related to the quantity of aluminum present in the zeolite framework. In such case, a low Si/Al ratio, in other words, high aluminum concentrations favors this process. In zeolites, this feature can be altered by dealumination.
4. The sieving and partial sieving effects of zeolites towards various cations are the one of the important features of them and have potential applicability in many areas.

4.3 Ion Exchange Equilibrium

The ion exchange process may be presented by the following equation:

$$z_A B^{Z_B^+}_{(z)} + z_B A^{z_A^+}_{(s)} \Leftrightarrow z_A B^{z_B^+}_{(s)} + z_B A^{z_A^+}_{(z)}$$

where z_A and z_B are the charges of the exchanging cations A and B and the subscripts z and s refer to the zeolite and solution, respectively.

Reaction proceeds until equilibrium is established. (Breck 1974, Helfferich, 1962) Equilibrium properties of a system have great importance because it is possible to obtain a measure of selectivity of the zeolite for one ion over another or group of other ions.

Equilibrium behavior is usually described in terms of equilibrium isotherms which depend on the system temperature, the total initial concentration of the solution in contact with the exchanger and on characteristics of the ion exchange system, such as solution composition, mineral type and pH.

Ion exchange equilibrium can be characterized by the by the ion exchange isotherm. Ion exchange isotherm shows the ionic composition of the ion exchanger as a function of the experimental conditions. It is plotted in terms of the equivalent fractions

of exchanging ion in solution and in zeolite phase by keeping total solution normality constant. Equivalent ionic fractions are expressed by the following equations:

for liquid phase:

$$X_A = \frac{C_{A(s)} z_A}{C_{A(s)} z_A + C_{B(s)} z_B} \quad 4.1$$

$$X_B = 1 - X_A \quad 4.2$$

where

$C_{A(S)}$ = the concentration of A ion (mole/ lt.) in the solution

$C_{B(s)}$ = the concentration of B ion (mole/ lt.) in the solution

for solid phase:

$$Y_A = \frac{number\ of\ equivalents\ of\ exchanging\ cation\ A}{total\ equivalents\ of\ cations\ in\ the\ zeolite} \quad 4.3$$

$$Y_A = 1 - Y_B \quad 4.4$$

According to Breck (1984), the ion exchange isotherm may be classified into six types. Breck's arrangements of isotherm indicate whether or not the cation in solution is preferably exchanged by zeolite. The exchange isotherms are illustrated in Figure 4.1. Six types of isotherms can be discriminated:

- a convex isotherm with ($\frac{\partial^2 y}{\partial x^2} < 0$): The relative exchanger phase loading is always greater than the relative liquid phase concentration. This means that the component is preferred.
- a concave isotherm with ($\frac{\partial^2 y}{\partial x^2} > 0$): This is the reverse case which shows that the component is not preferred.
- a s-shaped isotherm with separated regions of preference and non-preference.
- a linear isotherm y = x: In this case none of the two species is preferred. This case is very rare and occurs almost exclusively during isotope exchange.
- a "horizontal" isotherm x = 1: This is the so-called irreversible isotherm. For any x > 0 the relative exchanger phase concentration is y = 1.

- a second “horizontal” isotherm y = 0: This case indicates that there is no sorption and holds usually for co-ions.

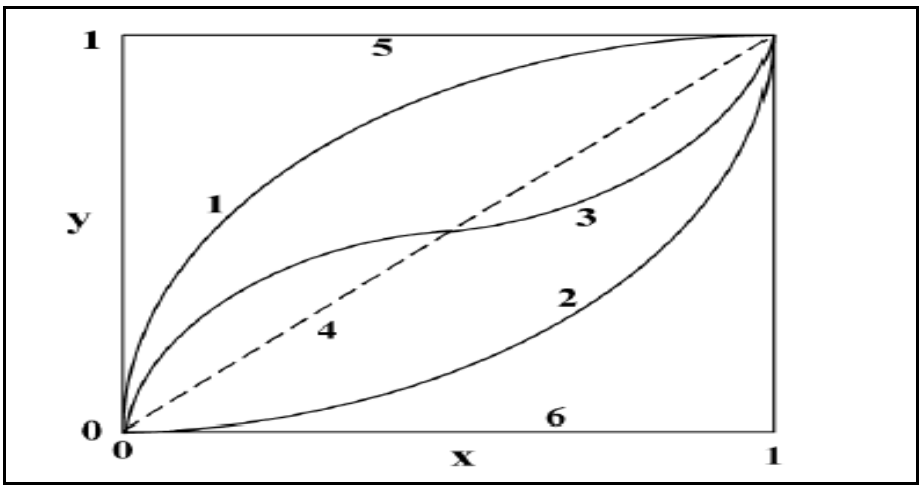

Figure 4.1. Ion exchange isotherms described by Breck (1984)

4.4 Separation Factor and Selectivity

The preference of the ion exchanger for one of the two counter ions is often expressed by the separation factor. This quantity is particular used for the practical applications, such as the calculations of the column performance. The separation factor α_B^A is defined by:

$$\alpha_B^A = \frac{Y_A * X_B}{Y_B * X_A} = \frac{Area\ I}{Area\ II} \qquad 4.5$$

There is a simple relationship between the separation factor and the ion exchange isotherm. Equation 4.5 and Figure 4.2 show that the separation factor is given by the ratio of the two rectangular areas which lie above and below the isotherm and intersect with each other at the point which corresponds to the experimental conditions.

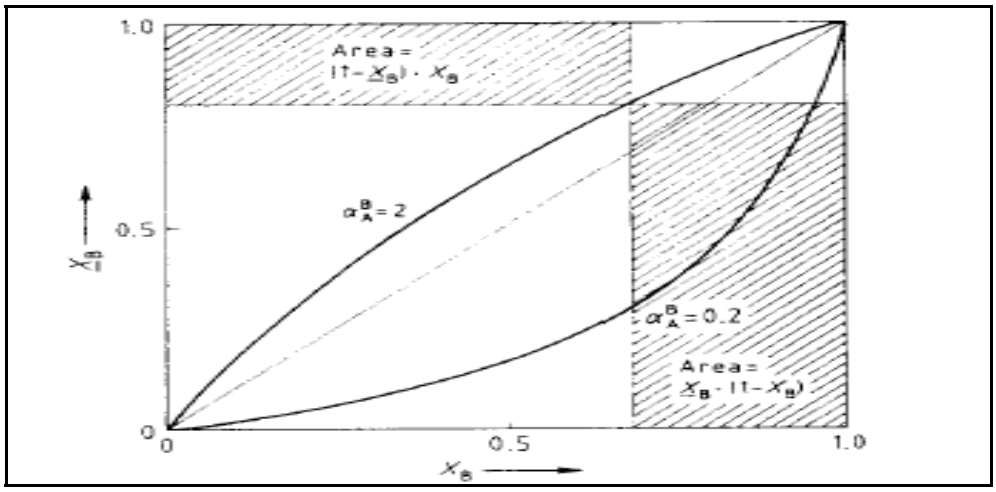

Figure 4.2. Derivation of the separation factor for the exchange reaction from the isotherms.

If the ion A is preferred, the separation factor α_B^A is larger than unity, and if B is preferred, the factor is smaller than unity. Ratio of the areas lying below and above an exchange isotherm gives an idea about which ion is preferred by ion exchanger.

In most crystalline exchangers, the isotherms terminate at the lower left and upper right corners of the diagrams. In zeolites, however, there are many exceptions due to exclusion of the entering ions or trapped cations in the zeolite structure. This is referred to as the ion-sieve effect, that is, the entering ions cannot reach all of the sites occupied by the ions initially in the zeolite. The isotherm then terminates at a point where the degree of exchange, x, is less than 1. (Breck, 1974) Ion sieving effects are observed with the zeolites having the smallest pore openings and with the largest cations. Some ions are exchanged even though their hydrated ionic diameters are much larger than the pore openings; an exchange of solvent molecules must occur for such cations to diffuse through the pore opening. Ions which have anhydrous diameters which are too large are totally excluded. Ions have sufficiently small anhydrous diameters to enter pores may differ in their exchange rates of exchange owing to differences in the activation energy required to exchange solvent molecules (Sherman, 1978).

In addition to some ion sieving effects, zeolites commonly exhibit high selectivities for ion exchange among ions which will easily enter the zeolites pores. Each zeolite provides a different pattern of ion exchange selectivity. The selectivity series of increasing preference for exchange of different cations for each of the most common zeolites are shown in Table 4.1. Some zeolites show marked selectivity for

some monovalent cations over common divalent cations. The observed ion exchange selectivities on zeolites are dependent upon the pH, temperature and aqueous solution chemistry. The competing cations, choice of solvent, presence of complexing agents, solution strength and type of anions present can alter the quality of the separation.

Table 4.1. Molecular Sieve Zeolite Ion Exchange Selectivity Patterns (Sherman, 1978)

Zeolite	Selectivity series	Reference
Chabazite	Li<Ca<Sr<Ba=Na<Pb<NH_4<Rb<Ag<K<Ti	Barrer, Davies and Breck
	Li<Na< K<Rb<Cs	Barrer and Klinowski
	Mg<Ca<Sr<Ba	Ames
	Li<Na< K<Cs	Ames
Clinoptilolite	$NC_4H_9NH_3^+$<$nC_3H_7NH_3^+$<NH_4^+<$C_2H_5NH_3^+$	Barrer, Papadopoulos, and Rees
	Li<Na<Rb<K<Cs	Sherry
	Li<Ca<Sr<Ba<Na<K<Rb	Filizova
	Na<K<Cs	Ames
	Na<NH_4^+<Cs	Howery and Thomas
	Cu<Zn<Cd<Pb<Ba	Semmens and Seyforth
	Zn<Cu<Cd<Pb	Fujimori and Moriya
	Mg<Ca<Na<NH_4^+<K	Sherman and Ross
	Li<Na<NH_4^+<K<Rb<Cs Mg<Ca<Sr<Ba	Ames
	Na<Ag<Pb At low loadings: Na<Cu<Zn<Cd<Ag<Pb	Chelishchev et al.
Heulandite	Ca< <Ba< Sr< Li<Na<Rb<K	Filizova
	Ca< Sr	Hawkins
Phillipsite	Li<Na<K< Rb< Cs Ca≤Sr<Na<Ba (Ba irreversible)	Barrer and Munday
	Ca<Na<NH_4<K	Sherman and Ross
	Na<K<Cs	Ames
Mordenite	Mg< Ca<Sr<<Ba Li<Na<H<K<Ag<Cs	Wolf, Furtig and Knoll

4.5 Factors Affecting Ion-Exchange Behaviour

Hundreds of technical papers have been written describing the characteristic ion exchange behavior of various zeolites. According to these studies, two conclusions are readily drawn. Cation exchange selectivities in zeolites do not follow the typical rules and patterns exhibited by organic and inorganic ion exchangers. And also, many molecular sieve zeolites provide certain combinations of selectivity, capacity and stability characteristics superior to the more common organic and inorganic ion exchangers (Sherman et al., 1978).

Cation exchange properties of zeolite depend on:

1. The nature of the cation species, cation valance and both anhydrous and hydrated size of cation.
2. Temperature
3. The cation concentration of cation species in the solution
4. The anion species associated with the cation in the solution.
5. The solvent
6. The structural characteristic of the particular zeolite.

Cation exchange in zeolites leads to alteration of stability, adsorption behaviour, and selectivity, catalytic activity and other important physical properties so ion exchange should also be considered as a modification process as well as a direct application.

The affinity of ion towards a given exchanger depends mainly on the charge of the ion, ionic radius and degree of hydration. There is a relation between ionic charge and hydration enthalpy. The higher charge shows the higher enthalpy. A large ion charge/size ratio results in an increase in the hydration energy. An increase in the ionic radius is accompanied by a decrease in the hydration enthalpy. Because of their size, certain cations may be able to exchange with cations within the crystal structure of the zeolite. Table 4.2 represents ionic radii, hydrated ionic radii and free energies of hydration for certain ions. If an ionic radius is compared with the free dimensions of the clinoptilolite channels (4.0x5.5-4.4x7.2 A), it is apparent that all of the unhydrated ions can pass readily through the channels, but since the hydrated ions are approximately the same size as the channel dimensions, they may exchange only with difficulty. (Semmens et al., 1974)

Eisenman indicated that selectivity of exchange cations is accounted for only in terms of their hydration free energies and their energies of electrostatic interaction with

the zeolite fixed anions. He separated the free energy of ion exchange reaction into two parts. The first part represents the difference between the free energy of the ions in zeolite while second part represents the free energy differences of hydration of the ions in the solution. If the electrostatic fields in zeolite are strong, then the first part dominates and small ions are preferred. Strong electrostatic fields occur in zeolites with a high framework charge and correspondingly low Si/Al ratio. However, if these electrostatic fields are weak (as in zeolites with a high Si/Al ratio), the hydration free energy is more important. So, weakly hydrated cations are preferred. Clinoptilolite has silicon to aluminum ratio of approximately 4.3 to 5.3 and a correspondingly low Si/Al ratio. The low Si/Al ratio provides a weak anionic field within the zeolite. Consideration of Eisenman's model in the case of exchange on zeolite in the presence of weakly anionic field indicates that selectivity is predominantly determined by the free energies of hydration of the competing cations.

According to Eisenman's Theory, the free energies of hydration listed in Table 4.2 indicate that the following selectivity sequence (Ba^{+2} >Pb^{+2}>Cd^{+2}>Cu^{+2}). Therefore, copper with the largest hydration energy, prefers the solution phase where it may satisfy its hydration requirements, and barium, with least hydration energy, prefers the zeolite phase.

Table 4.2. Properties of Certain Cations (Semmens, 1974)

Cation	Ionic Radius (A)	Hydrated Radius (A)	Free Energy of Hydration (kcal/gr ion)
Ba^{+2}	1.43	4.04	-315.1
Cd^{+2}	1.03	4.26	-430.5
Cu^{+2}	0.82	4.19	-498.7
Pb^{+2}	1.32	4.01	-357.8
Zn^{+2}	0.83	4.30	-484.6
Na^{+}	0.98	3.58	-98.2
K^{+}	1.30	3.31	-76.67
Mg^{+2}	0.65	4.28	-459.04
Ca^{+2}	0.99	4.12	-380.22

Considerable research has been conducted to characterize the mechanism of ammonium from wastewater and aqueous solution by natural zeolite. It was revealed that a number of factors contribute to the maximization of ammonium removal by ion exchange, including the initial concentration of the solution (Fredickson et al., 1993), the particle size of the zeolite (Jorgensen et al., 1976), properties of the zeolite such as porosity and density of the zeolite (Fredickson, 1993), chemical pretreatment leading to

the particular homoionic form of the zeolite (Koon et al., 1975; Jorgensen, 1976; Mercer et al., 1970; Yücel et al., 1989; Townsend et al., 1984), pH of the solution (Koon et al., 1975; Jorgensen, 1976), and the presence of competing cation (Koon et al., 1975; Jorgensen, 1976; Schoeman, 1986; Czaran, 1988).

Many authors stated that the pretreatment operation has effected on the cation exchange capacity. Practically, the result of any pretreatment operation is the increase of the content in a single cation, what is called homoionic form (Semmens et al., 1988). Therefore, pretreatment aims to remove certain ions from the structure of the material and locates more easily removable ones, prior to any ion exchange application of it. The final homoionic or near homoionic state of the zeolites was found to improve their effective exchange capacity and performance in ion exchange applications (Kesraoui et al., 1993; Klieve et al., 1980; Semmens et al., 1988; Chmielewska et al., 1995).

Pretreatment with sodium ions has been shown to improve the selectivity and ammonium exchange capacity of the zeolite more than pretreatment with magnesium and calcium ions (Jørgensen et al., 1979; Booker et al., 1996). The calcium form of the clinoptilolite had an even lower ammonium exchange capacity than untreated clinoptilolite (Hlavay et al, .1982), which was explained in terms of cation size. Because the calcium ion is larger than the sodium ion, it cannot approach the exchange sites as closely as sodium, which is smaller and freer to migrate through the zeolite channels (Koon et al., 1975).

Cooney et al., (1999) have studied the removal of ammonium ion from wastewaters using natural Australian Zeolite. It has been found that pretreatment with NaCl enhances the capacity of zeolite. The ion-exchange capacity for ammonium of the sodium-form zeolite was found to be 1.5 meq/gr. Klieve et al., (1980) studied the effects of pretreatment with NaOH,HNO_3, steam and heat (600 °C, 1 hour) on the performance of ammonium removal as well as the total ammonium capacity. NaOH treated clinoptilolite was observed to have highest capacity, whereas the heat treated was the lowest. On the other hand, pretreatment of clinoptilolite with NaOH, HNO_3 and steam did little to improve the zeolite's performance, while heat treatment improved the zeolite's selectivity significantly.

As a consequence of this concern, the process of converting original samples to the Na-form can be suggested as the appropriate pretreatment method for increasing exchange capacity.

Washing the zeolite sample is different effective way for increasing exchange capacity of the zeolite. Inglezakis et al., (2001) have investigated the effect of washing surface dust of the zeolite sample on the exchange capacity. According to their results, they concluded that surface dust is clogging part of the pore openings in zeolite structure leading in slower ion exchange kinetics.

Jorgensen et al., (1976) studied that ammonium removal from wastewater, distilled water and tap water by using clinoptilolite. According to his results; clinoptilolite works by a combination of ion exchange and adsorption process. With a small concentration of the counter ion in the solution only ion exchange takes place. With a higher concentration, adsorption takes place. They indicated that there are many factors which affect the ion exchange and adsorption of ammonium cations from either synthetic or real municipal wastewater. They included the concentration of ammonium ion in the solution, concentrations of counter ions such as Ca^{+2} or Na^{+} or other cations. Therefore, tap water and wastewater have a considerably lower NH_4^{+} removal capacity than distilled water due to mainly to Ca^{+2} ions present in tap water and wastewater. And also, clinoptilolite was used in the pilot scale application. A very high wastewater effluent quality can be achieved by applying a combination of chemical precipitation, activated carbon column, anion exchange media and clinoptilolite (Jorgensen et al., 1976). The removal efficiency of such pollutants like ammonium, phosphorous, suspended solids and organic matter were %90, 90-99%, 99% and 94% respectively.

Hlavay et al. (1980) investigated the performance of the Hungarian natural zeolite for ammonium removal from synthetic and municipal wastewater. The optimal ion exchange conditions found were as follows: Na-form clinoptilolite and 0.5-1.0 mm in particle size. The loading flow rate used is a very important factor regarding the column performance. By changing the flow rate 10 to 5 BV/h the ammonium breakthrough capacity increased as much as 35%. So, optimum conditions were chosen 5-7 BV/h for loading rate. For regeneration of the ion exchange bed, 10-20 BV of regenerant were necessary to remove the 98-99% of ammonium with a flow rate of a 5-7 BV/h. The ammonium breakthrough capacity was found as 2.4 mg/gr zeolite, less than a half of the value (4.5 mg/gr zeolite) obtained with synthetic wastewater.

Ülkü (1984) studied the effect of natural zeolites on the pollution control of Porsuk River to which wastewater of Kutahya Fertilizer Plant is discharged. In this study, natural zeolites provided from Balıkesir region of Turkey have been used. At the end of the study, 91% ammonium removal efficiency has been obtained. It has been

concluded that natural zeolites could be good material that can be used in the pollution control, especially ammonium removal applications.

Yücel et al., (1990) investigated the sodium-ammonium, potassium-ammonium and calcium-ammonium exchanges on the clinoptilolite. Prior to exchange experiments, all sample converted to homoionic form with appropriate salt solutions. Their experimental results indicate that the clinoptilolite show a very high preference for ammonium ion over sodium and calcium but not over potassium. It can be explained with the poor ion exchange behaviour of the K^+ ion. Potassium ion exchange does not exchange significantly with other ions in the solution. This behaviour of K indicates that a low mobility of K in the clinoptilolite structure as compared to other ions. The selectivity sequence for the exchange studies were given as follows: $K^+ > NH_4^+ > Na^+ > Ca^{+2}$.

A combination of the natural zeolite as ion exchanger for ammonium recovery and/or anionic resin fro the removal of phosphorous from wastewater in the RIMNUT process, which were discussed by the Liberti et al. (1991). After the regeneration of the exhausted zeolite and resin with Na-solution an acid solution was occurred, respectively, and by adding $MgCl_2.6H_2O.H_3PO_4.Na_2CO_3$ and NaOH to the regeneration eluate, high quality slow release fertilizers ($MgNH_4PO_4.6H_2O$) were produced. The ammonium removal efficiency achieved higher than % 80, the effluent concentration of ammonium was lower than 15 mg/lt.

Garcia Hernandez et al., (1992) found that the tertiary treatment of wastewater using phillipsite rich tuff is very useful not just for removing ammonium but also for the removal of phosphor, calcium, magnesium, inorganic contaminants, bacteria and soluble organic matter. Depending amount of ammonium, phosphor and other plant nutrients, they suggested that the exhausted zeolite could be used as a slow-release fertilizer.

Metropoulos et al., (1993) compared natural zeolite and synthetic zeolite for ammonium uptake. In this study, clinoptilolite, mordenite and ferrierite were used in their sodium forms. And also, Zeolite A was used in its sodium, potassium and calcium forms. The three natural zeolites show higher selectivies for ammonium compared to the synthetic zeolite A, in any of the three forms. Clinoptilolite and ferrierite show similar behaviour regarding the selectivity for ammonium ions. Although mordenite has similar exchange capacity with clinoptilolite, its selectivity for the ammonium ion is

much lower. Despite the theoretical high exchange capacity of Zeolite A, low ammonium quantities are retained.

Alsoy et al., (1993) investigated that the treatment of wastewater with natural zeolite. Prior to exchange experiments, all sample converted to Na- form with appropriate salt solution. In this study, sodium-ammonium, sodium-lead, sodium-copper exchange equilibrium studies were investigated. Experimental results show that, clinoptilolite has a good selectivity especially lead and ammonium ions. Selectivity sequence was given as follows: Pb^{+2}>Cu^{+2}, NH_4^+. And also, thermodynamic parameters were calculated. Ka and ΔG^0 was found as 3.119 and -2.9067 kJ/equiv for $Na^+ \leftrightarrow NH_4^+$ equilibria.

Clinoptilolite- rich tuffs were reported to be utilized in two stages of treatment of municipal wastewater. The clinoptilolite tuffs of 40-160 μm grain size were added to 1 m^3 of raw sewage before the aeration tank. Kallo (1995) found that the addition of 40-80 mg of clinoptilolite samples to 1 lt of raw sewage resulted in an increase of the settling rate of suspended solid as well as an increase in the biological activity of living sludge and that with the composting and de-watering of the produced sludge is made easier when compared with normal sludge. In addition, elimination of phosphor was observed. After the biological treatment, residual ammonium was removed by ion exchanger bed filled with 0.5-2.0 mm granules of the clinoptilolite tuffs. The clinoptilolite was regenerated using an alkaline solution of KCl/ NaCl. Ammonia was then stripped from the regenerating solution with air and adsorbed in phosphoric acid; hence, the ammonia removed from the sewage was used to produce an ammonium hydrophosphate fertilizer.

Şenatalar et al., (1995) studied that ammonium removal from wastewaters using by using Bigadiç clinoptilolite. In this study, the effects of influent ammonium concentration and loading rate on the breakthrough capacity and the effects of regenerant concentration and pH on the regeneration efficiency were investigated using synthetic wastewaters containing no competing cations. The ammonium exchange capacity of the zeolite sample was found as 0.52 meq/gr at 20°C. Breakthrough and total ammonium exchange capacities were observed to increase with increasing feed concentration and decreasing flow rate. 212.5 BV of a solution containing 25 mg/lt could be treated at a flow rate of 11 BV/h until the breakthrough concentration of 2 mg/lt was reached in the effluent. Regeneration efficiency increases with increasing the pH of the solution. 30 gr NaCl/lt at a pH of 12.5 was found to be sufficient to regenerate

the clinoptilolite bed with 99% efficiency. Their results indicate that Bigadiç clinoptilolite can be potential candidate to be used in several ammonium removal applications.

Booker et al., (1996) studied that ammonium removal from sewage by using natural Australian Zeolite. In this study different homoionic forms were tested. Their results indicate that the sodium form shows the highest ammonium removal capacity. The zeolite ion exchange process has proved effective, at pilot scale in reducing ammonium ions in sewage from concentrations ranging from 25 to 50 mg/lt down to levels below 1 mg/lt. The ammonium removal capacity was found as 4.5 mg/gr for this range of initial ammonium concentrations. The rate of treatment by the pilot zeolite column makes it ideally suited as retrofit to high rate secondary sewage treatment process, for the removal of the soluble ammonium component.

An alternative to chemical regeneration is biological regeneration, which actually is a combination of chemical regeneration and nitrification. One reason given for the development of biological regeneration was to decrease brine consumption. A second reason was to achieve a more efficient nitrification process in a small volume with minimal competition between autotrophic nitrifying bacteria and heterotrophic bacteria caused by a low concentration of organic compounds (Lahav et al, 1996). Green et al., (1996) investigated the application of the biological ion exchange process. In the first mode (ion exchange), a column filled with zeolite (chabazite) is used for ammonium ion exchange from secondary or primary effluents. When $NH4^+$ concentration breakthrough occurs the system switches to the bioregeneration mode. In the second mode (bioregeneration), the same column containing the ammonium-rich chabazite is used during the bioregeneration mode as a fluidized bed reactor for biological nitrification with the chabazite acting as the carrier for the bio-film. After a short time, the solution reaches an apparent equilibrium concentration of ammonium (Reaction I), while simultaneously, the biomass starts to oxidize ammonia (Reaction II).

I. desorption: $Z - NH_4^+ + Na^+ \leftrightarrow Z - Na^+ + NH_4^+$

II. nitrification: $NH_4^+ + 2O_2 \rightarrow NO_3^- + 2H^+ + H_2O$

During the regeneration phase, oxygen and sodium bicarbonate were supplied for the nitrification process and to maintain a constant pH. Sodium salt was added to the recirculating solution to facilitate the ammonium desorption. Because the ammonium was oxidized to nitrate, the regeneration solution could be used during several cycles

with no addition of external regenerant. After the regeneration phase, it was suggested that the nitrate-rich backwash water could be used for agricultural purposes or conveyed to a denitrification reactor. At the end of the adsorption and regeneration modes, backwash is practiced.

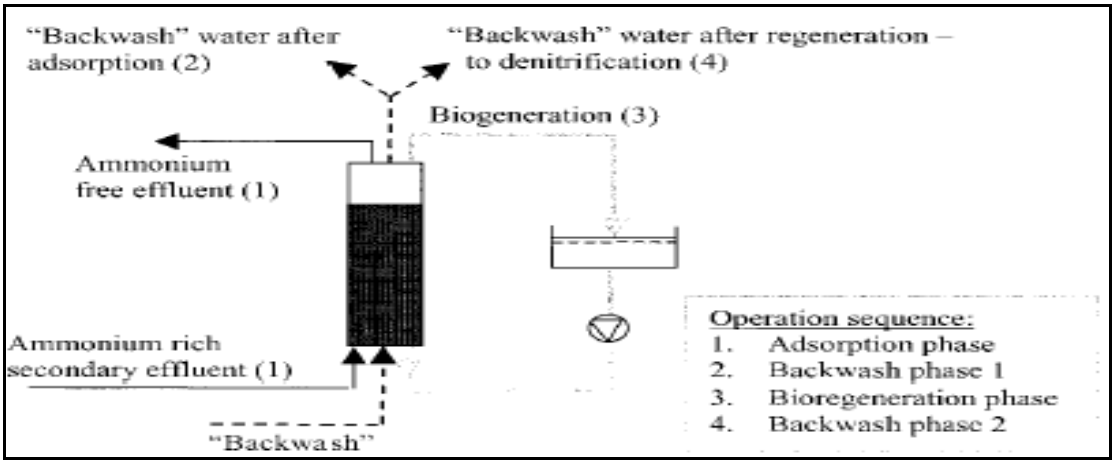

Figure 4.3. Biological Regeneration of Ammonium Exchanger in Single Reactor [from Lahav et al., (1996)]

Komarowski et al., (1997) studied that ammonium ion removal from wastewater and synthetic solution by using Australian natural zeolite. They concluded that the ammonium ion removal capacity for pure ammonium chloride solution is approximately % 40 greater than that for wastewater, for the initial ammonium ion concentration range of 5 to 50 mg/lt. The decreased ammonium ion removal for wastewater may be attributed to by existence of competing cations in the wastewater, which reduce the ammonium removal capacity. Their results were good agreement with the Jorgensen et al. (1976) study.

Kithome et al., (1998) worked on the adsorption–desorption properties of ammonium on the natural clinoptilolite. They indicated the ability of clinoptilolite to adsorb and desorb ammonium from simulated ammonium solution where the pH value and the ammonia concentration have significant effects. They found that the sorbed amount of ammonium increased by increasing the initial ammonium concentration. By increasing the initial ammonium concentration, the NH_4^+ concentration, the NH_4^+ exchange rate was decreased. They indicated the potential use of clinoptilolite as adsorbent for ammonium which could be used as slow release fertilizer.

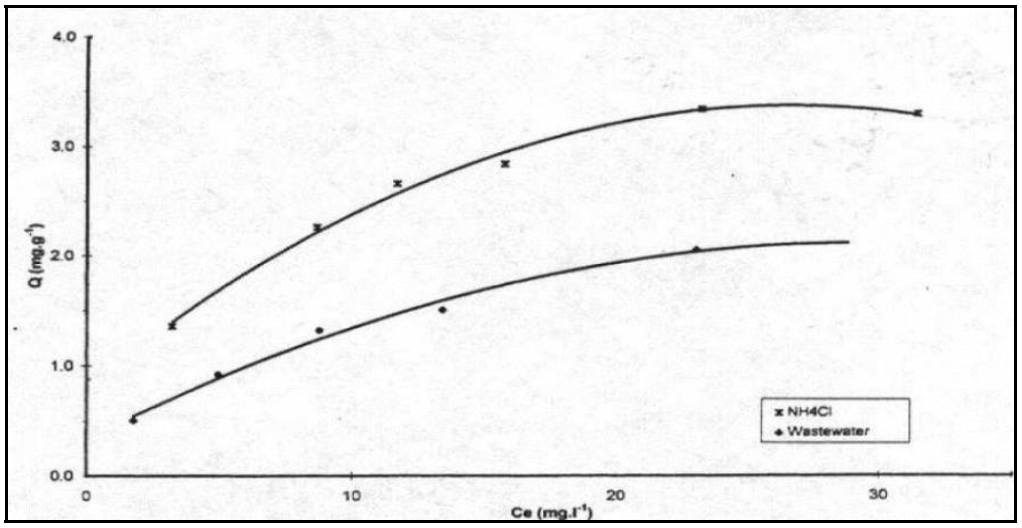

Figure 4.4. Comparison of ammonium removal capacity for wastewater and synthetic solution [Komarowski and Yu, 1997]

Langella et al., (2000) investigated the exchange equilibria of the Na-form Sardinian clinoptilolite with some of the hazardous cations, such as; ammonium, copper, zinc and lead. In this study, isotherms of NH_4^+, Cu^{+2}, Zn^{+2}, Cd^{+2} and Pb^{+2} exchanges for Na^+ at 25°C and 0.1 total normality were obtained and the related thermodynamic quantities computed. Exchange isotherm describing NH_4^+ and Na^+ was given in Figure 4.5. The maximal exchange level was obtained as 0.901 for ammonium ion. It means that, clinoptilolite has shown good selectivity for the ammonium ion. And also, Ka and ΔG^0 was found as 10.21 and -5.72 kJ/equiv for $Na^+ \leftrightarrow NH_4^+$ equilibria.

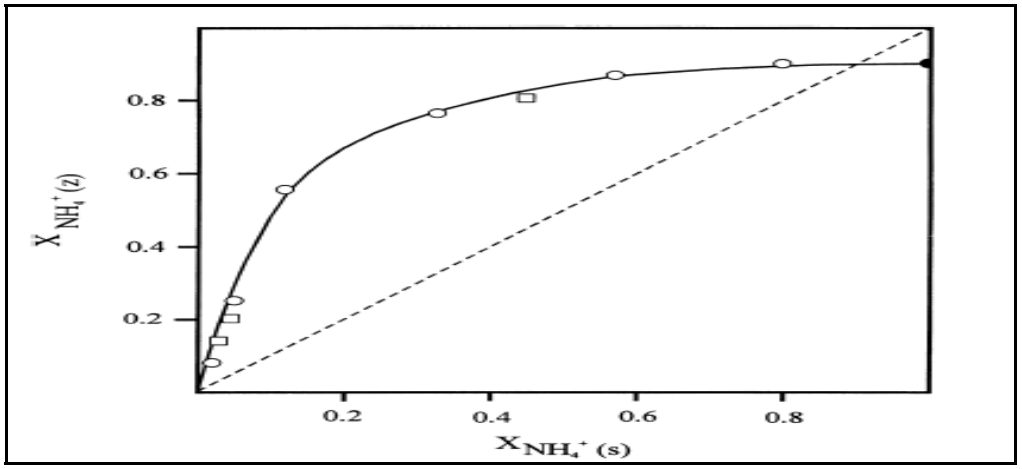

Figure 4.5. Isotherm at 25°C for the exchange of NH_4^+ into Na-clinoptilolite at 0.1 total solution normality. (Langella et al., 2000)

Ammonium removal from aqueous solution by a natural Bigadiç clinoptilolite was investigated by considering the factors affecting the ammonium-exchange capacity including the zeolites particle size, the loading flow rates and the impact of a number of regenerations upon the ion-exchange capacity. (Demir et al., 2001)The resin column was exhausted by down flow at 10, 25, 50 and 75BV/h, until effluent ammonium concentration of more than 10 mg/l $NH4^+$ was achieved. The results indicate that conditioning of the zeolite improves the ion-exchange capacity and that the smaller particle size also causes a higher ion-exchange capacity due to greater available surface area. The actual ion-exchange capacity of the conditioned fine 1 mm and coarse 2 mm clinoptilolite was found to be 0.57 and 0.38 meq/g zeolite, respectively. The capacity to 1 mg/lt $NH4^+$ breakthrough was reached in 450 BV for the fine clinoptilolite column with superficial velocities of both 25 and 50 BV/h. On the other hand, the capacity of 1 mg/l $NH4^+$ breakthrough was reached in 350 BV for the fine zeolite column with superficial velocity of 75 BV/h. A flow rate of 25 to 50 BV/h loading is advocated. In this study, the capacity increases considerably with the first regeneration. After the 2^{nd} and 3^{rd} regenerations ammonium adsorption capacity of zeolite remained constant.

Depending on the studies mentioned above, ammonium ion exchange behaviour depends on the solution and ion exchange material properties. Particle size of the zeolite, the amount of zeolite addition, initial concentration of the solution, chemical and physical treatment of the zeolite, operating conditions(flow rate, number of regeneration, etc.) presence of competing cation, pH of the solution, temperature and zeolite mineral composition are effected the ammonium exchange mechanism in the zeolite.

4.6 Ion Exchange Kinetics and Ion Diffusion

In order to determine experimental mass transfer coefficients and other kinetic parameters necessary to design an ion exchange plant, it is necessary to investigate kinetics of the ion exchange process. Batch system is widely used for the kinetic investigations. In this system, proper volumes of zeolite and solution of known initial concentration are mixed and stirred in a thermostated water bath, while the time variation of concentration is taken as output.

The kinetics of ion exchange process using zeolite may be divided into four steps:

1. Diffusion of the counterions through the film solution to the surface of the zeolite (film diffusion)
2. Diffusion of the counterions within the zeolite (particle phase diffusion)
3. Diffusion of the displaced ions out of the zeolite
4. Diffusion of the displaced ions from the zeolite surface into the bulk solution

The slowest step of the ion-exchange process for a given system controls the speed of ion exchange and is said to be the rate-limiting step. Two mechanisms generally control the rate of ion exchange within porous solids: these are either film diffusion (Step 1) or particle diffusion (Step 2). Both mechanisms are present in practice, although normally one mechanism (the slower) dominates. If the ion exchanger is nonporous, ion exchange is occurred only the external surface. So, the rate of ion exchange will be controlled by diffusion through the laminar fluid film surrounding the particle. Film diffusion is a measure of the resistance to the transport of ions from the bulk solution through the hydrodynamic boundary layer or through a real surface barrier, if existing, to the outer surface of the ion-exchange particle. Film diffusion depends mainly on particle size, solution concentration, film thickness and the effective film-diffusion coefficient of the ions (Karger et al., 1992). If the ion exchanger is microporous, ion exchange is occured only the microparticle.Particle diffusion relates to the ion diffusion rate within the exchange matrix. It is directly proportional to the concentration of the fixed charges and the particle-diffusion coefficient, which depends on the intracrystalline structure of the zeolite. In zeolites, particle diffusion is usually the rate-controlling step.

It is known that in the crystalline zeolites, ion exchange controlled by the diffusion of the ion within the crystal structure (Breck, 1974). In this case, the relevant diffusion equation for a set of uniform spherical particles is:

$$\frac{\partial Q}{\partial t} = \frac{1}{r^2}\frac{\partial}{\partial r}\left(r^2 D_e \frac{\partial Q}{\partial r} \right) \qquad 4.6$$

and the relevant initial and boundary conditions for a step change in sorbate concentration are:

$$t=0 \quad \begin{cases} Q(r,0) = Q_0' \\ Q(r_p,t) = Q_0 \\ \left.\frac{\partial Q}{\partial r}\right|_{r=0} = 0 \end{cases} \qquad 4.7$$

The solution for the uptake curve for this situation is:

$$\frac{Q_t}{Q_\infty} = 1 - \frac{6}{\pi^2}\sum_{n=1}^{\infty}\frac{1}{n^2}\exp\left(\frac{-n^2\pi^2 D_e \cdot t}{r_p^2}\right) \qquad 4.8$$

or equivalently:

$$\frac{Q_t}{Q_\infty} = 6\left(\frac{D_e \cdot t}{r_p^2}\right)^{1/2}\left[\frac{1}{\sqrt{\pi}} + 2\sum_{n=1}^{\infty} i \cdot erfc\left(\frac{nr_p}{\sqrt{D_e \cdot t}}\right)\right] - 3\frac{D_e \cdot t}{r_p^2} \qquad 4.9$$

For long time [($\frac{Q_t}{Q_\infty}$)>0.7] and short time [($\frac{Q_t}{Q_\infty}$<0.3) regions, the expressions can be simplified;

$$1 - \frac{Q_t}{Q_\infty} \cong \frac{6}{\Pi^2}\exp\left(-\frac{\Pi^2 D_e t}{r_p^2}\right) \quad \left[\left(\frac{Q_t}{Q_\infty}\right)>0.7\right] \qquad 4.10$$

$$\frac{Q_t}{Q_\infty} = \frac{6}{\sqrt{\pi}}\left(\frac{D_e \cdot t}{r_p^2}\right)^{1/2} \qquad \left[\left(\frac{Q_t}{Q_\infty}\right)<0.3\right) \qquad 4.11$$

respectively. Using these simple expressions, from the slopes of plots ln [1-$\frac{Q_t}{Q_\infty}$] vs. t (in the long time region) and $\frac{Q_t}{Q_\infty}$ versus $\sqrt{t}$ (in the short time region) effective diffusion coefficient can be calculated. According to the Equation 4.10, the effective diffusion coefficients for all concentrations were computed. For zeolites, D_e varies from $1*10^{-8}$-$1*10^{-13}$ cm^2/sec.

The factors that affect the rate of cationic exchange are:

- The charge of the inter-diffusing cations. Monovalent cations move faster in zeolites and have lower activation energies than divalent cations.

- The structure of the zeolite, or more specifically the dimensions of zeolite channels and cavities.
- The cationic radius. The cation exchange rate decreases with increasing cationic radius.
- The concentration of the exchange solution. The rate of the ionic exchange increase with the solution concentration.

Based on above, an intraparticle diffusion rate model is used to calculate the initial uptake constant. The initial uptake constant is given by Weber and Morris:

$$Q = k.t^{1/2} \qquad 4.12$$

Using this expression, from the slope of Q versus the square root of time, initial uptake constant k (mg ammonium ion per gram zeolite.minute$^{-0.5}$) can be calculated. A linear plot of Q versus the square root of time suggests intraparticle diffusion to be rate limiting step in the overall kinetic process. This dependence, according to the Fickien's Law, is deduced by considering the ion exchange process as being influenced by diffusion in the particle and by convective diffusion in the solution.

CHAPTER 5

EXPERIMENTAL

5.1 Materials

Clinoptilolite rich natural zeolite samples used in this study were taken from Gördes, Western Anatolia.

During the experimental studies, all solutions were made using the deoinozied water (Barnstead Ultrapure-UV). pH values were measured with a pH-meter namely, pH Metrohm 744. The ion exchange experiments were carried out in 250 ml cylindrical flask placed in thermostat shaker at 25 °C. In the experiment, the ammonium ion concentration of the samples taken with certain time intervals were analyzed before and after equilibrium by using the ammonia selective electrode (Metrohm, 781/pH-Ionmeter). The ammonium was converted to ammonia by raising pH to above 11 with 10 M NaOH (Fluka) solution as required by use of ammonia selective electrode method. The competing cation concentrations of the samples after equilibrium were analyzed by using Inductively Coupled Atomic Emission Spectroscopy (ICP-AES 96, Varian). In the ICP analyses, 1 wt. % Nitric Acid (HNO3) solution (Merck) was used.

In the experiment, ammonium chloride synthetic solution was prepared by dissolving NH_4Cl (Sigma, 99.9% pure) in deoinozied water. The dilution of the solutions was made by using the stock ammonium chloride solution (1000 ppm) of Metrohm, 776 DOSIMAT Unit. To understand the effect of the competing cations, $CaCl_2.2\ H_2O$ (Aldrich, 98% pure), $MgCl_2.6H_2O$ (Aldrich, 99 % pure) and KCl (Panreac, 99.9% pure) were used in the experiment.

Experiments were also conducted using samples of treated Izmir Çiğli domestic wastewater effluent. Five liter samples were collected after Parshall Flumes and prior to Oxidation Ditch Tank at the plant. After collecting samples, pH of the samples was adjusted to preserve the composition of the samples. For this purpose, concentrated H_2SO_4 solution was used. Prior to the ion exchange experiment, the pH of the samples were raised by using concentrated NaOH solution. BOD and COD test of the domestic wastewater samples were made at the Izmir Çiğli Domestic Wastewater Plant. For measuring the COD value; potassium dichromate (Merck) and silver sulfate (Merck) were used. Also, BOD value was measured by using BOD test bottles.

5.2 Methods

Measurements of the ammonium ion concentration in solution were conducted by using the combination of 781/pH-Ionmeter (Metrohm), 776 Dosimat Unit (Metrohm) and Ammonia Selective Electrode (Metrohm) system. The ammonium ion concentration of the samples were taken against the time and analyzed before and after equilibrium by using this system. This system was shown in Figure 5.1.

Figure 5.1. 781/pH-Ionmeter, 776 Dosimat Unit and Ammonia Selective Electrode.

Two methods were used to measure the ammonium ion concentration with ammonia selective electrode system. Direct method is a simple, fast method for measuring a large number of samples over a wide range of concentration. Only one meter reading is required for each sample. This method involves measuring the mV potential of known standards to produce a calibration graph of mV versus concentration. The mV potential of the sample is then measured and correlated to a concentration on the calibration graph. Standard addition method is convenient fro measuring occasional samples because no calibration is needed. Since accurate measurement requires that the concentration approximately doubles as a result of addition, sample concentration must be known within a factor of five. In this method, we have a large volume of unknown to which small amounts of a standard solution are added. From the change in electrode voltage before and after addition, the original sample concentration is determined.

In this study, direct and standard addition methods results were compared to check the effect of interference on the selective electrode system. For this reason, known ammonium concentration was prepared in the range of 1-200 mg/lt. to construct

the calibration curve for direct method. This calibration curve was given in Appendix A. Some direct and standard method concentration results were tabulated in Table 5.1.

Table 5.1 shows that there are no significant differences between two methods. The differences were very small. The results indicate that both methods are useful to determine the ammonium ion concentration in the solution. Also, there is no effect of interference on the selective electrode system.

Table 5.1.Direct and Standard Addition Method Concentration Results

C_0(ppm)	C_{eq} (direct)	C_{eq} (standard)
10	0.51	0.5
30	2.21	2.2
50	6.44	6.5
70	13.71	13.8
100	27.62	27.9
150	66.81	67.5
200	108.66	109.4

In order to establish the extent to which the presence of potassium, calcium and magnesium ions influenced ammonium ion uptake further equilibration experiments were conducted. Some experiments were performed to understand the effect of the competing cation on the ion exchange mechanism. For this reason, Inductively Coupled Atomic Emission Spectroscopy (ICP-AES 96, Varian) was used to measure the competing cation concentration in the solution after equilibrium. ICP method analyze procedure was given in Appendix A.2.

5.3 Material Preparation

Clinoloptilolite rich natural zeolite rock samples used in this study were taken from Manisa Gördes region. These rock samples from Gördes deposits were first crushed mechanically into small pieces and sieved into different size ranges. The final clinoptilolite rich natural zeolites sample were ground and sieved to 2-0.85 mm & 2-2.8 mm particle size and used in ion exchange experiments. Prior to the ion exchange experiments, samples were washed with deionized water to remove any non-adhesive impurities and small particles, and then dried at 105° C for 24 h to remove moisture.

5.4 Ion Exchange Experiments

Ion exchange experiments were performed in order to see the effect of different parameters on the ammonium uptake efficiency of clinoptilolite rich natural zeolites and to investigate the applicability of these minerals in the areas of wastewater treatment. In this part of study, initial concentration of the solution, particle size of the zeolite, solid: solution ratios, the presence of competing cation in the solution, pH of the solution were considered as parameters.

The ion exchange experiments were carried out in 250 ml cylindrical flask placed in thermostat shaker at 25 °C for 5 days. Kinetic ion exchange studies for ammonium were performed at 25°C for seven different initial concentrations. The equilibration procedure adopted was as follows: 2.5 gr samples of material were continuously shaken with 250 ml aliquots of ammonium chloride solution, having concentrations in the range 0-200 mg/L NH_4^+. The ammonium ion concentration of the samples were taken against the time and analyzed before and after equilibrium.

In order to compare the ammonium removal efficiency of with different solid: solution ratios, 10 mg/L NH_4^+ solution and 50 mg/L NH_4^+ were shaken at 170 ppm shaking speed with 2-0.85 mm particle size. 1%, 1.5%, 2% and 5% zeolite content was added to these solutions. After that, samples were taken against the certain time interval.

In the ion exchange experiment, three different particle sizes (2.8-2, 2-0.85 mm and 0.85-0.60 mm) were used to see the effect of particle size on the ammonium removal efficiency of zeolite. In this part of the study, 10 mg/L NH_4^+ solution and 50 mg/L NH_4^+ were shaken at 170 rpm shaking speed with 2.5 gr sample. After that, samples were collected at the certain time interval.

In order to establish the extent to which the presence of potassium, calcium and magnesium ions influenced ammonium ion uptake further equilibration experiments were conducted. These were confined to determination of the effect of each individual ion alone upon ammonium ion uptake. The starting solutions were dosed with the appropriate cation at a concentration of 30 mg/L and equilibration in the presence of ammonium ion repeated as before. In this part of the study, ammonium chloride solution with the presence of competing cation, which have the concentration in the range of 10-200 mg/lt, were shaken at 170 rpm shaking speed with 2.5 gr sample. After that, samples were taken against the certain time interval.

In the experiment, initial and equilibrium pH values were recorded. For specific experiments the pH was initially adjusted to fixed value with solutions of NaOH or H_2SO_4. To understand the effect of pH of the solution on the ammonium uptake capacity, different pH value was tested.

Experiments were conducted using the samples of treated domestic wastewater effluent using a clinoptilolite-rich natural zeolite. The average ammonium ion concentration in the wastewater effluent was measured as 40 mg/lt. After collecting samples, pH of the samples was adjusted in the range of 1.5-2 to preserve the composition of the samples. Prior to the ion exchange experiments, the pH values were raised to 7-7.5 using concentrated NaOH solution. After that, domestic wastewater samples were prepared to give ammonium concentrations of 5, 10, 15, 20, 30 and 40 mg/l by diluting treated wastewater samples with deionized water. After ion exchange experiment, BOD and COD values of the samples were measured to understand the effect of the clinoptilolite on the organic and inorganic matter.

In the COD test, the oxygen equivalent of the organic matter is calculated by using strong chemical oxidizing agent. Potassium dichromate is used for this purpose. The test must be performed at elevated temperature. Potassium dichromate was mixed with silver sulfate and sulfuric acid solution. Then, the solution was placed in furnace at 200 °C for 2 hours. After that, this solution was titrated with ferrous ammonium sulfate until the first red brown endpoint. The COD value of the domestic wastewater was calculated.

In BOD test, wastewater samples are placed in BOD test bottles. The samples are stored at a constant temperature of 20 °C. Common incubation period is five days. At the end of the incubation period, the BOD value of the domestic wastewater was calculated by automatically.

CHAPTER 6

RESULTS AND DISCUSSION

The ion exchange of ammonium ion on clinoptilolite was examined in batch mode experiments. Ion exchange experiments were carried out to investigate the equilibrium uptake of ammonium ion onto Gördes clinoptilolite by the presence of effective parameters. The effect of solid: solution ratio, particle size of the zeolite, initial concentration of the ammonium ion, competing cation such as potassium, calcium and magnesium ion on the ammonium ion uptake capacity and the percentage of ammonium removal efficiency were discussed. These effective parameters were given in Table 6.1.

In the experiment, the amount of ammonium accumulated on the clinoptilolite was calculated by the using equation 6.1 as the difference between the amount present in the initial ammonium concentration and that remaining in solution after equilibrium with the clinoptilolite. The kinetic curve of ammonium uptake Q(t) was determined by using the equation 6.2

$$Q = \frac{(C_0 - C_E) * V}{m} \qquad 6.1$$

$$Q(t) = \frac{(C_0 - C_{(t)}) * V}{m} \qquad 6.2$$

where;

Q : (mg/gr) is the ammonium uptake capacity

Q(t): (mg/gr) is the ammonium uptake capacity at time t

C_0: (mg/l) represents initial ammonium concentration

C(t):(mg/lt) represents ammonium concentration at time

C_E: (mg/l) represents equilibrium ammonium concentration

V: (l) volume of solution

m: (gr) mass of clinoptilolite

Ammonium removal efficiency was calculated by using the equation 6.3.

$$\% NH_4^+ = (\frac{C_0 - C_{eq}}{C_0}) * 100 \qquad 6.3$$

where C_0 and C_{eq} are the initial and equilibrium concentration of ammonium, mg/lt.

Table 6.1.Effective Parameters on the Ammonium Exchange Process

Effective Parameters	
Solid: Solution Ratio	1/100, 1/80,1/50, 1/20
Grain size (mm)	2.8-2.0 , 2.0-0.85,0.85-0.6
Initial Concentration(ppm)	10,30,50,70,100,150,200
Competing Cation	Ca^{+2}, K^+, Mg^{+2}
pH of the Solution	pH<7
Temperature	25 °C

6.1. The Effect of Solid: Solution Ratio:

In this part of the study, different solid: solution ratios (1:100, 1:80, 1:50, 1:20) were tested to investigate the ammonium uptake capacity and the ammonium removal efficiency of zeolites. A measured quantity of clinoptilolite sample (1% to 5%) was added to a vessel containing measured volume of ammonium chloride solutions (250 ml) at two different initial ammonium concentrations (10 and 50 mg/lt). Figure 6.1 and 6.2 show the change in ammonium concentration versus time for two different initial ammonium concentration and four different solid: solution ratios. According to the results; 10 mg/lt initial ammonium concentration decreased to 0.5 mg/lt with 1% solid: solution ratio, 0.42 mg/lt with % 1.25 solid: solution ratio, 0.28 mg/lt with 2 % solid: solution ratio and 0.1 mg/lt with 5 % solid: solution ratio. At higher concentration, 50 mg/lt initial ammonium concentration decreased to 6.5 mg/lt with 1% solid: solution ratio, 4.82 mg/lt with % 1.25 solid: solution ratio, 3.62 mg/lt with 2 % solid: solution ratio and 2.4 mg/lt with 5 % solid: solution ratio at the end of the shaking period.

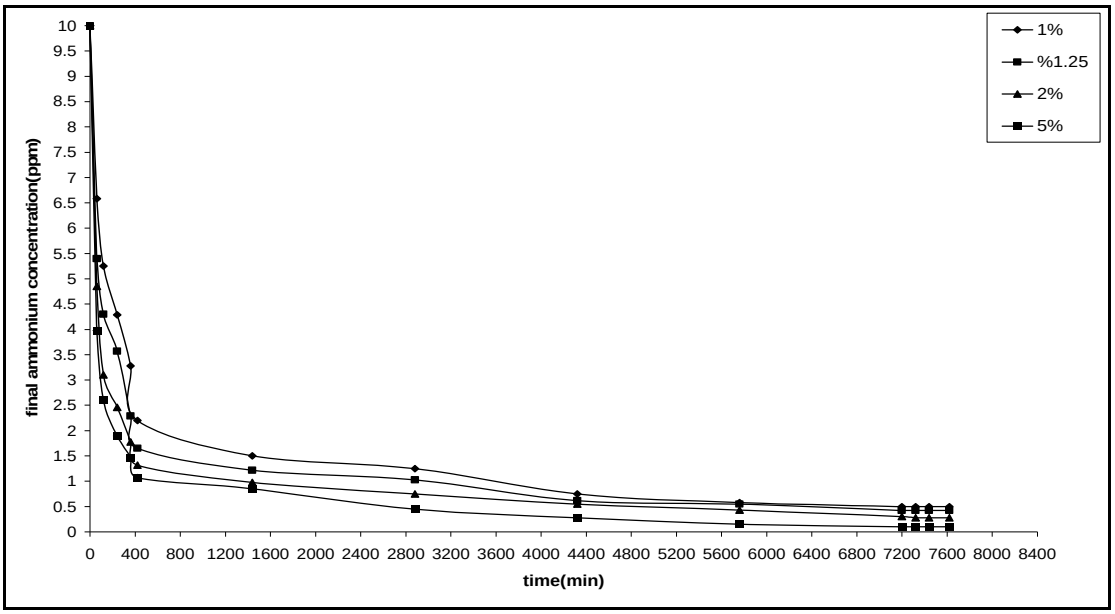

Figure 6.1. Change in NH_4^+ concentration with time for different solid: solution ratios. C_0= 10 mg/lt, particle size=2.0-0.85 mm, pH<7.0, shaking rate= 170 rpm, no competing cation.

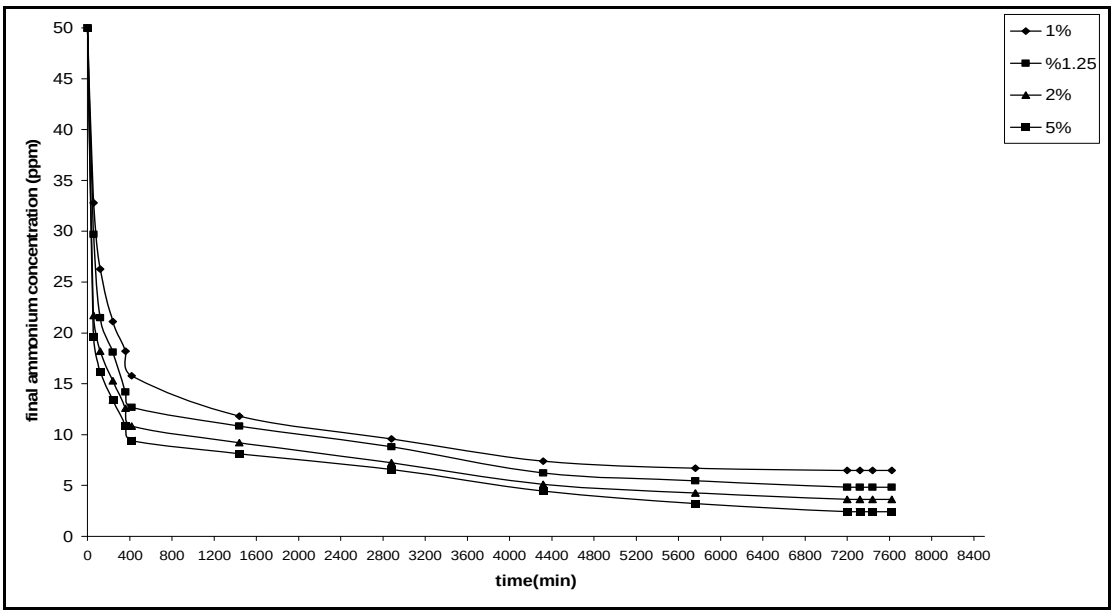

Figure 6.2. Change in NH_4^+ concentration with time for different solid: solution ratios. C_0= 50 mg/lt, particle size=2.0-0.85 mm, pH<7.0, shaking rate= 170 rpm, no competing cation.

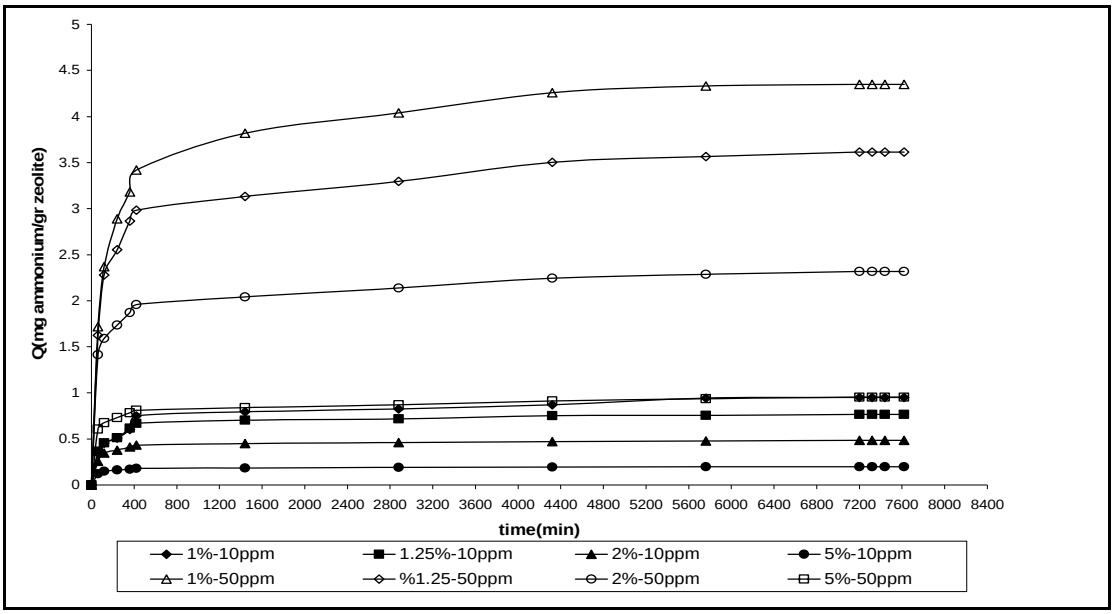

Figure 6.3. The kinetic curves of ammonium uptake for ammonium chloride solution at different initial ammonium ion concentrations and solid: solution ratios (initial ammonium ion concentrations: 10 mg/lt and 50 mg/lt, particle size=2.0-0.85 mm, pH<7.0, shaking rate= 170 rpm, no competing cation)

Figure 6.3 shows the batch kinetics of ammonium ion removal by plotting the ammonium uptake capacity versus time for two different initial ammonium concentrations and four different solid: solution ratios without any competing cations. The results obtained (Figure 6.3) show that ammonium uptake capacity and initial rate decreased with increasing the solid: solution ratios for different initial ammonium concentrations. Highest amount of ammonium removal per gram zeolite was found in the solution having 1% solid: solution ratio without competing cations.

Figure 6.4 and Figure 6.5 show the percent of ammonium ion removal versus time for four different solid: solution ratios and two different initial ammonium concentrations. When increasing the solid: solution ratio %1 to %5, the percent ammonium ion increases since for the same concentration more zeolite is available for exchange and hence more ammonium ion is removed. The increase in efficiency is expected result because of increasing the solid: solution contact surface. For example, 95 % and 99 % ammonium removal was observed with 1% and 5% solid: solution ratio for 10 ppm initial ammonium concentration. Komarowski and Yu had obtained similar results with the Australian clinoptilolite for different amount of zeolite addition. They have stated that 20 % and 80 % ammonium removal was observed with 1% and 5 %

content for 50 and 25 mg/lt initial ammonium concentration. Their results indicate that increasing the amount of zeolite cause higher ammonium removal.

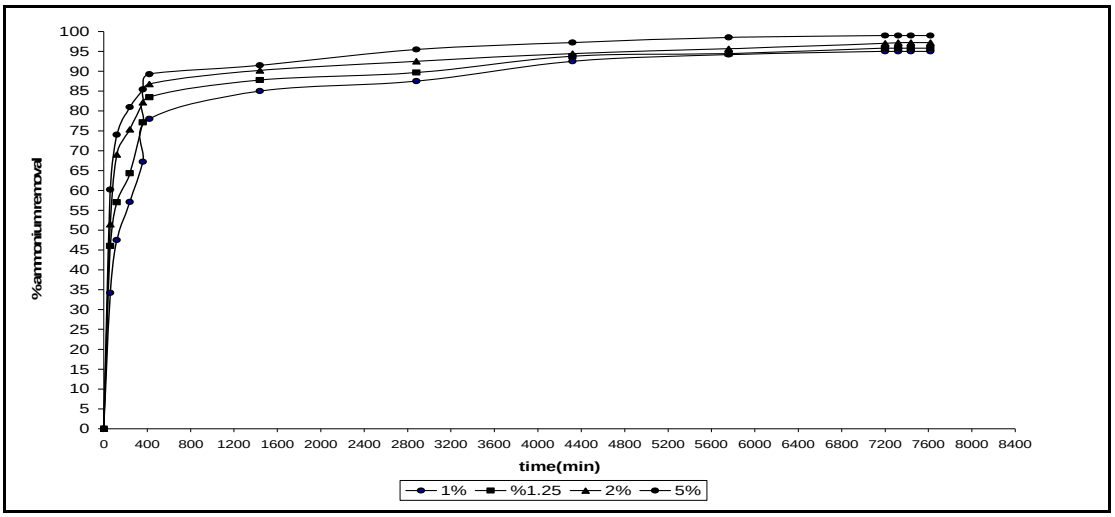

Figure 6.4. The percentage of removed ammonium ion with versus time for different solid: solution ratios %, C_0=10 mg/lt, particle size=2.0-0.85 mm, pH<7.0, shaking rate= 170 rpm.

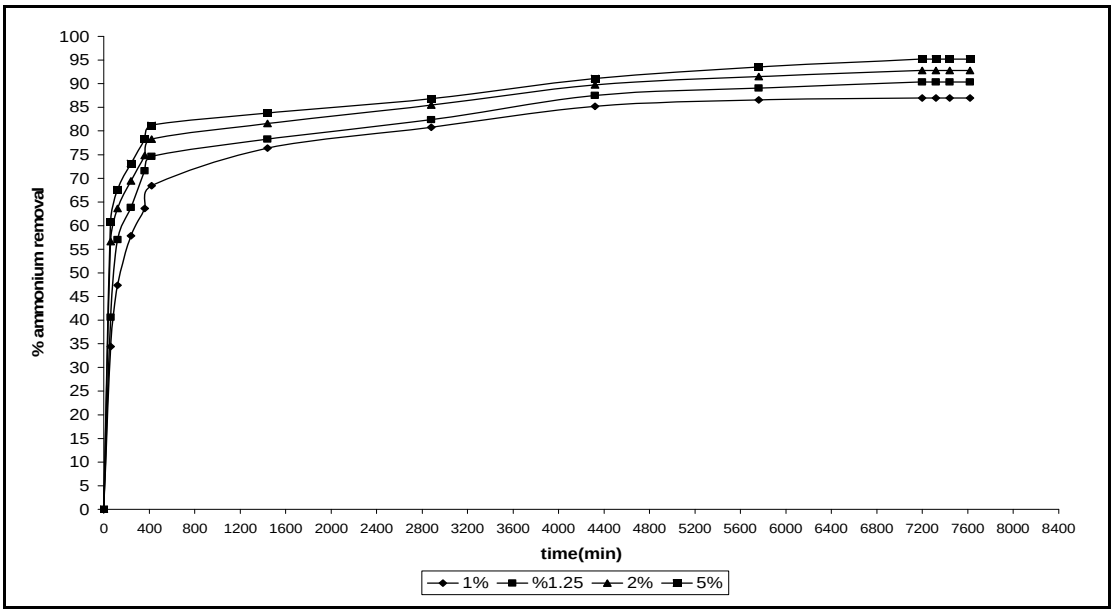

Figure 6.5. The percentage of removed ammonium ion with versus time for different solid: solution ratios %, C_0=50 mg/lt, particle size=2.0-0.85 mm, pH<7.0, shaking rate= 170 rpm.

The effect of the solid: solution ratios on the ammonium ion uptake were investigated in the presence of Ca^{+2} Mg^{+2} and K^{+}. Figure 6.6 and 6.7 shows the change in ammonium concentration versus time for two different initial ammonium concentration and four solid: solution ratios. As it can be seen from the Figure 6.6, 10

mg/lt initial ammonium concentration in the presence of potassium ion decreased to 1.4 mg/lt with 1% solid: solution ratio , 1 ppm 5% solid: solution ratio. And also, 10 mg/lt initial ammonium concentration in the presence of magnesium and calcium ion decreased to 0.90 and 1.1 mg/lt with 1% solid: solution ratio, 0.52 and 0.75 mg/lt 5 % solid: solution ratio, respectively at the end of the shaking period. At higher concentration, similar results were obtained for different solid: solution ratios.

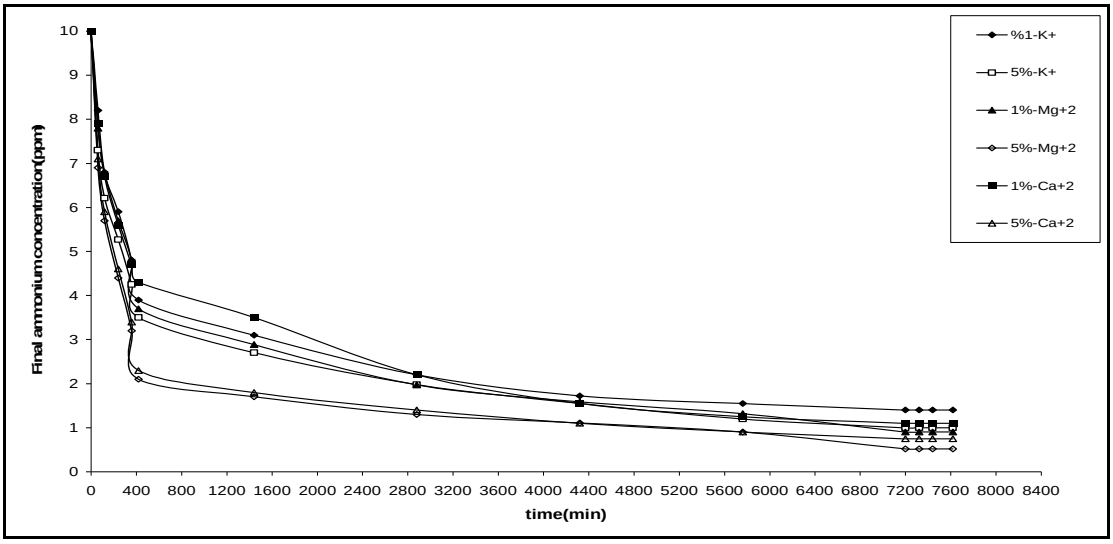

Figure 6.6. Change in NH_4^+ concentration with time for different solid: solution ratios. C_0= 10 mg/lt in the presence of Ca^{+2} Mg^{+2} and K^+, particle size: 2.0-0.85 mm, pH<7.0, shaking rate= 170 rpm.

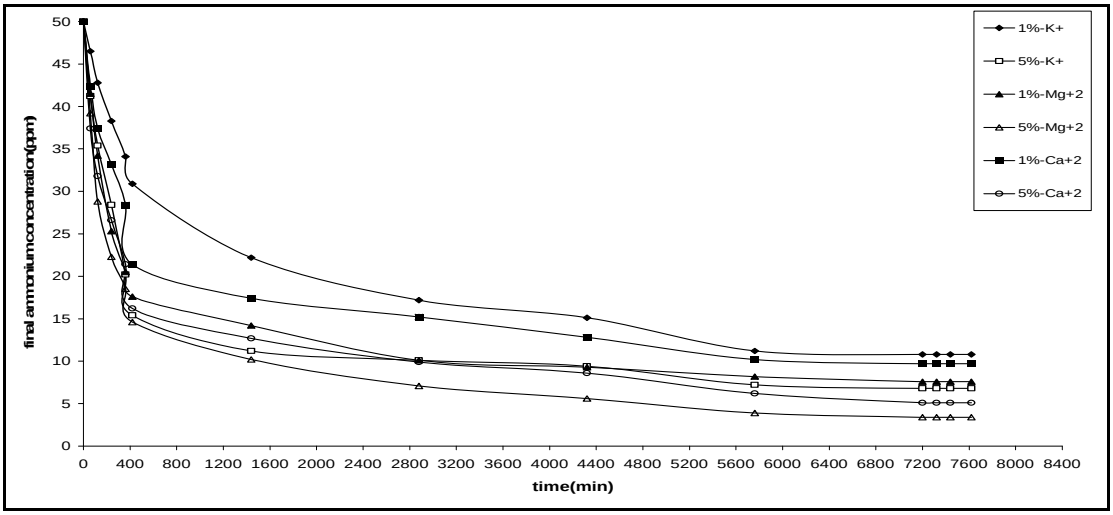

Figure 6.7. Change in NH_4^+ concentration with time for different solid: solution ratios. C_0= 50 mg/lt in the presence of Ca^{+2} Mg^{+2} and K^+, particle size: 2.0-0.85 mm, pH<7.0, shaking rate= 170 rpm.

Table 6.2 and 6.3 show the ammonium uptake capacity results with different %solid: solution ratios at two different initial ammonium concentrations in the presence

of competing cations. Highest amount of ammonium removal per gram zeolite was found in the solution having 1% zeolite content with competing cations. Similar to the previous experiments performed for without competing cations, ammonium uptake capacity decreased with increasing the solid: solution ratio.

Figure 6.8 and 6.9 show the percent ammonium removal versus time for % different solid: solution ratios with presence of Ca^{+2} Mg^{+2} and K^{+} at two different initial ammonium concentration. Similar to the previous experiments performed for without any competing cations, ammonium ion removal efficiency increases with increasing the amount of zeolite. For example, 86 % and 90 % ammonium removal was observed with 1% and 5% solid: solution ratio for 10 ppm initial ammonium concentration with the presence of potassium ion. And also, 91 % and 89 %, 94.8 % and 92.5 % ammonium removal was observed with 1% and 5% solid: solution ratio for 10 ppm initial ammonium concentration with the presence of magnesium and calcium ion, respectively. As it can be seen from the figures, ammonium removal increases with increasing the solid: solution ratio % 1 to 5 %. This is an expected result because of increasing the solid: solution contact surface.

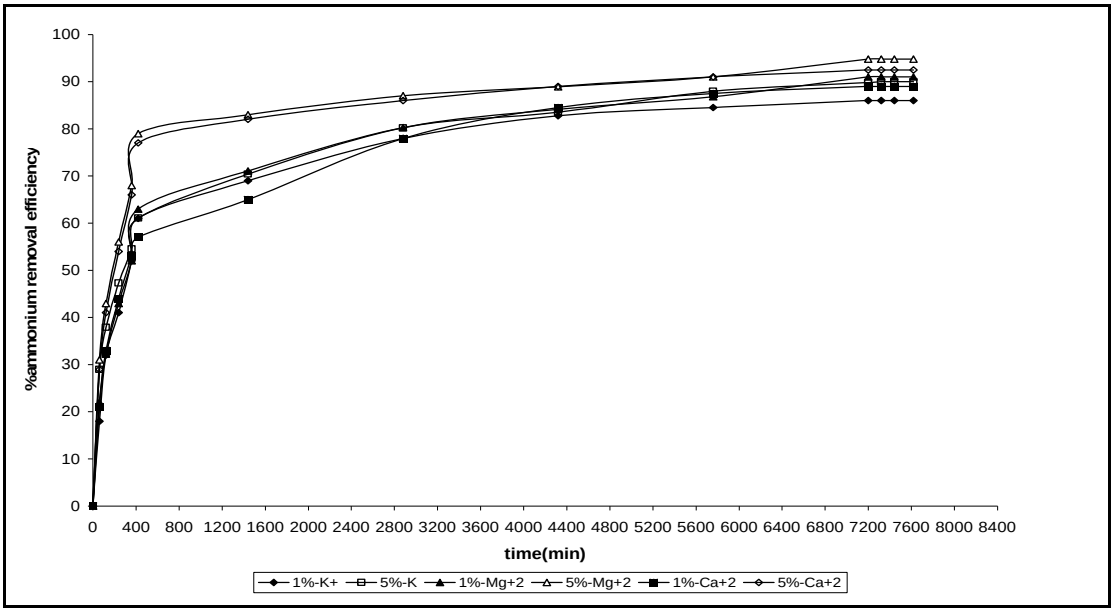

Figure 6.8. The percentage of removed ammonium ion with the presence of Ca^{+2} Mg^{+2} and K^{+} versus time for different solid: solution ratios %, C_0=10 mg/lt, particle size=2.0-0.85 mm, pH<7.0, shaking rate= 170 rpm.

Table 6.2. Ammonium uptake results with the presence of Ca^{+2}, Mg^{+2} and K^{+} for different solid: solution ratio %, C_0= 10 mg/lt, particle size=2.0-0.85 mm, pH<7.0, shaking rate= 170 rpm.

	NH_4^+		NH_4^+-K^+		NH_4^+-Mg^{+2}		NH_4^+-Ca^{+2}	
Time (min)	%1	% 5	%1	% 5	%1	% 5	%1	% 5
0	0	0	0	0	0	0	0	0
60	0.34	0.12	0.18	0.05	0.22	0.06	0.21	0.06
120	0.46	0.15	0.32	0.08	0.32	0.09	0.33	0.08
240	0.51	0.16	0.41	0.09	0.43	0.11	0.44	0.11
360	0.60	0.171	0.52	0.11	0.52	0.14	0.53	0.13
420	0.75	0.179	0.61	0.13	0.63	0.16	0.57	0.15
1440	0.79	0.183	0.69	0.15	0.71	0.17	0.65	0.16
2880	0.83	0.191	0.78	0.16	0.80	0.174	0.78	0.17
4320	0.87	0.194	0.83	0.17	0.84	0.178	0.85	0.18
5760	0.94	0.197	0.85	0.18	0.87	0.182	0.88	0.182
7200	0.95	0.198	0.86	0.18	0.91	0.19	0.89	0.185
7320	0.95	0.198	0.86	0.18	0.91	0.19	0.89	0.185
7440	0.95	0.198	0.86	0.18	0.91	0.19	0.89	0.185
7620	0.95	0.198	0.86	0.18	0.91	0.19	0.89	0.185

Table 6.3. Ammonium uptake results with the presence of Ca^{+2}, Mg^{+2} and K^{+} for different solid: solution ratio %, C_0= 50 mg/lt, particle size=2.0-0.85 mm, pH<7.0, shaking rate= 170 rpm.

	NH_4^+		NH_4^+-K^+		NH_4^+-Mg^{+2}		NH_4^+-Ca^{+2}	
Time (min)	%1	% 5	%1	% 5	%1	% 5	%1	% 5
0	0	0	0	0	0	0	0	0
60	1.72	0.61	0.35	0.18	0.85	0.22	0.76	0.25
120	2.37	0.68	0.72	0.29	1.58	0.42	1.26	0.36
240	2.89	0.73	1.17	0.43	2.47	0.55	1.68	0.47
360	3.18	0.78	1.59	0.60	2.95	0.63	2.16	0.57
420	3.42	0.81	1.91	0.69	3.24	0.71	2.86	0.68
1440	3.82	0.84	2.78	0.78	3.58	0.80	3.26	0.75
2880	4.04	0.87	3.28	0.80	3.99	0.86	3.48	0.80
4320	4.26	0.91	3.49	0.81	4.07	0.89	3.72	0.83
5760	4.33	0.94	3.88	0.86	4.18	0.92	3.98	0.88
7200	4.35	0.95	3.92	0.86	4.24	0.93	4.03	0.90
7320	4.35	0.95	3.92	0.86	4.24	0.93	4.03	0.90
7440	4.35	0.95	3.92	0.86	4.24	0.93	4.03	0.90
7620	4.35	0.95	3.92	0.86	4.24	0.93	4.03	0.90

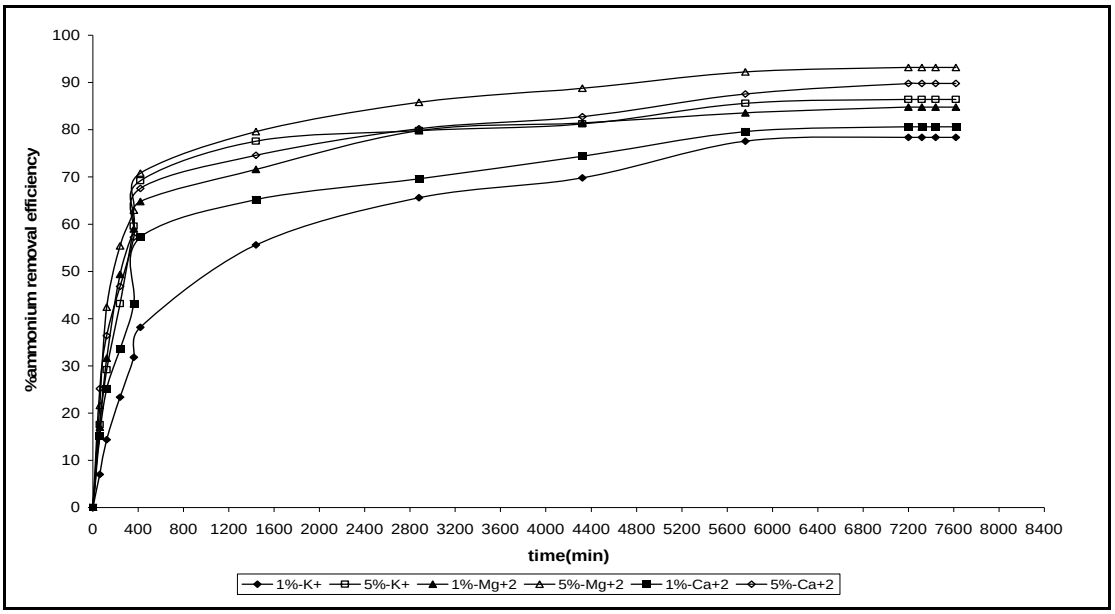

Figure 6.9. The percentage of removed ammonium ion with the presence of Ca^{+2} Mg^{+2} and K^{+} versus time for different solid: solution ratios %, C_0=50 ppm, particle size=2.0-0.85 mm, pH<7.0, shaking rate= 170 rpm.

6.2. The Effect of Grain Size:

In this study, three different particle sizes (2-2.8, 2-0.85, 0.85-0.6 mm) and two different initial ammonium ion concentrations (10 and 50 ppm) were used to see the effect of particle size on the ammonium removal efficiency of zeolite. The results were given in Figure 6.10-6.14 to show the changes in final ammonium concentration, percent ammonium removal and ammonium removal per gram of zeolite (Q) as a function of time for two different particle sizes of the zeolite. According to the results, 10 mg/lt initial concentration decreased to 0.5 mg/lt with 2-2.8, 2-0.85 and 0.85-0.6 mm particle size of zeolites. At the end of the shaking period, 50 mg/lt initial concentration decreased to 6.5 mg/lt with 2-2.8, 2-0.85 and 0.85-0.6 mm particle size of zeolites. Figure 6.10 and 6.11 shows the effect of different particle sizes on the equilibrium time of clinoptilolite, which was longer as the clinoptilolite particle size was larger. The results show that the particle size of the clinoptilolite did not affect the equilibrium ammonium concentration.

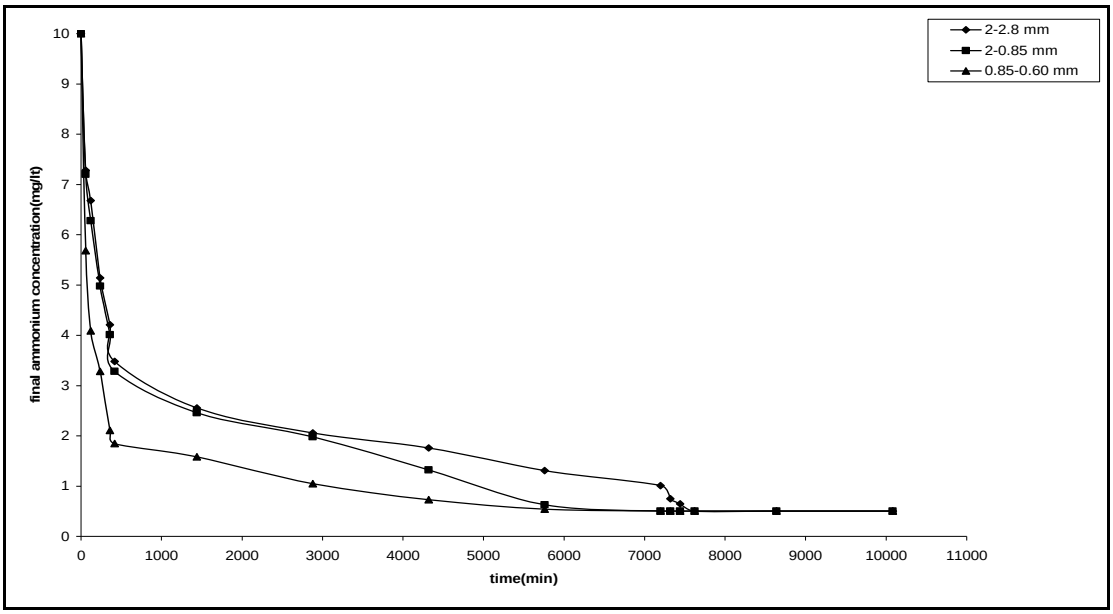

Figure 6.10. Change in NH_4^+ concentration with time for different particle sizes of the zeolite. C_0= 10 mg/lt, 1% solid: solution ratio, pH<7.0, shaking rate= 170 rpm, no competing cation.

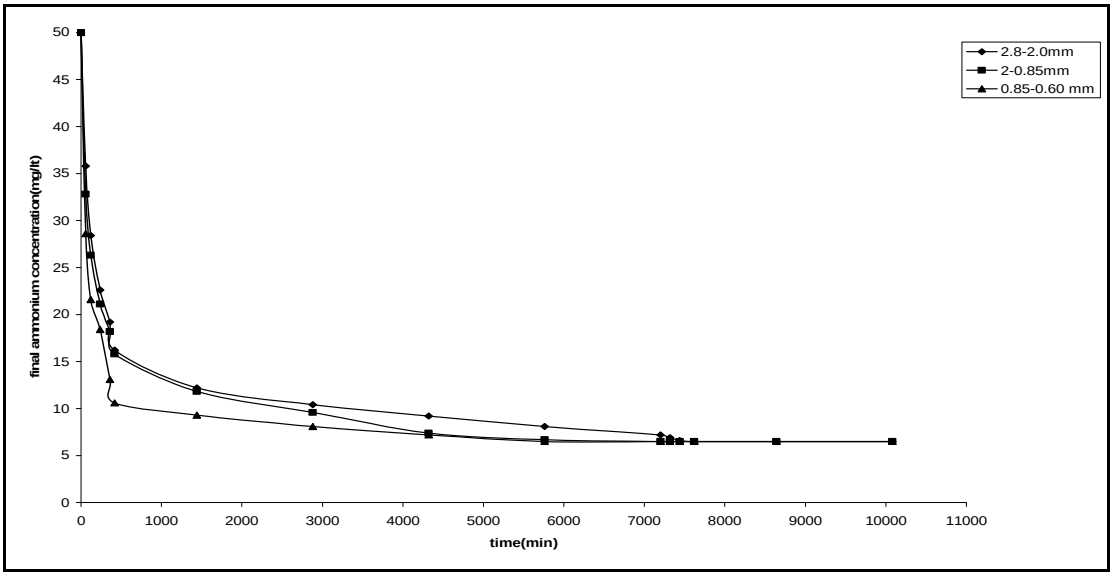

Figure 6.11. Change in NH_4^+ concentration with time for different particle sizes of the zeolite. C_0= 50 mg/lt, 1% zeolite content, pH<7.0, shaking rate= 170 rpm, no competing cation.

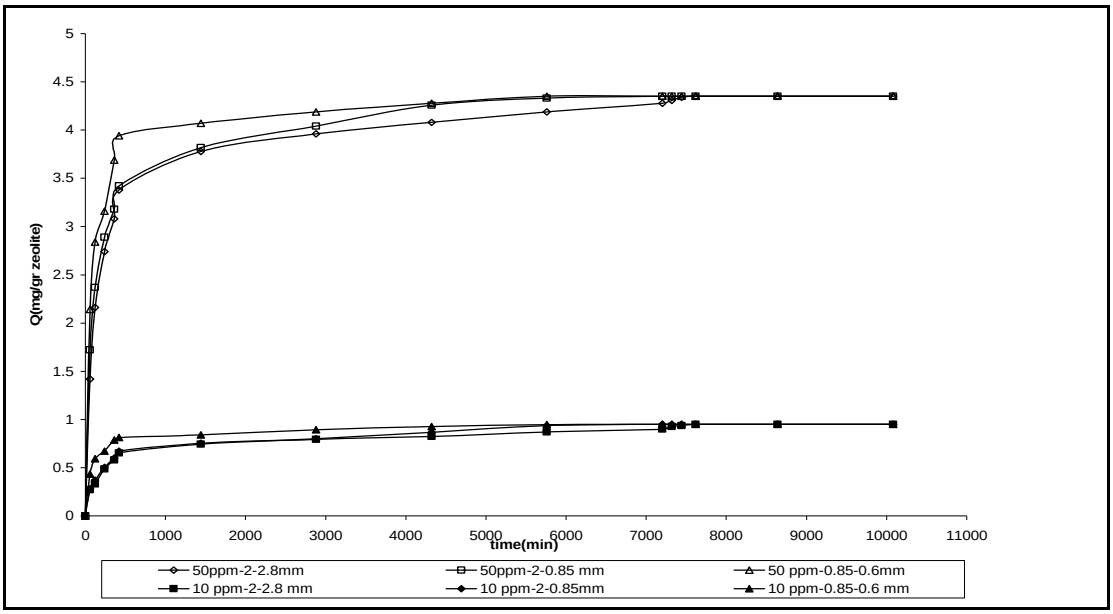

Figure 6.12. The kinetic curves of ammonium uptake for ammonium chloride solution at different initial ammonium ion concentrations and different particle size of the zeolite (initial ammonium ion concentration: 10 mg/lt and 50 mg/lt, 1% solid: solution ratio, pH<7.0, shaking rate= 170 rpm, no competing cation)

Figure 6.12 shows the batch kinetics of ammonium ion removal by plotting the ammonium uptake capacity versus time for two different initial ammonium concentrations and two particle sizes of the zeolite without any competing cations. Experimental results show that ammonium uptake capacity (Q) was independent of the particle size of the clinoptilolite. At the end of the shaking period, ammonium uptake capacity values were found to be 0.95 mg/gr zeolite for the samples with 2.8-2, 2-0.85, 0.85-0.6 mm particle size at low initial ammonium concentration, respectively. Same results were obtained for the higher ammonium concentration. Booker et al., (1996) had obtained similar results with the Australian clinoptilolite for different particle sizes of zeolite. They have stated that ammonium uptake capacity was observed 0.88 mg/gr with 1-1.2, 1-0.85, 0.85-0.60 mm particle size for 25 ppm initial ammonium concentration. At higher concentration, ammonium uptake capacity values were found to be 3.9 mg/ gr with 1-1.2, 1-0.85, 0.85-0.60 mm particle size. Their results indicate that ammonium uptake capacity was independent of the particle size of the zeolite. Our experimental results are coinciding with their studies.

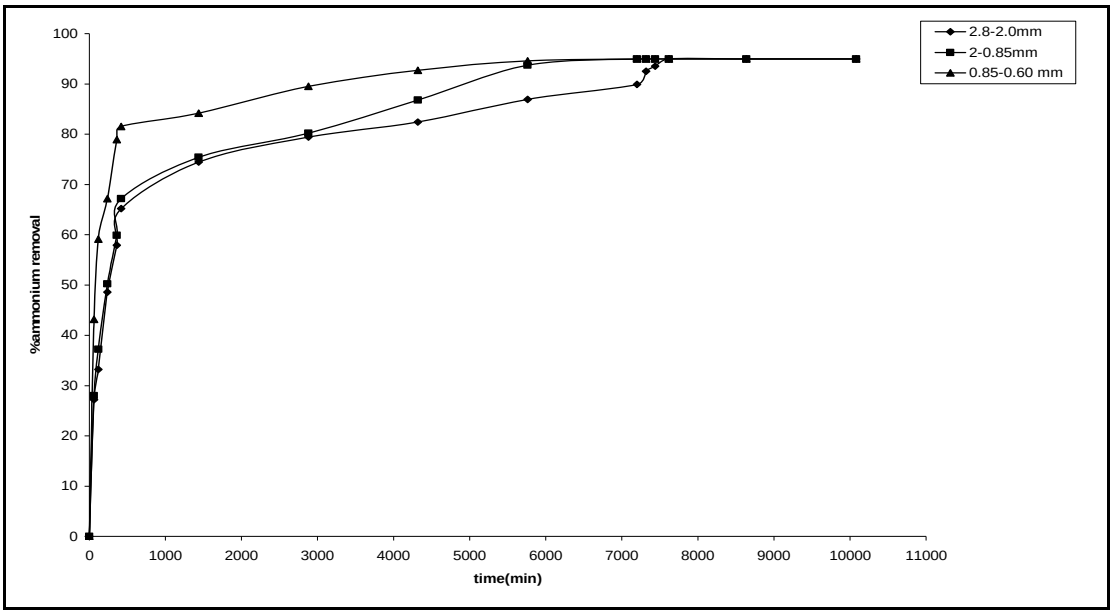

Figure 6.13. The percentage of removed ammonium ion versus time for different particle sizes, C_0:10 mg/lt, 1% solid: solution ratio, pH<7.0, shaking rate= 170 rpm, no competing cation]

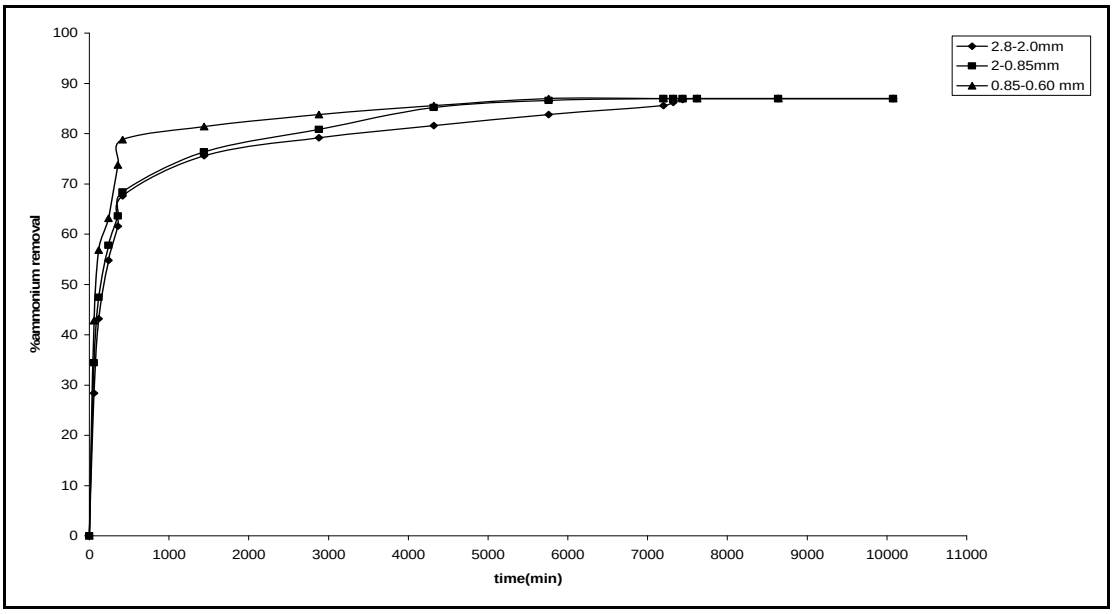

Figure 6.14. The percentage of removed ammonium ion versus time for different particle sizes, C_0:50 mg/lt, 1% solid: solution ratio, pH<7.0, shaking rate= 170 rpm, no competing cation]

Figure 6.13 and Figure 6.14 shows the percent ammonium removal versus time for three different particle sizes of the zeolite and two different initial ammonium

concentrations. For instance, 95 % ammonium removal was observed with 2-2.8, 2-0.85, 0.85-0.60 mm particle size for 10 ppm initial ammonium concentration. The results show that the particle size of the clinoptilolite did not affect the percent of ammonium removal. Total surface area of the clinoptilolite takes into account both external surface area of the particle and its internal surface area. The internal surface area is due to the pores and channels of the clinoptilolite. When reducing the particle size, the external surface area is considerably but not the internal surface area. In porous materials, the contribution of the external surface area to total surface area is very slight and for this reason, size reduction increases the total surface area very slight. Based on above, it can be assumed that the ammonium exchange capacity is not dependent on the particle size of zeolite since most of cationic sites are located inside the pores of the zeolitic rock and the channels and cavities of zeolite crystalline structure. Considering spherical geometry for these particle sizes, the external surface area increases from the coarser to the finer particles. The internal area should not change significantly with the particle size. It can be concluded that the external surface area of clinoptilolite has an insignificant role in cation retention and that the internal sites are responsible for the cation exchange.

As comprehended from the results, the particle size of the clinoptilolite did not affect ammonium removal capacity and the percent of ammonium removal but only reflected the initial uptake rate. Initial uptake constants (Discussed in Chapter 4.6) were calculated for three different particle sizes of the zeolite. Table 6.4 indicate that the effect of the particle size on uptake rate constant (k). Uptake rate constants for different particle size were in the range of 0.03-0.182 $mg.gr^{-1}.min^{-0.5}$. The results indicate that smaller particle size of the clinoptilolite shows the more rapid initial uptake rate.

Table 6.4.Initial uptake rate, k ($mg.gr^{-1}.min^{-0.5}$) values for different particle size of the clinoptilolite.

Particle size (mm)	C_0=10 mg/lt	C_0=50 mg/lt
2.8-2	0.031	0.161
2-0.85	0.032	0.162
0.85-0.6	0.039	0.182

Effective diffusion coefficients were calculated from the experimental uptake curves (Discussed in Chapter 4.6). Table 6.5 gives the effective diffusion coefficient

obtained for various particle sizes. It can be seen that effective diffusion coefficient values slightly change with different particle size of the zeolite. Booker et al., (1996) was calculated the effective diffusion coefficient for different particle sizes of the Na-clinoptilolite. In their study, effective diffusion coefficient values were determined in the range of 3.21-3.49 $*10^{-12}$ for 1.2-1, 1-0.85, 0.85-0.6 mm particle size of the clinoptilolite. Their results show that particle size did not affect on the effective diffusion coefficient values. Our experimental results are coinciding with their studies.

Table 6.5. Effective Diffusion Coefficient for different particle sizes of clinoptilolite.

Particle size (mm)	Effective Diffusion Coefficient$*10^{12}$ (m^2/sec)
2.8-2	1.44
2-0.85	2.02
0.85-0.6	2.22

The effect of particle sizes of the zeolite on the ammonium ion uptake was investigated with the presence of Ca^{+2} Mg^{+2} and K^{+}. Table 6.6 and 6.7 shows the change in ammonium concentration versus time for two different initial ammonium concentration and different particle size of the zeolite. According to these tables, 10 mg/lt initial ammonium concentration with the presence of potassium ion decreased to 1.4 mg/lt with 2-2.8, 2-0.85, 0.85-0.6 mm particle size. At the end of the shaking period, 10 mg/lt initial ammonium concentration with the presence of magnesium and calcium ion decreased to 0.90 and 1.1 mg/lt with 2-2.8, 2-0.85, 0.85-0.6 mm particle size. At higher concentration, 50 mg/lt initial ammonium concentration with the presence of potassium ion decreased to 10.8 mg/lt with 2-2.8, 2-0.85, 0.85-0.6 mm particle size. Also, 50 mg/lt initial ammonium concentration with the presence of magnesium and calcium ion decreased to 7.6 and 9.7 ppm with 2-2.8, 2-0.85, 0.85-0.6 mm particle size, respectively.

Table 6.8 and 6.9 show the ammonium uptake capacity results with different particle size of zeolite for two different initial ammonium concentrations with presence of competing cations. Similar to the previous experiments performed for without competing cations, ammonium uptake capacity and percent of ammonium removal was independent of the particle sizes of the clinoptilolite. For example, 86 % ammonium removal was observed with 2-2.8, 2-0.85, 0.85-0.6 mm particle size for 10 mg/lt initial ammonium concentration with the presence of potassium ion. At the end of the shaking

Table 6.6. Change in NH_4^+ concentration with time for different particle sizes of the zeolite.C_0= 10 ppm with the presence of Ca^{+2}, Mg^{+2} and K^+, 1% solid: solution ratio, pH<7.0, shaking rate= 170 rpm.

	NH_4^+-K^+			NH_4^+-Mg^{+2}			NH_4^+-Ca^{+2}		
Time (min)	2-2.8 (mm)	2-.0.85 (mm)	0.85-0.6 (mm)	2-2.8 (mm)	2-.0.85 (mm)	0.85-0.6 (mm)	2-2.8 mm	2-.0.85 (mm)	0.85-0.6 (mm)
0	10	10	10	10	10	10	10	10	10
60	8.6	8.2	7.21	7.9	7.80	6.42	8.1	7.9	6.78
120	7.2	6.8	5.45	6.82	6.78	5.04	6.92	6.7	5.22
240	6.2	5.9	4.25	5.85	5.7	4.08	5.81	5.6	4.12
360	5.1	4.8	3.15	4.85	4.8	3.04	4.85	4.7	3.05
420	4.1	3.9	2.12	3.74	3.7	2.02	4.34	4.3	2.09
1440	3.2	3.1	1.75	2.92	2.89	1.58	3.65	3.5	1.63
2880	2.32	2.2	1.63	2.04	1.97	1.28	2.34	2.2	1.34
4320	1.85	1.72	1.45	1.75	1.59	1.02	1.75	1.55	1.25
5760	1.68	1.55	1.4	1.55	1.32	0.9	1.55	1.25	1.1
7200	1.52	1.4	1.4	1.22	0.9	0.9	1.32	1.1	1.1
7320	1.48	1.4	1.4	1.05	0.9	0.9	1.22	1.1	1.1
7440	1.42	1.4	1.4	0.98	0.9	0.9	1.12	1.1	1.1
7620	1.4	1.4	1.4	0.9	0.9	0.9	1.1	1.1	1.1
8640	1.4	1.4	1.4	0.9	0.9	0.9	1.1	1.1	1.1
10080	1.4	1.4	1.4	0.9	0.9	0.9	1.1	1.1	1.1

Table 6.7. Change in NH_4^+ concentration with time for different particle sizes of the zeolite.C_0= 50 ppm with the presence of Ca^{+2}, Mg^{+2} and K^+, 1% solid: solution ratio, pH<7.0, shaking rate= 170 rpm.

	NH_4^+-K^+			NH_4^+-Mg^{+2}			NH_4^+-Ca^{+2}		
Time (min)	2-2.8 (mm)	2-.0.85 (mm)	0.85-0.6 (mm)	2-2.8 (mm)	2-.0.85 (mm)	0.85-0.6 (mm)	2-2.8 mm	2-.0.85 (mm)	0.85-0.6 (mm)
0	50	50	50	50	50	50	50	50	50
60	48.2	46.5	40.2	44.2	41.5	38.4	44.4	42.4	39.2
120	43.4	42.8	35.6	36.4	34.2	29.2	39.4	37.4	32.6
240	39.8	38.3	30.2	29.8	25.3	22.4	35.2	33.2	25.3
360	35.3	34.1	24.6	22.3	20.5	19.4	30.4	28.4	17.2
420	31.9	30.9	18.2	19.9	17.6	14.8	23.4	21.4	14.5
1440	24.2	22.2	15.3	16.2	14.2	10.8	19.4	17.4	12.1
2880	18.2	17.2	12.5	12.2	10.1	9.2	16.2	15.2	10.6
4320	16.8	15.1	11.2	11.8	9.3	8.3	14.8	12.8	9.9
5760	13.2	11.2	10.8	10.2	8.2	7.6	13.5	10.2	9.7
7200	12.6	10.8	10.8	9.2	7.6	7.6	11.2	9.7	9.7
7320	11.6	10.8	10.8	8.4	7.6	7.6	10.2	9.7	9.7
7440	11.2	10.8	10.8	7.8	7.6	7.6	9.9	9.7	9.7
7620	10.8	10.8	10.8	7.6	7.6	7.6	9.7	9.7	9.7
8640	10.8	10.8	10.8	7.6	7.6	7.6	9.7	9.7	9.7
10080	10.8	10.8	10.8	7.6	7.6	7.6	9.7	9.7	9.7

Table 6.8. Ammonium uptake results with the presence of Ca^{+2}, Mg^{+2} and K^{+} for different particle size of the zeolite C_0= 10 ppm, particle size=2.0-0.85 mm, pH<7.0, shaking rate= 170 rpm.

	NH_4^+-K^+			NH_4^+-Mg^{+2}			NH_4^+-Ca^{+2}		
Time (min)	2-2.8 (mm)	2-.0.85 (mm)	0.85-0.6 (mm)	2-2.8 (mm)	2-.0.85 (mm)	0.85-0.6 (mm)	2-2.8 mm	2-.0.85 (mm)	0.85-0.6 (mm)
0	0	0	0	0	0	0	0	0	0
60	0.14	0.18	0.28	0.21	0.22	0.358	0.19	0.21	0.322
120	0.28	0.32	0.45	0.318	0.322	0.496	0.308	0.33	0.478
240	0.38	0.41	0.575	0.415	0.43	0.592	0.419	0.44	0.588
360	0.49	0.52	0.69	0.515	0.52	0.696	0.515	0.53	0.695
420	0.59	0.61	0.79	0.626	0.63	0.798	0.566	0.57	0.791
1440	0.68	0.69	0.83	0.708	0.711	0.842	0.635	0.65	0.837
2880	0.768	0.78	0.84	0.796	0.803	0.872	0.766	0.78	0.866
4320	0.815	0.828	0.855	0.825	0.841	0.898	0.825	0.845	0.875
5760	0.832	0.845	0.86	0.845	0.868	0.91	0.845	0.875	0.89
7200	0.848	0.86	0.86	0.878	0.91	0.91	0.868	0.89	0.89
7320	0.852	0.86	0.86	0.895	0.91	0.91	0.878	0.89	0.89
7440	0.858	0.86	0.86	0.902	0.91	0.91	0.888	0.89	0.89
7620	0.86	0.86	0.86	0.91	0.91	0.91	0.89	0.89	0.89
8640	0.86	0.86	0.86	0.91	0.91	0.91	0.89	0.89	0.89
10080	0.86	0.86	0.86	0.91	0.91	0.91	0.89	0.89	0.89

Table 6.9. Ammonium uptake results with the presence of Ca^{+2}, Mg^{+2} and K^{+} for different particle size of the zeolite C_0= 50 ppm, particle size=2.0-0.85 mm, pH<7.0, shaking rate= 170 rpm.

	NH_4^+-K^+			NH_4^+-Mg^{+2}			NH_4^+-Ca^{+2}		
Time (min)	2-2.8 (mm)	2-.0.85 (mm)	0.85-0.6 (mm)	2-2.8 (mm)	2-.0.85 (mm)	0.85-0.6 (mm)	2-2.8 mm	2-.0.85 (mm)	0.85-0.6 (mm)
0	0	0	0	0	0	0	0	0	0
60	0.18	0.35	0.98	0.58	0.85	1.16	0.56	0.76	1.08
120	0.66	0.72	1.44	1.36	1.58	2.08	1.06	1.26	1.74
240	1.02	1.17	1.98	2.02	2.47	2.76	1.48	1.68	2.47
360	1.47	1.59	2.54	2.77	2.95	3.06	1.96	2.16	3.28
420	1.81	1.91	3.18	3.01	3.24	3.52	2.66	2.86	3.55
1440	2.58	2.78	3.47	3.38	3.58	3.92	3.06	3.26	3.79
2880	3.18	3.28	3.75	3.78	3.99	4.08	3.38	3.48	3.94
4320	3.32	3.49	3.88	3.82	4.07	4.17	3.52	3.72	4.01
5760	3.68	3.88	3.92	3.98	4.18	4.24	3.65	3.98	4.03
7200	3.74	3.92	3.92	4.08	4.24	4.24	3.88	4.03	4.03
7320	3.84	3.92	3.92	4.16	4.24	4.24	3.98	4.03	4.03
7440	3.88	3.92	3.92	4.22	4.24	4.24	4.01	4.03	4.03
7620	3.92	3.92	3.92	4.24	4.24	4.24	4.03	4.03	4.03
8640	3.92	3.92	3.92	4.24	4.24	4.24	4.03	4.03	4.03
10080	3.92	3.92	3.92	4.24	4.24	4.24	4.03	4.03	4.03

period, 91 % and 89 % ammonium removal was observed with 2-2.8, 2-0.85, 0.85-0.6 mm particle size for 10 mg/lt initial ammonium concentration with the presence of magnesium and calcium ion, respectively. Our experimental results indicate that particle size of the zeolite did not effect on the ammonium exchange in the presence of competing cations.

6.3. The Effect of Initial Ammonium Concentration:

This experiment was performed to see the effect of the initial ammonium concentration on the ammonium ion exchange process. For this reason, eight different initial ammonium concentrations (10, 30, 50, 70, 100, 150,200 and 300 mg/lt) were used. The reason for working with different concentrations of ammonium chloride solution is to construct the equilibrium isotherm for the determination of the equilibrium behaviour of the system. Figure 6.15 shows the change in ammonium concentration versus time for different initial ammonium concentrations.

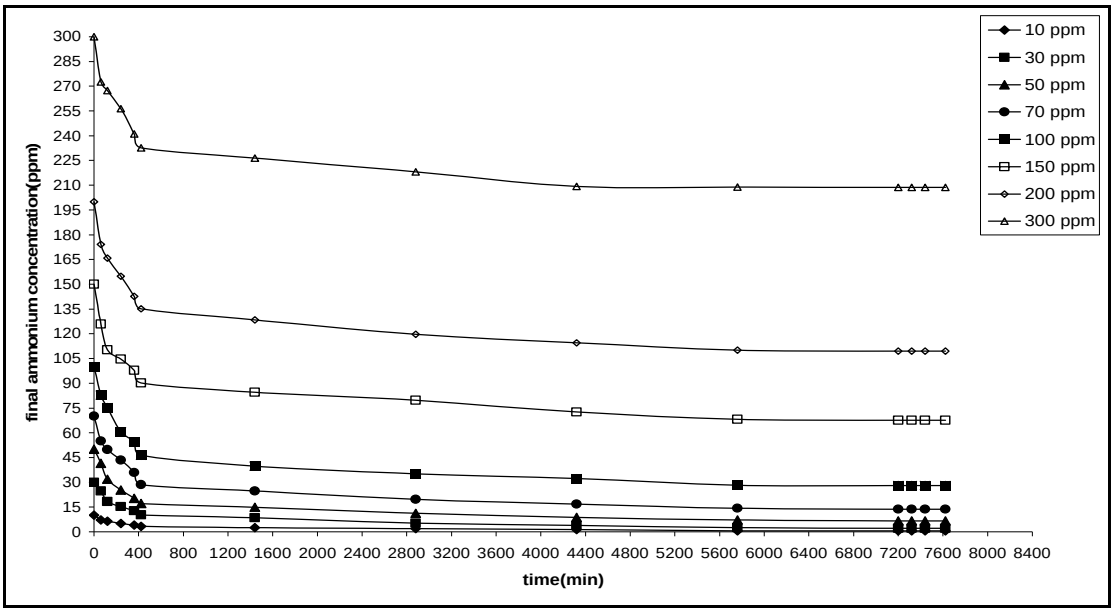

Figure 6.15. Change in NH_4^+ concentration with time for different initial ammonium concentrations, 1% solid: solution ratio, particle size= 2-0.85 mm, pH<7.0, shaking rate= 170 rpm, no competing cation

Figure 6.16 shows the batch kinetics of ammonium ion removal by plotting the ammonium uptake capacity versus time for different initial ammonium concentrations without any competing cations. Experimental results show that the ammonium uptake

capacity increases with increasing initial ammonium concentration. The initial ammonium concentration provides the necessary driving force to overcome all mass-transfer resistances of ammonium between the aqueous and solid phases. Hence, higher initial ammonium concentration will have a beneficial effect on the exchange capacity. Such an effect was clearly shown in Figure 6.16. The ammonium uptake capacity seems to increase essentially linearly with an increase in the ammonium concentration. The uptake rate of ammonium by clinoptilolite was initially fast in the 400 min depending on the initial concentration. After 400 min, the ammonium uptake rate decreases with increasing the contact time. Finally, the uptake rate approaches zero when equilibrium is attained. These changes in the rate of ammonium uptake could be due to the fact that, all exchange sites of the clinoptilolite were vacant. Afterwards, the ammonium uptake rate by the clinoptilolite decreased significantly, due to decrease in exchange sites. A decreasing removal rate, particularly towards the end of the experiment, indicated a possible monolayer of ammonium ions on the outer surface and pores of the zeolite and pore diffusion onto the inner surface of zeolite particles through the film due to continuous agitation maintained during the experiment.

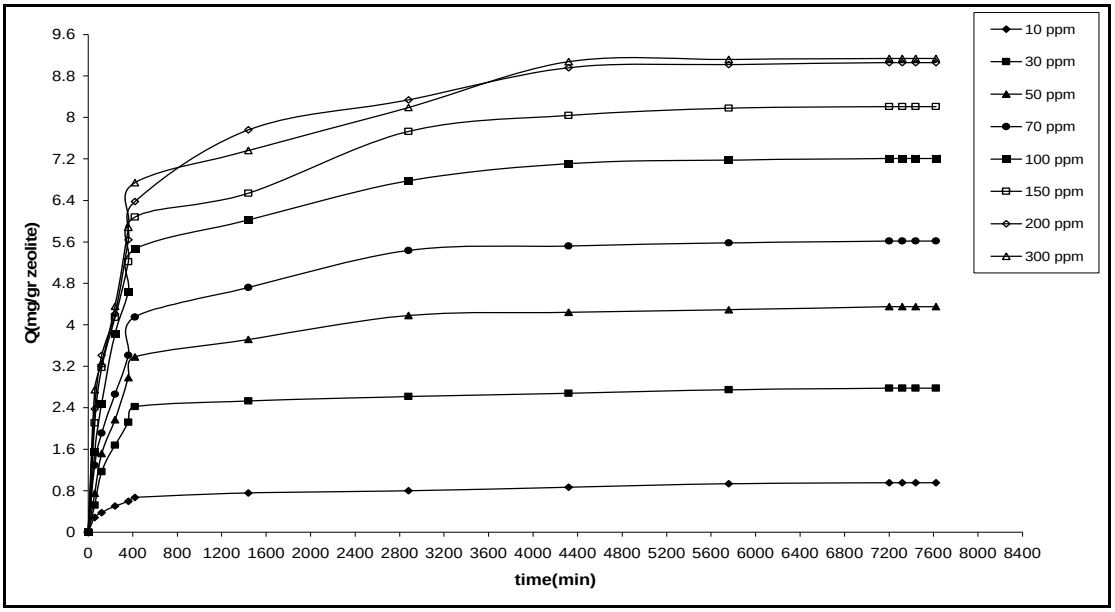

Figure 6.16. The kinetic curves of ammonium uptake for ammonium chloride solution at different initial ammonium ion concentrations, 1% solid: solution ratio, particle size: 2-0.85 mm, pH<7.0, shaking rate= 170 rpm, no competing cation.

To understand the initial concentration effect on the intraparticle diffusion rate constants ammonium removal capacity versus square time was plotted. Initial uptake rate constant values for different initial concentration were tabulated in Table 6.10. Table 6.10 indicates that the effect of the initial concentration on initial uptake rate constant (k). Initial uptake constants for pure ammonium chloride solution were in the range of 0.03-0.3112 $mg.gr^{-1}.min^{-0.5}$. The more concentrated solution shows the more rapid initial uptake rate. This may be due to a greater driving force with increasing initial ammonium ion concentration.

Table 6.10. Initial uptake rate, k ($mg.gr^{-1}.min^{-0.5}$) values for different initial ammonium ion concentration.

C_0 (ppm)	Initial rate constant ($mg.gr^{-1}.min^{-0.5}$)
10	0.0317
30	0.0969
50	0.1643
70	0.1897
100	0.2571
150	0.279
200	0.3043
300	0.3112

Effective diffusion coefficients were calculated from the experimental uptake curves. Effective diffusion coefficient values were given in Table 6.11. It is noticed that; effective diffusion coefficients for ammonium ion slightly change with different initial concentration. Effective diffusion coefficients reported previously in the literature were tabulated in Table 6.12. Our experimental results are coinciding with literature studies.

Table 6.11. Effective Diffusion Coefficients calculated from the Experimental Uptake Curve for NH_4^+ exchange

C_0 (ppm)	D_e (m^2/sec)*10^{12}
10	2.02
30	2.10
50	2.18
70	2.28
100	3.08
150	3.29
200	3.70
300	4.11

Table 6.12. Effective diffusion coefficients reported previously in the literature

Initial NH_4^+ Concentration (mg/lt)	Explanation	Effective Diffusion Coefficient*10^{-12}	References
6.7-1199	Na-form Clinoptilolite 4.76 mm	220-3.974	Alsoy, 1993
6.7-336.6	Na-form Clinoptilolite 4.76-3.36, 1.19-0.84	4-5	Suzuki, 1996
25-50	Na-form Clinoptilolite 1.2-1,1-0.85, 0.425-0.6 mm	3.26-3.49	Booker, 1996

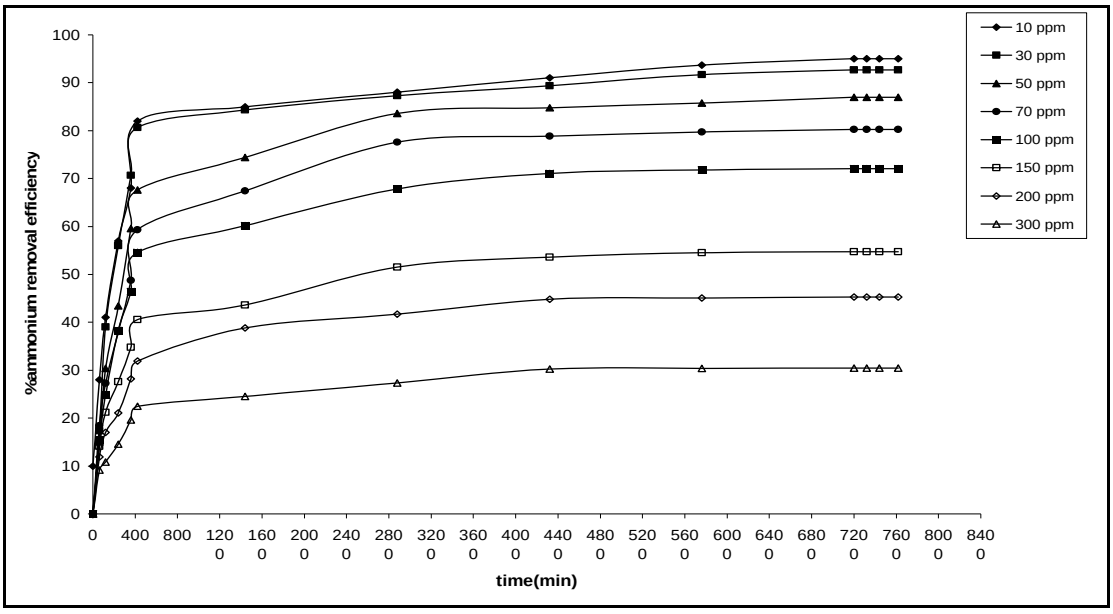

Figure 6.17. The percentage of removed ammonium ion versus time for different initial ammonium concentrations, % 1 solid: solution ratio, particle size=2.0-0.85 mm, pH<7.0, shaking rate= 170 rpm, no competing cation.

Figure 6.17 shows the percent ammonium removal versus time for different initial ammonium concentration without any competing cations. For instance, the higher NH_4^+ ion concentrations show the 30.5-55 % removal. Also, lower NH_4^+ ion concentrations show the 87-95 % removal. The results indicate that percent of ammonium removal decreases with increasing the initial ammonium concentration. It would be expected that there would be some relationship between C_0 and the percentage

of removed ammonium ion from solution since ion exchange of any cation by a cation exchanger is a function of the concentration of the cation in the solution. McLaren et al., [1973] studied certain factors suspected to affect the ammonium ion removal efficiency of zeolite and suggested that initial ammonium concentration had the greatest effect on the removal. As comprehended from the results; the initial concentration of the solution shows the significant effect on the ammonium exchange process.

6.4. The Effect of Competing Cation:

In this study, the effect of the individual presence of potassium, calcium and magnesium ion on the ammonium ion uptake was examined. The results were given in Figure 6.18-6.26 to show the changes in final ammonium concentration, percent ammonium removal and ammonium removal per gram of zeolite (Q) as a function of time with the presence of magnesium, calcium and potassium ions. These results were compared with results that obtained from the pure ammonium chloride solution.

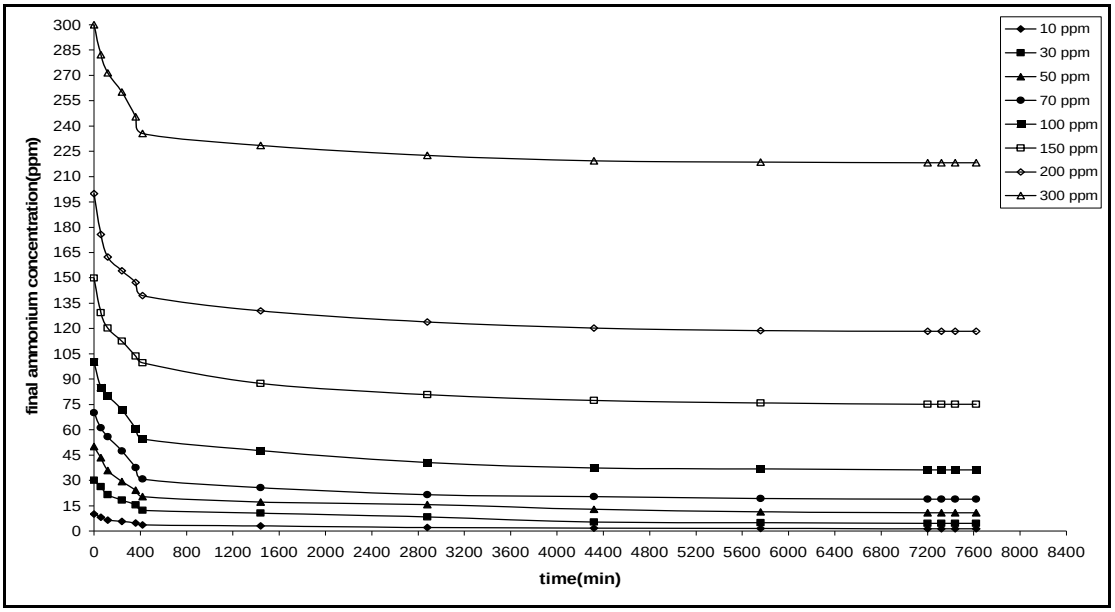

Figure 6.18. Change in NH_4^+ concentration with time for different initial ammonium concentration, %1 solid: solution ratio, K^+ as a competing cation, particle size=2.0-0.85 mm, pH<7.0, shaking rate= 170 rpm.

Figure 6.19, Figure 6.22 and Figure 6.25 shows the batch kinetics of ammonium ion removal by plotting the ammonium uptake capacity versus time for different initial ammonium concentrations in the presence of competing cations. Experimental results

show that the ammonium uptake capacity increases with increasing initial ammonium concentration in the presence of competing cations. Also, ammonium removal efficiency decreases with increasing initial ammonium concentration in the presence of competing cations.

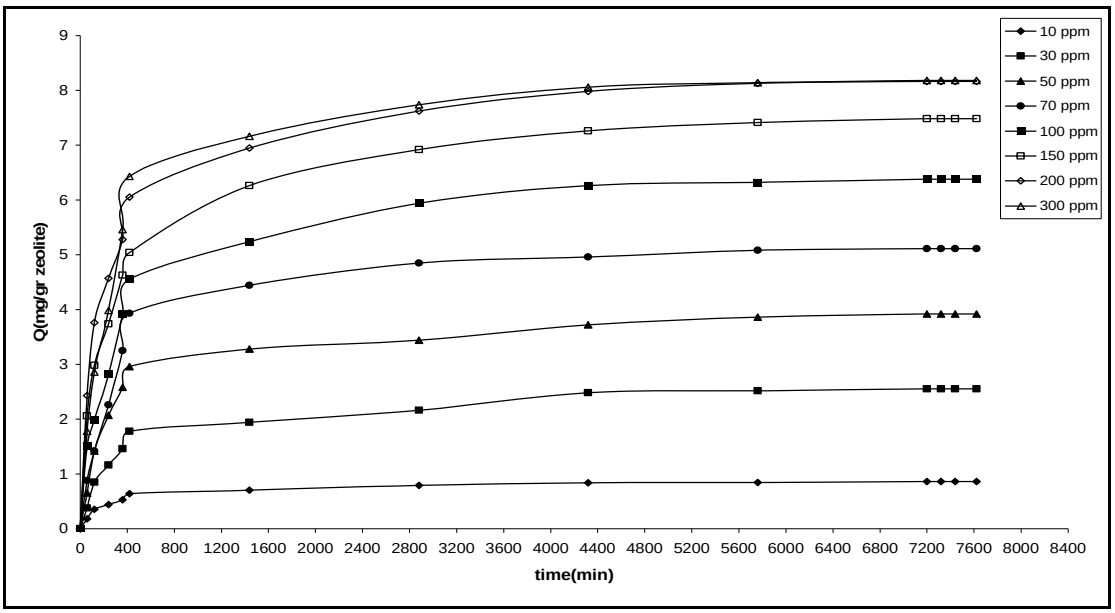

Figure 6.19. The kinetic curves of ammonium uptake for ammonium chloride solution at different initial ammonium ion concentrations, 1% solid: solution ratio, K^+ as a competing cation, particle size= 2-0.85 mm, pH<7.0, shaking rate= 170 rpm.

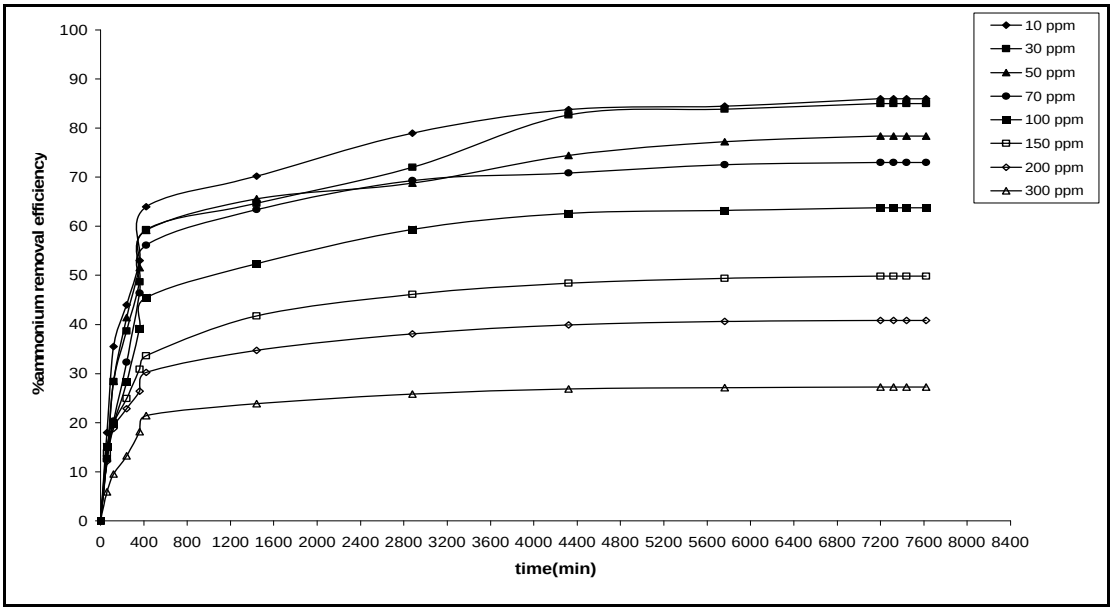

Figure 6.20. The percentage of removed ammonium ion versus time for different initial ammonium concentrations, %1 solid: solution ratio, K^+ as a competing cation, particle size=2.0-0.85 mm, pH<7.0, shaking rate= 170 rpm.

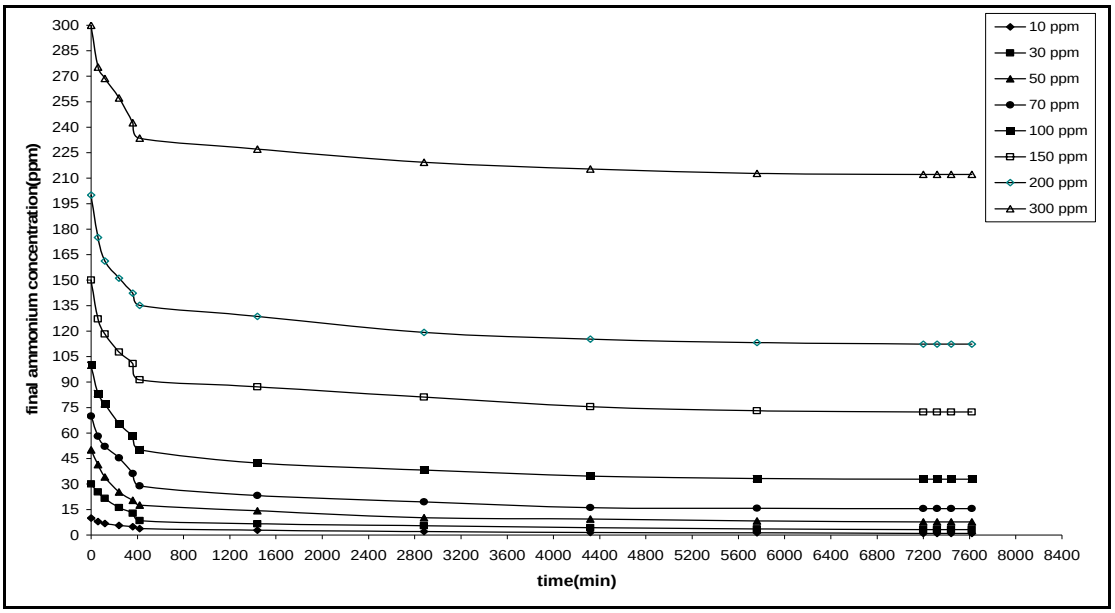

Figure 6.21. Change in NH_4^+ concentration with time for different initial ammonium concentrations, %1 solid: solution ratio, Mg^{+2} as a competing cation, particle size=2.0-0.85 mm, pH<7.0, shaking rate= 170 rpm.

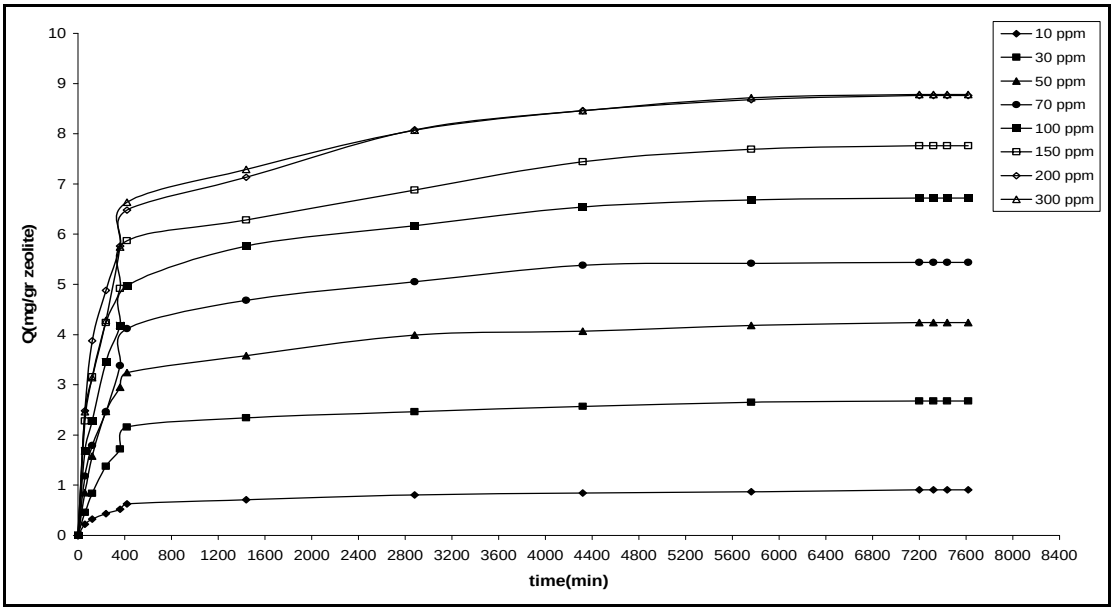

Figure 6.22. The kinetic curves of ammonium uptake for ammonium chloride solution at different initial ammonium ion concentrations, 1% solid: solution ratio, Mg^{+2} as a competing cation, particle size= 2-0.85 mm, pH<7.0, shaking rate= 170 rpm.

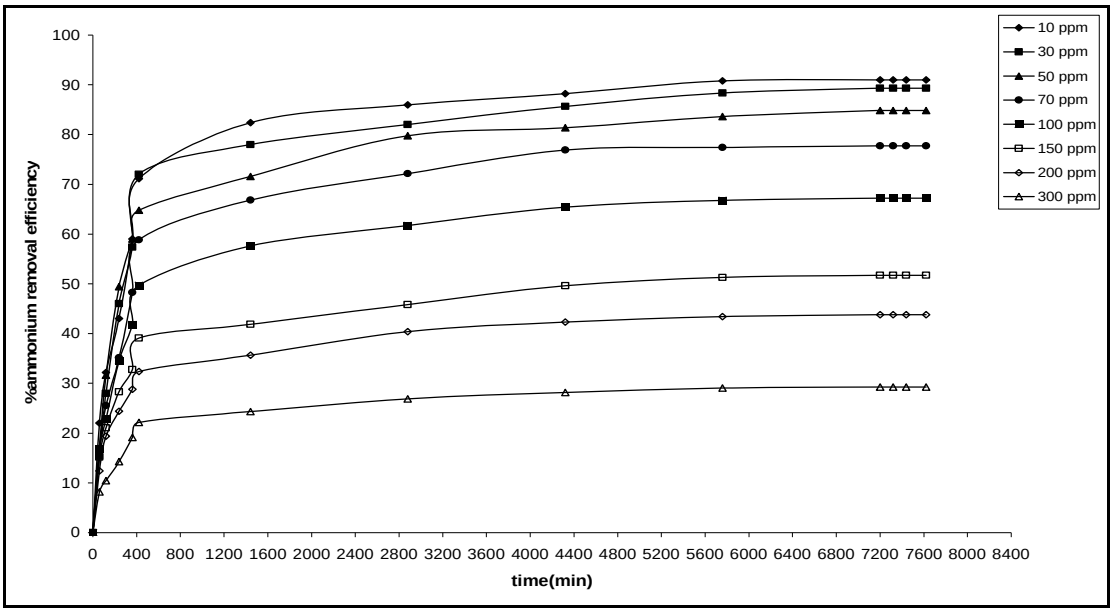

Figure 6.23. The percentage of removed ammonium ion versus time for different initial ammonium concentrations, % 1 solid: solution ratio, Mg^{+2} as a competing cation, particle size=2.0-0.85 mm, pH<7.0, shaking rate= 170 rpm

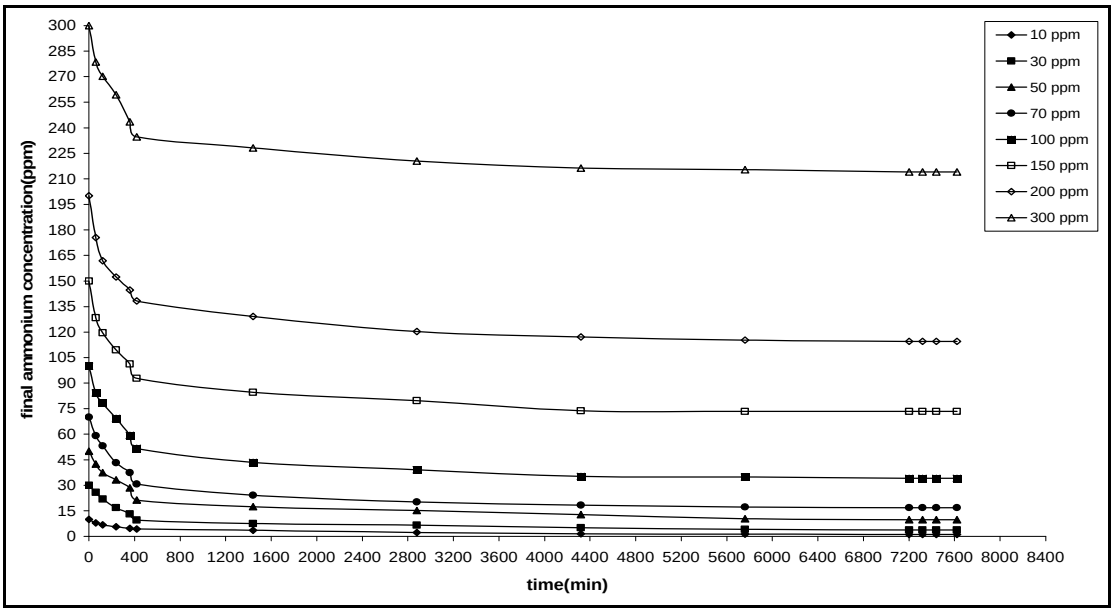

Figure 6.24. Change in NH_4^+ concentration with time for different initial ammonium concentrations, %1 solid: solution ratio, Ca^{+2} as a competing cation, particle size=2.0-0.85 mm, pH<7.0, shaking rate= 170 rpm.

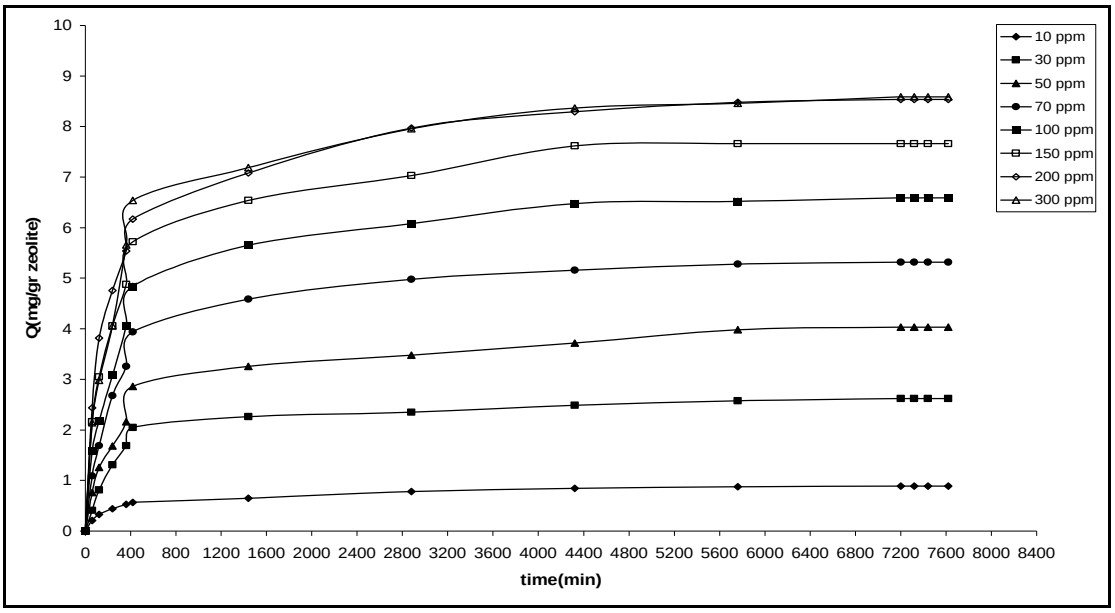

Figure 6.25. The kinetic curves of ammonium uptake for ammonium chloride solution at different initial ammonium ion concentrations, 1% solid: solution ratio, Ca^{+2} as a competing cation, particle size= 2-0.85 mm, pH<7.0, shaking rate= 170 rpm.

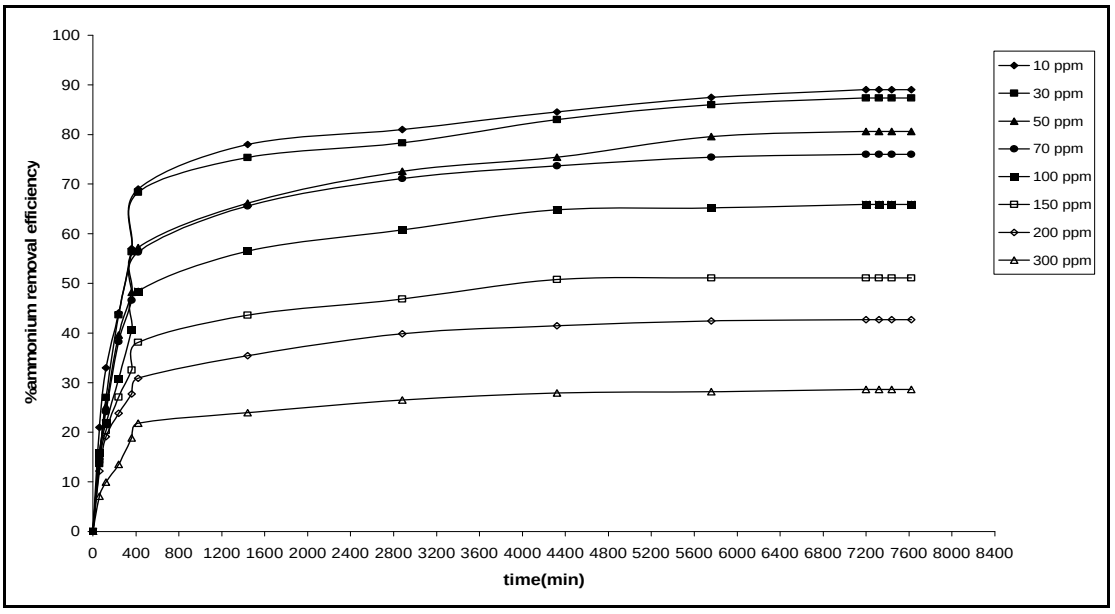

Figure 6.26. The percentage of removed ammonium ion versus time for different initial ammonium concentrations, %1 solid: solution ratio, Ca^{+2} as a competing cation, particle size=2.0-0.85 mm, pH<7.0, shaking rate= 170 rpm.

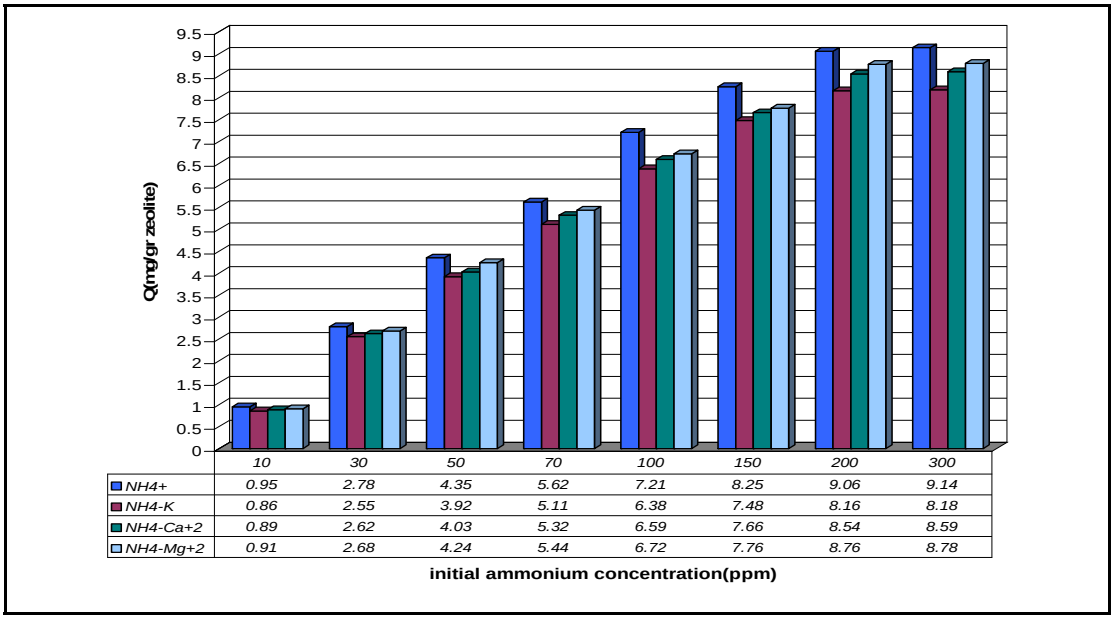

Figure 6.27. Comparison of ammonium uptake capacity data for with and without competing cations.

Figure 6.27 show the ammonium uptake capacity data versus initial ammonium concentration with and without competing cations. Similar to the previous experiments performed for without competing cations, ammonium uptake capacity values were lower than pure ammonium chloride solution. Ammonium uptake capacity in the presence of potassium ion is less than in the presence of magnesium, and that in the presence of calcium ion. The effect of the competing cations suggest an order of preference $K^{+}>Ca^{+2}>Mg^{+2}$ since the greatest reduction in the presence of potassium ion. As a comprehended from the results, the presence of potassium ion had the most significant effect upon ammonium uptake followed by calcium. Magnesium ion had the least effect. Our experimental results were shown good agreement with the Eisenman theory. Consideration of Eisenman's model, in the case of exchange on a zeolite in the presence of a weakly anionic field indicates that selectivity is predominantly determined by the free energies of hydration of the competing ions. The free energies of hydration and hydrated radius of the ions were listed in Table 6.13. As it can be seen from the Table 6.13, Mg^{+2} with the largest hydration energy prefers the solution phase where it may satisfy its hydration requirements, and K^{+} with the least hydration energy, prefers the zeolite phase. For this reason, magnesium ion had the least effect on the ammonium uptake capacity.

Table 6.13. Properties of Competing Cations (Semmens, 1978)

Cation	Ionic Radius (A°)	Hydrated Radius (A°)	Free Hyd. Energy (kcal/gr)
K^{+}	1.33	3.31	-76.67
NH_4^{+}	1.43	3.35	-77.99
Ca^{+2}	0.99	4.12	-380.22
Mg^{+2}	0.65	4.28	-459.04

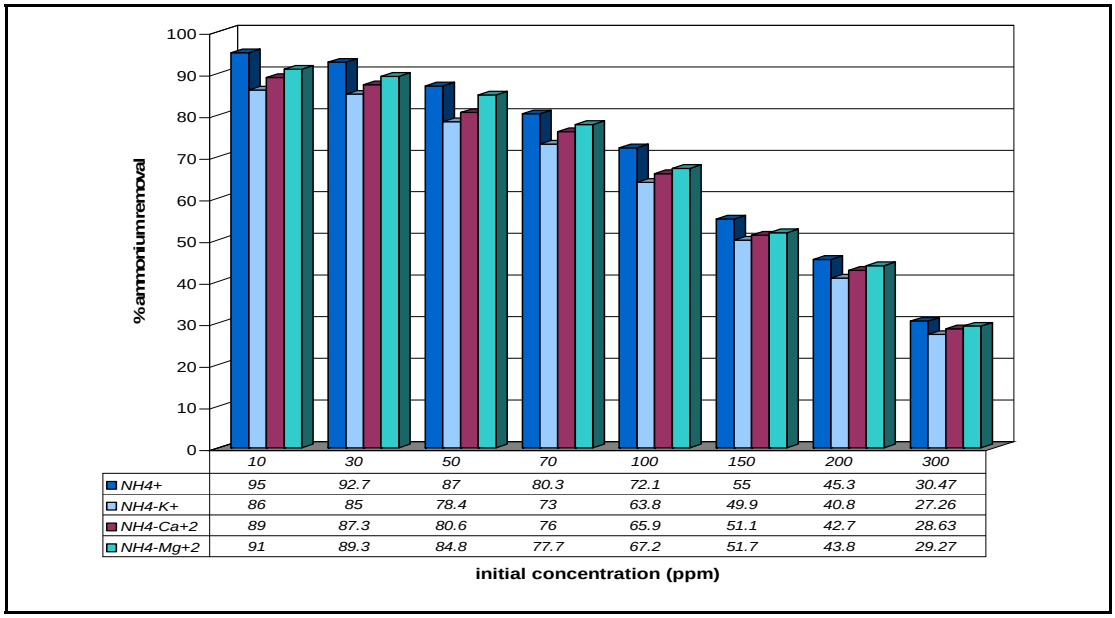

Figure 6.28. Comparison of the percentage of ammonium removal data for with and without competing cations.

Figure 6.28 shows the percentage of ammonium removal versus initial ammonium ion concentrations with and without competing cations. Similar to the previous experiments performed for without competing cations, the percentages of ammonium removal values were lower than pure ammonium chloride solution. For example, the higher NH_4^{+} ion concentrations with the presence of magnesium, calcium and potassium ions show the 29.3-51.7%, 28.63-51.7% and 49.9-27.6 % removal, respectively. And also, lower NH_4^{+} ion concentrations with the presence of magnesium, calcium and potassium ions show the 84.8-91 %, 80.6-89% and 78.4-86 % removal, respectively. The results were compared with the pure ammonium chloride solution; ammonium removal efficiency values decreased to 78.4-86% in the presence of potassium. The results indicate that, the presence of potassium ion decreases in effect relative to magnesium and calcium as the initial ammonium ion concentration increases.

As comprehended from the results; potassium ion had the largest effect on the percentage of ammonium removal. Maximum removal percentage values were observed for the pure ammonium chloride solution. Our experimental results indicated that the presence of competing cation in the solution was highly critical for the percentage of ammonium ion removal.

6.5 The Effect of pH of the Solution

In this study, pH of the solution was recorded. The pH profiles of zeolite in varying concentrations of ammonium chloride solutions, 10 to 300 mg/lt, as a function of time is shown in Figure 6.29. The initial pH of all solutions was about 5.5-5.8. After zeolite addition, the solution pH was raised to 5.87, 6.02, 6.24 and 6.35 in 60 min and then increased. Finally, they reached the equilibrium around 6.93, 6.97, 6.98 and 7.01 after 4320 min, for initial ammonium ion concentrations of 10, 50, 100 and 300 mg/lt. The reason for the rapid rise in the suspension pH in the first 60 min is ascribed to the rapid adsorption of H^+ ions in solution both onto the negatively charged clinoptilolite surface and as a potential determining ion (pdi) in the electrical double layer (EDL) in order to provide electroneutrality (Ersoy et al., 2002). Rivera et al, 2000 investigated the pH profile of purified natural clinoptilolite in aqueous medium. They have found that, pH of the solution was increased quickly after zeolite addition. After that, a decrease of the pH values towards the neutral area was observed, followed by its stabilization at around 6000 min. These results indicate that clinoptilolite tends to neutralize the aqueous medium acting either as proton acceptor or as proton donor, which makes evident its amphoteric character.

In order to understand the effect of the pH of the solution on the ammonium uptake capacity, different pH values were tested. Figure 6.30 shows the effect of initial pH on the ammonium uptake capacity. It can be observed that the ammonium uptake capacity is slightly reduced at pH values lower than 6. The experimental results indicate that an optimal pH value of 7 for ammonium removal by zeolite.

The ammonia in aqueous solution can be found in a dissociated form as ammonia, NH_4^+, or without dissociating as dissolved ammonia, $NH_3(aq)$. The equilibrium between these two species is dependent upon solution pH and can be represented by the following chemical reaction. According to the equilibrium Bronsted-Lowry acid-base reaction, the ammonium removal should be greater at lower pH values

and smaller at higher pH values, if ion exchange mechanism occurs only by means of the ammonium ion.(Demir et al., 2002)

$$NH_3 + H_2O \leftrightarrow NH_4^+ OH^- \qquad 6.4$$

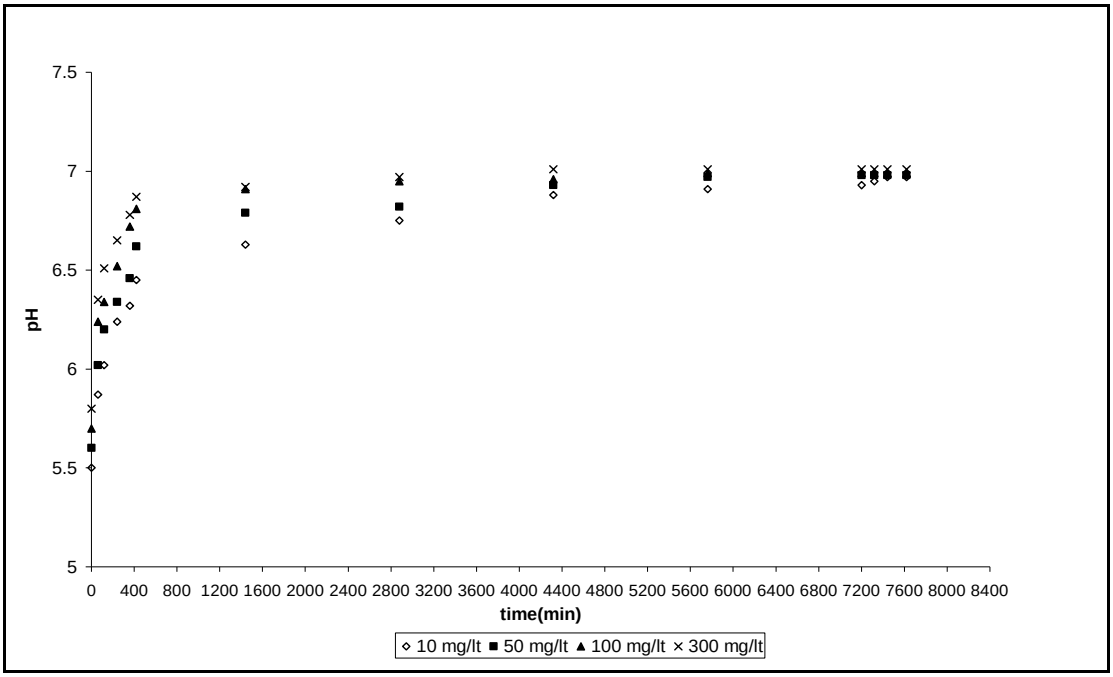

Figure 6.29. Investigation of pH of the Solutions at varying Initial Ammonium Ion Concentrations (%1 solid: solution ratio, 2-0.85 mm, no competing cation, shaking rate: 170 rpm).

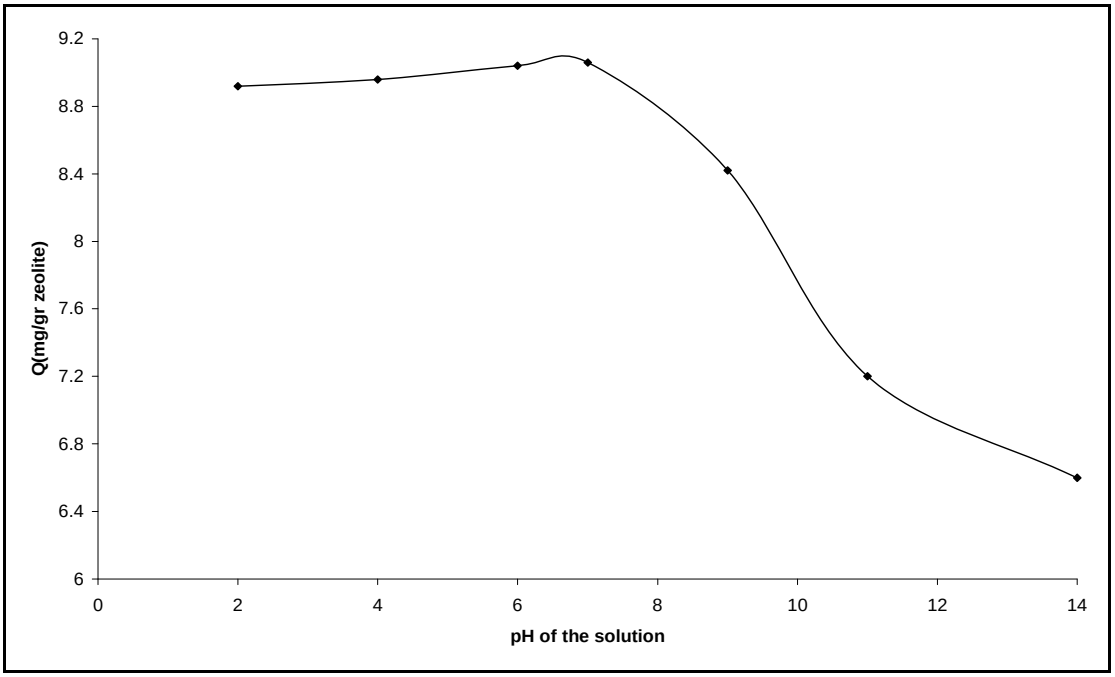

Figure 6.30. The effect of pH of the solution on the ammonium uptake capacity

The chemical speciation diagram of ammonium aqueous solution was prepared by using Minteq Computer Program and was shown in Figure 6.31. It can be noted that at pH lower than 7, the predominant species is the NH_4^+ ion but at pH greater than 11.5 it is the dissolved ammonia, $NH_3(aq)$. Thus, ammonium was exchanged on the zeolite as the ammonium ion since all experiments were carried out at pH 7. The slightly lower ammonium uptake capacities results obtained under low pH conditions may be due to the H^+-NH_4^+ competition for the exchange sites in the zeolite surface (Inglezakis et al., 2001), as seen in the chemical species diagram for aqueous solution system. In addition, the ammonium uptake capacity is drastically reduced at pH values higher than 9 because of the NH_3 gaseous species begin to be significant.

Koon et al, 1975 investigated the impact of pH on ammonium exchange in zeolites by varying the pH between 4 to 10 and obtained the highest ammonium exchange at pH 6. They can be explained that at low pH, the ammonium ions had to compete with hydrogen ions among the exchange sites; however, when the pH was high, the ammonium were transformed to ammonia gas. For practical applications, they recommended that a pH value within interval 4-8 during loading phase. Kithome et al., (1998) found that, when they performed experiments where the pH was varied between 4 and 7, most ammonium was adsorbed at pH 7. They gave the same explanation for low pH values as Koon et al. (1975). Our experimental results are coinciding with their studies.

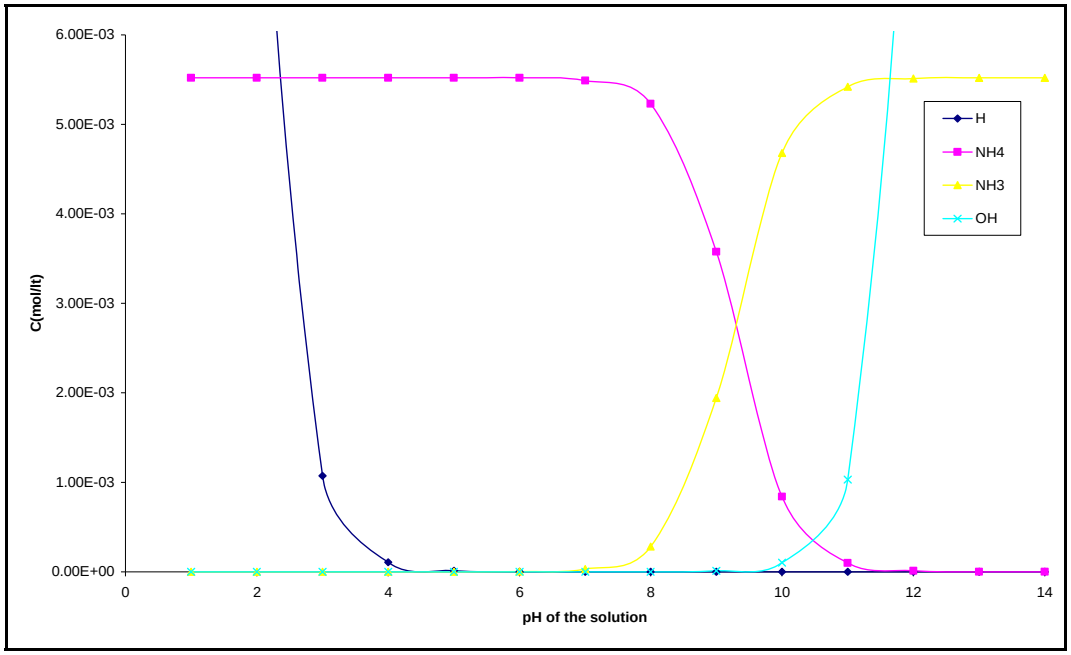

Figure 6.31. Chemical species diagram for ammonium aqueous solution

6.6 Ion Exchange Mechanism

ICP-AES was used to understand the ion exchange mechanism between the ammonium and the exchangeable cations of the clinoptilolite rich mineral. Figure 6.32-6.35 shows the kinetic curves for ion exchange between ammonium and magnesium, sodium, potassium and calcium ions with 2.5 gr of zeolite, 10 ppm ammonium chloride solution with and without competing cations. Figure 6.29 indicate that ammonium ion concentration decreased from 10 to 0.5 mg/lt, while sodium, potassium, calcium and magnesium increased to approximately 2.61, 3.24, 3.22 and 0.50 mg/lt, respectively.

It is noticed that, an ion exchange mechanism exists between the ammonium ion and the exchangeable cations of the zeolite. Ion exchange is a stoichiometric reaction. Therefore, in any ion exchange reaction, the equivalent of the major cations released to the solution should be equal to those of the equivalent cations sorbed. For this reason, a balance of equivalent of cations was constructed between the major exchangeable cations released to the solution phase and equivalent of change of ammonium ion in solution with and without competing cations. In Table 6.14 , equivalent of NH_4^+ ion sorbed by solid phase was determined by the difference in the concentration of NH_4^+ ion in equivalents and also it was calculated by the summation of the equivalents of Na^+, Mg^{+2}, Ca^{+2} and K^+ ions released to the solution. Table 6.14 indicates that, adsorption and ion exchange process is significant mechanism for the ammonium removal process. The differences found from NH_4^+ equivalent change and exchange cation equivalent change indicated 14 to 34% of NH_4^+ ions were adsorbed by physical adsorption and remaining was exchanged by cation.

Table 6.14. Experimental Data for Ammonium Exchange of the Clinoptilolite Samples at 25°C

System	q_{eq}^a(meq /g)	q_{eq}^b(meq /g)	% differences
NH_4^+	0.131	0.100	24
NH_4^+- Mg^{+2}	0.165	0.109	34
NH_4^+- Ca^{+2}	0.228	0.185	19
NH_4^+- K^+	0.228	0.196	14

a=from NH_4^+ measurements directly

b=from Na^++ Ca^{2+} + K^++ Mg^{2+} measurements

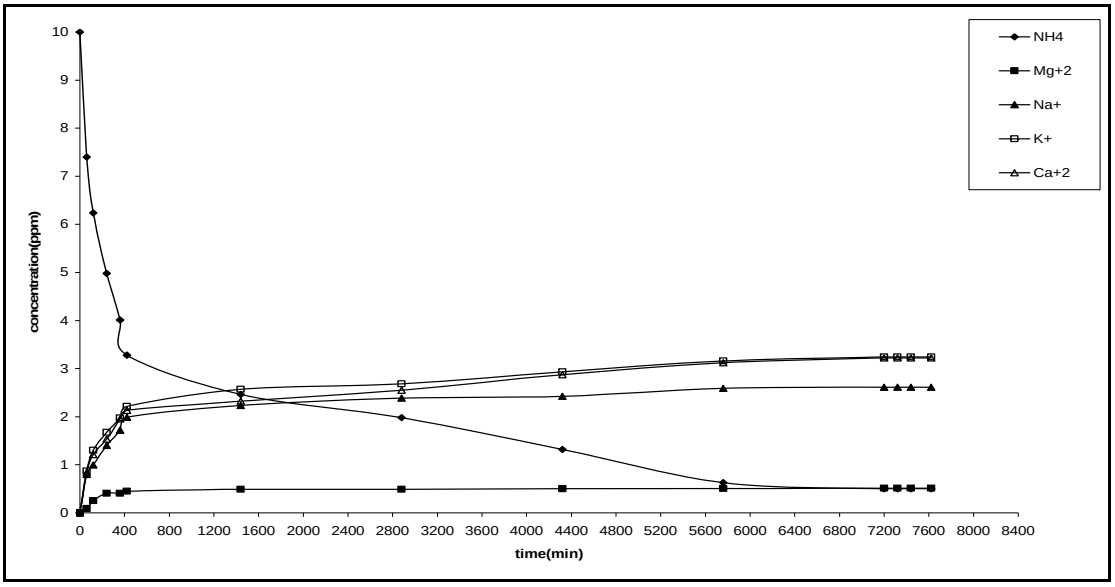

Figure 6.32. The kinetic curves for ion exchange between NH_4^+ and Na^+, K^+, Ca^{+2}, Mg^{+2} ions with 2.5 gr of zeolite, 10 mg/lt NH_4Cl solution (no competing cation, shaking rate=170 rpm)

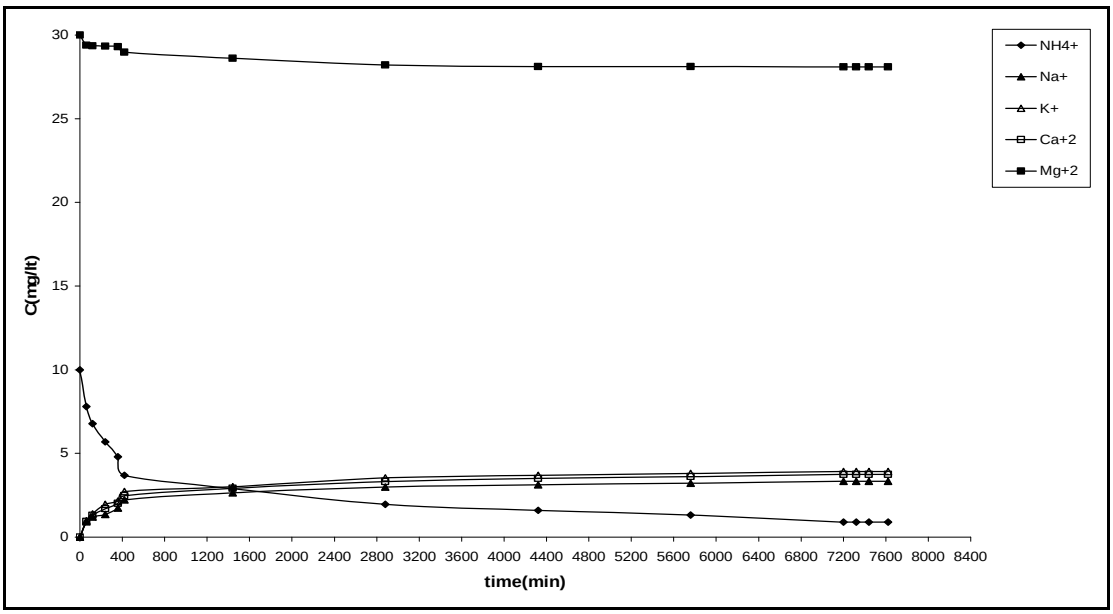

Figure 6.33. The kinetic curves for ion exchange between NH_4^+ and Na^+, K^+, Ca^{+2}, Mg^{+2} ions with 2.5 gr of zeolite, 10 mg/lt NH_4Cl solution (Mg^{+2} as competing cation, shaking rate=170 rpm)

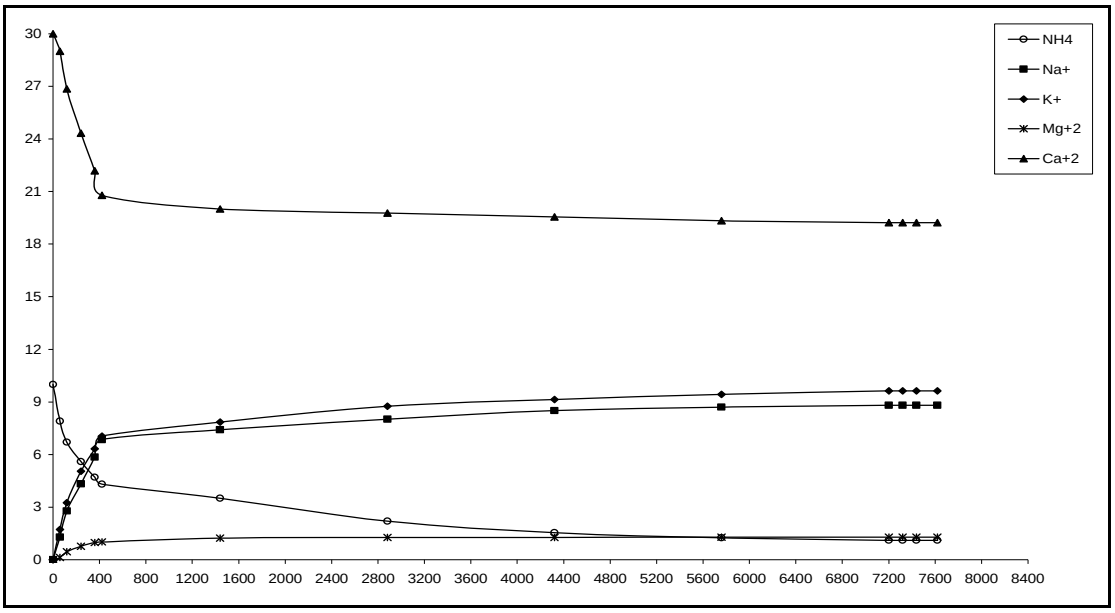

Figure 6.34. The kinetic curves for ion exchange between NH_4^+ and Na^+, K^+, Ca^{+2}, Mg^{+2} ions with 2.5 gr of zeolite, 10 mg/lt NH_4Cl solution (Ca^{+2} as competing cation, shaking rate=170 rpm)

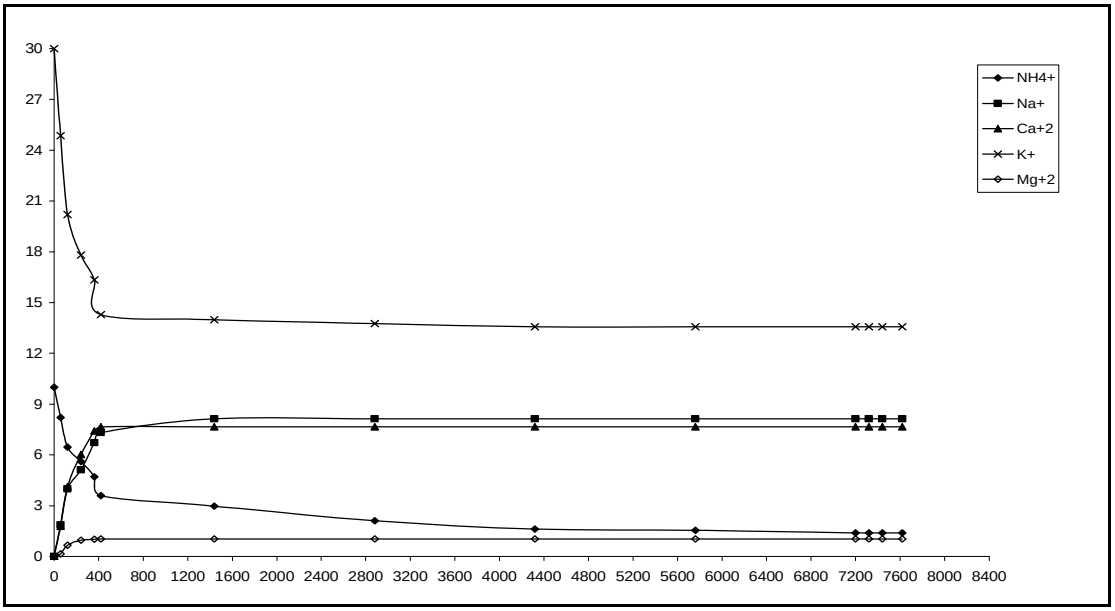

Figure 6.35. The kinetic curves for ion exchange between NH_4^+ and Na^+, K^+, Ca^{+2}, Mg^{+2} ions with 2.5 gr of zeolite, 10 mg/lt NH_4Cl solution (K^+ as competing cation, shaking rate=170 rpm)

Figure 6.33, 6.34, 6.35 indicates that ion exchange mechanism ammonium ion between exchangeable cations of the clinoptilolite in the presence of competing cations. As it can be seen from the figures; ammonium ion is highly exchange with major exchangeable cations, especially Na^+, K^+ and Ca^{+2}. Two possible reasons exits why

Mg^{+2} will exchange out of the samples slower than other exchangeable cations. The first could be explained by the structural location of Mg^{+2} in the clinoptilolite and the second by the difference in the hydration spheres associated with each. As stated in literature, magnesium ion is situated in M (4) site and this site is coordinated by six water molecules, which theoretically give this cation great facility for ion exchange (Ackley et al., 1991). However, magnesium ion exhibit lower mobility than Na^{+} and Ca^{+2} in solution, because of the competition that competing cations present in solution phase. Another explanation, recently put forward by Wüst et al., (1999), involves variables sizes of the associated hydration spheres for the ingoing and outgoing cations. Magnesium ion only exchanged into the center of the A-channel along with its large hydration sphere. When its properties was compared to other exchangeable cations, hydrated radius and free hydration energy values were higher than the others. In general, hydrated radius is inversely proportional to cationic radius, and divalent radius have higher hydrated radius than monovalent cations. For this reason, Mg^{+2} ions can not move easily out of the channels due to its considerably higher hydrated radius and free hydration energy. As a consequence of these concerns, other exchangeable cations with fewer, more weakly bonded waters are actually smaller and more mobile than magnesium ion with larger, more tightly bonded water molecule. Therefore, ammonium ion in solution does not exchange significantly with magnesium ion in the clinoptilolite structure.

6.7. Composition Change of the Solid Phase by Ion Exchange

Analyses of solid phase were carried out using SEM-EDX microanalysis. Figure A.3.3 shows the SEM images of the clinoptilolite rich mineral samples before and after ion exchange process. EDX results of the clinoptilolite samples before and after ion exchange process were shown in Figure 6.36-6.39. Each bar represents the average results of 6 EDX analyses taken from different parts of Gördes clinoptilolite rich mineral structure in 5000 magnification. Standard deviations were calculated. The calculated percent errors were presented on the bar graph as error bars in each figure.

Table 6.15. Composition of the clinoptilolite after ion exchange process with 10 ppm pure ammonium chloride (2-0.85)

ELEMENT	1	2	3	4	5	6
N	3.36	3.47	3.44	3.49	3.38	3.59
O	48.77	48.65	48.4	48.2	48.11	48.1
Na	0.60	0.53	0.54	0.53	0.59	0.55
Mg	1.14	0.98	1.1	0.98	1.1	1.11
Al	7.85	7.87	7.92	7.85	7.83	7.84
Si	33.98	33.9	34.2	34.63	34.66	34.2
K	2.71	2.97	2.69	2.69	2.72	2.93
Ca	1.57	1.63	1.63	1.63	1.61	1.68
TOTAL	100	100	100	100	100	100

The main exchangeable cation (Na^+, K^+, Mg^{2+}, Ca^2) are present in the clinoptilolite structure. K^+ and Ca^{+2} are the major exchangeable cations in the structure. When Figure 6.36 is investigated, it is seen that after ion exchange with pure ammonium chloride solution, weight percentages of Na^+, K^+, Mg^{2+} and Ca^{2+} ions were decreased while weight percent of NH_4^+ ions was increased. Also, the least exchange was observed between Mg^{2+} and NH_4^+ ions as was proved by the ICP results of batch studies for Gördes Clinoptilolite rich material sample.

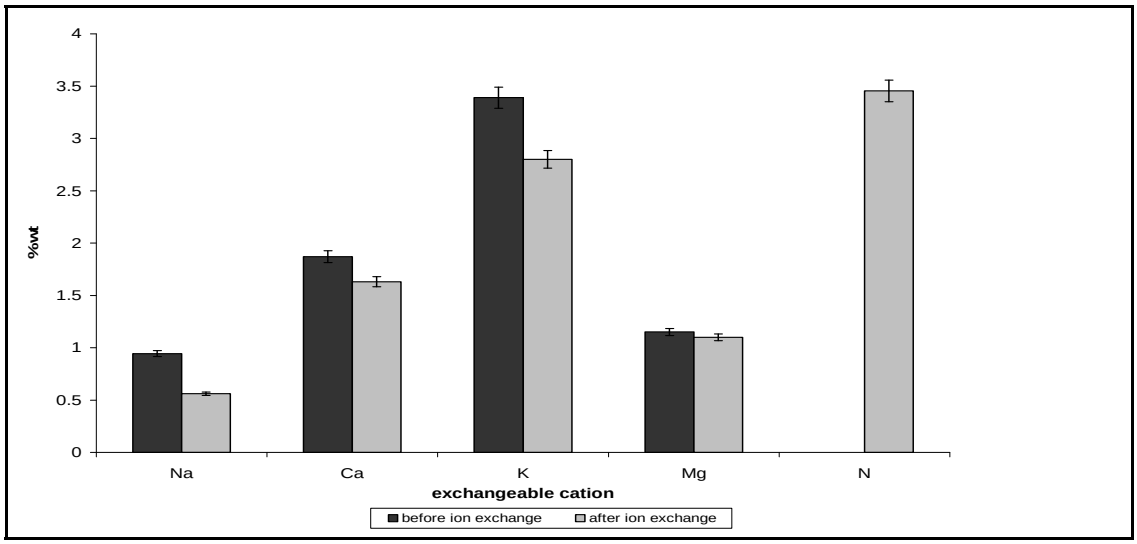

Figure 6.36. Results of the exchangeable cation composition of the clinoptilolite (black: before ion exchange, gray: after ion exchange with 10 ppm pure ammonium chloride solution)

Table 6.16. Composition of the clinoptilolite after ion exchange process with 10 ppm pure ammonium chloride with competing cation Ca^{+2} (2-0.85)

ELEMENT	1	2	3	4	5	6
N	2.86	2.89	2.92	2.96	2.93	2.96
O	48.57	48.55	48.42	48.25	48.35	48.49
Na	0.69	0.59	0.57	0.51	0.50	0.52
Mg	1.09	1.01	1.04	1.07	1.1	1.11
Al	7.85	7.87	7.86	7.85	7.83	7.84
Si	34.21	34.11	34.2	34.63	34.5	34.2
K	2.75	2.94	2.93	2.67	2.75	2.83
Ca	2.02	2.04	2.06	2.06	2.04	2.05
TOTAL	100	100	100	100	100	100

Table 6.17. Composition of the clinoptilolite after ion exchange process with 10 ppm pure ammonium chloride with competing cation K^{+} (2-0.85)

ELEMENT	1	2	3	4	5	6
N	3.04	3.09	3.14	3.12	3.06	3.16
O	48.57	48.51	48.32	48.25	48.35	48.33
Na	0.51	0.46	0.52	0.54	0.48	0.47
Mg	1.03	1.04	1.05	1.07	1.12	1.11
Al	7.86	7.88	7.89	7.84	7.87	7.88
Si	34.21	34.11	34.2	34.25	34.19	34.2
K	3.42	3.46	3.49	3.51	3.50	3.48
Ca	1.36	1.45	1.39	1.42	1.43	1.37
TOTAL	100	100	100	100	100	100

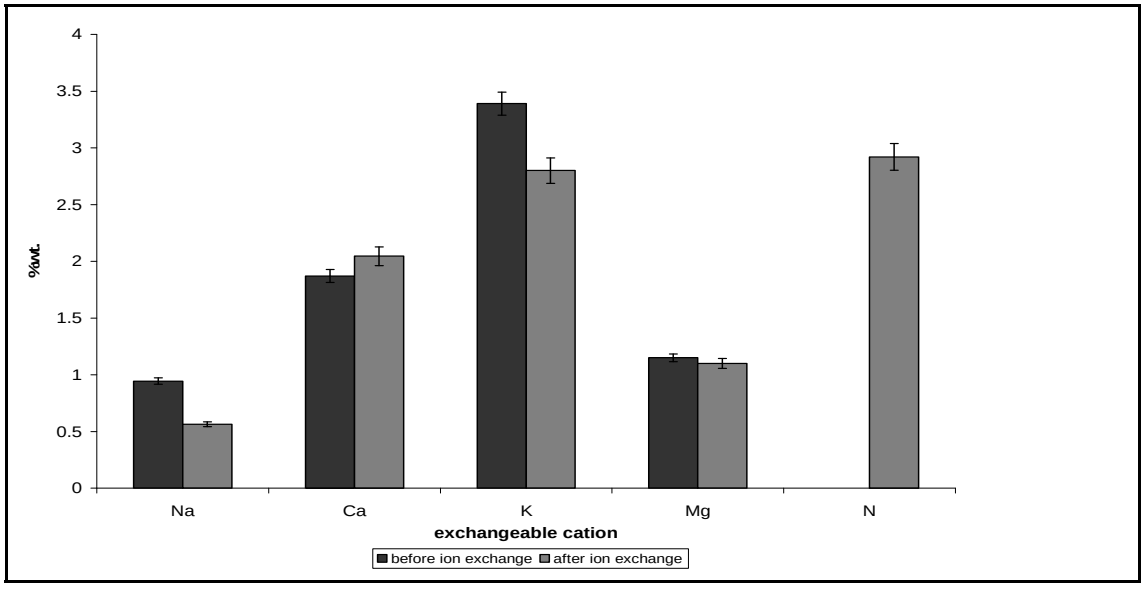

Figure 6.37. Results of the exchangeable cation composition of the clinoptilolite (black: before ion exchange, gray: after ion exchange with 10 ppm pure ammonium chloride solution with competing cation Ca^{+2})

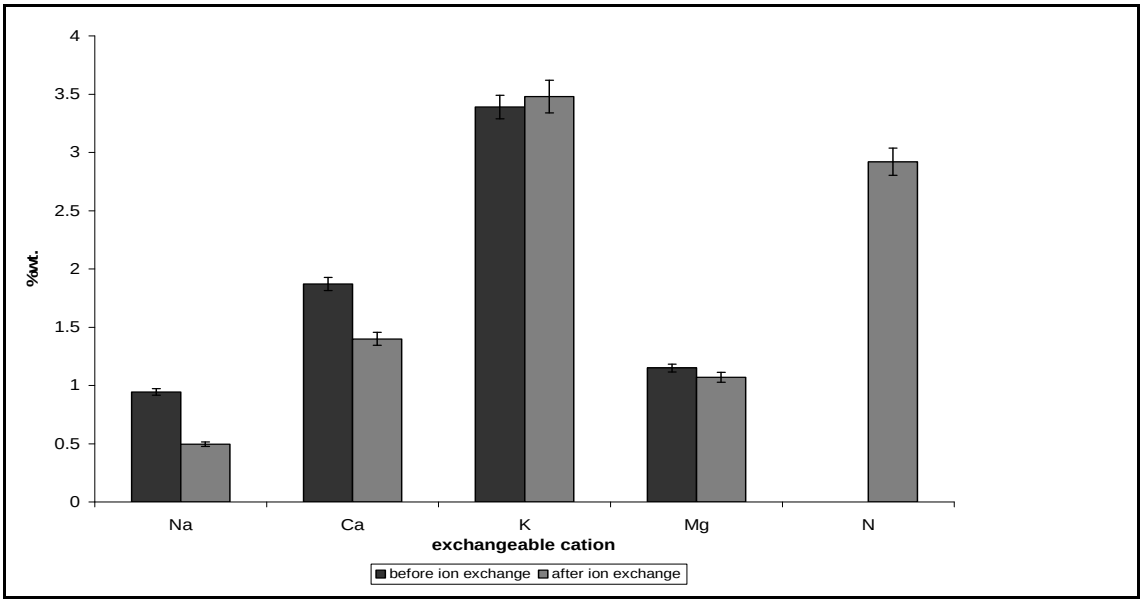

Figure 6.38. Results of the exchangeable cation composition of the clinoptilolite (black: before ion exchange, gray: after ion exchange with 10 ppm pure ammonium chloride solution with competing cation K^{+})

Table 6.18. Composition of the clinoptilolite after ion exchange process with 10 ppm pure ammonium chloride with competing cation Mg^{+2} (2-0.85)

ELEMENT	1	2	3	4	5	6
N	2.69	2.72	2.75	2.68	2.71	2.66
O	48.47	48.75	48.72	48.75	48.68	48.68
Na	0.62	0.55	0.57	0.49	0.50	0.53
Mg	1.27	1.26	1.24	1.28	1.26	1.29
Al	7.89	7.87	7.89	7.91	7.93	7.86
Si	34.99	34.78	34.72	34.82	34.89	34.88
K	2.71	2.75	2.82	2.77	2.75	2.83
Ca	1.36	1.32	1.29	1.30	1.28	1.27
TOTAL	100	100	100	100	100	100

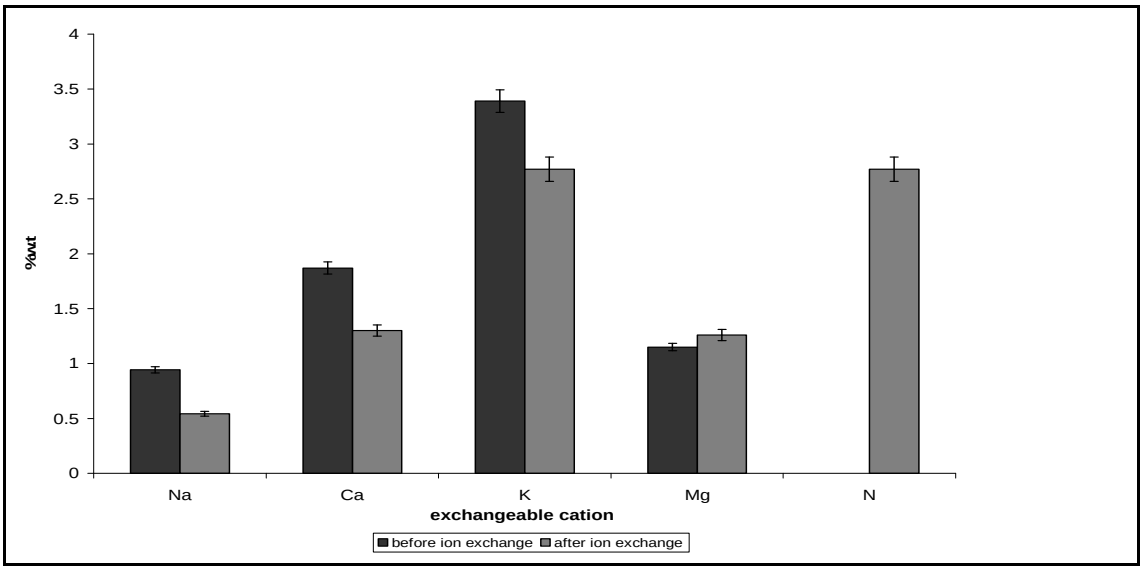

Figure 6.39. Results of the exchangeable cation composition of the clinoptilolite (black: before ion exchange, gray: after ion exchange with 10 ppm pure ammonium chloride solution with competing cation Mg^{+2})

Figure 6.37, Figure 6.38 and Figure 6.39 show that the effect of competing cation on the EDX results of the exchangeable cation of the clinoptilolite sample. In the presence of calcium ion, ammonium exchange with K and Na in the clinoptilolite structure. Weight percentage of Ca^{+2} ions in the structure increases with the addition of competing cation (Ca). Similar results were obtained with the presence of competing cations (K and Mg). In each case, weight of the competing cations in the structure increases with the addition of competing cations to solution. EDX results show good agreement with the ICP results.

6.8. Interpreting Equilibrium Data

There are several isotherms which can be employed for describing the ion exchange process. The Langmuir and Freundlich isotherms are the most commonly used. The Langmuir model assumes only one solute molecule per site, and also assumes a fixed number of sites. The Freundlich model suggests the energetic distribution of the sites is heterogeneous, due to the diversity of the sorption sites.

The Langmuir isotherm relates Q (mg of ammonia adsorbed / g of clinoptilolite) and C_E (the equilibrium ammonium concentration in solution) as shown in equation 6.4

$$Q = \frac{Q_m * C_E}{1 + b * C_E} \qquad 6.4$$

Rearranging the Langmuir equation gives equation 6.5, where linear relation is obtained. It can be seen that by plotting Ce/Q versus Ce the coefficients Q_m and k can be calculated.

$$\frac{C_e}{Q} = \frac{C_e}{Q_m} + \frac{1}{Q_m b} \qquad 6.5$$

The Freundlich isotherm relates uptake capacity and concentration in solution as shown in equation 6.6.

$$Q = \mathrm{K_f} * C_e^{\,1/n} \qquad 6.6$$

Rearranging the Freundlich equation gives equation 6.7, where linear relation is obtained. When log Q is plotted against log Ce the coefficients K_f and n can be calculated. Knowing all coefficients and using experimental data for Ce, the Langmuir and Freundlich theoretical Q_E can be calculated according to equations 7.1 and 7.3.

$$\log Q = \log K_f + (1/n)\log C_e \qquad 6.7$$

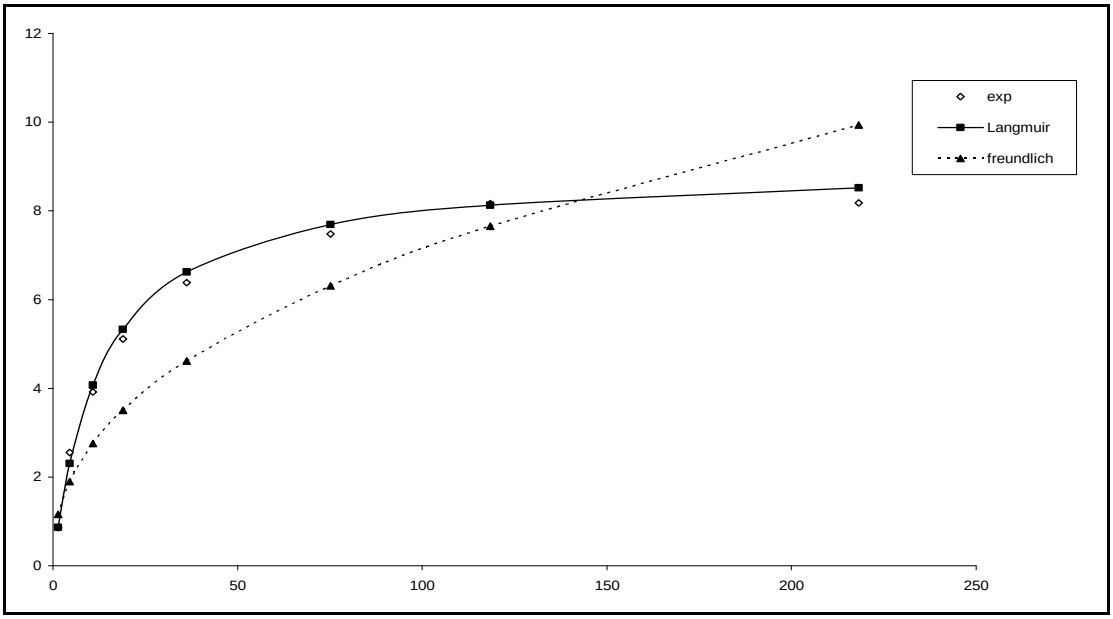

Figure 6.40. Equilibrium isotherm data for ammonium uptake onto clinoptilolite fitted to the Langmuir and the Freundlich uptake models.

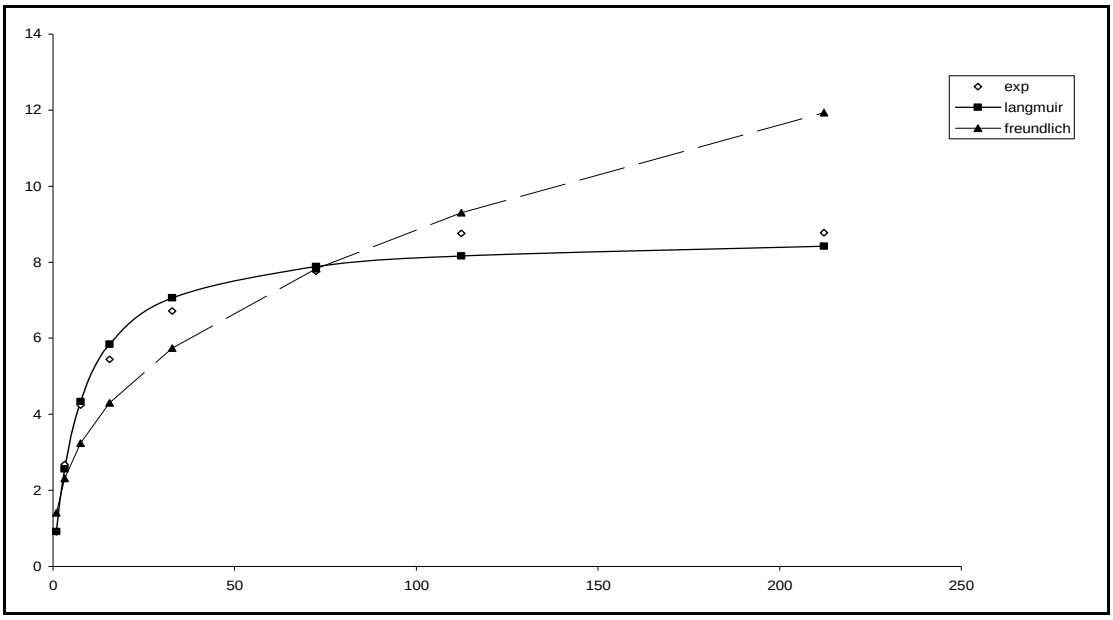

Figure 6.41. Equilibrium isotherm data for ammonium uptake onto clinoptilolite in the presence of magnesium ions fitted to the Langmuir and the Freundlich uptake models.

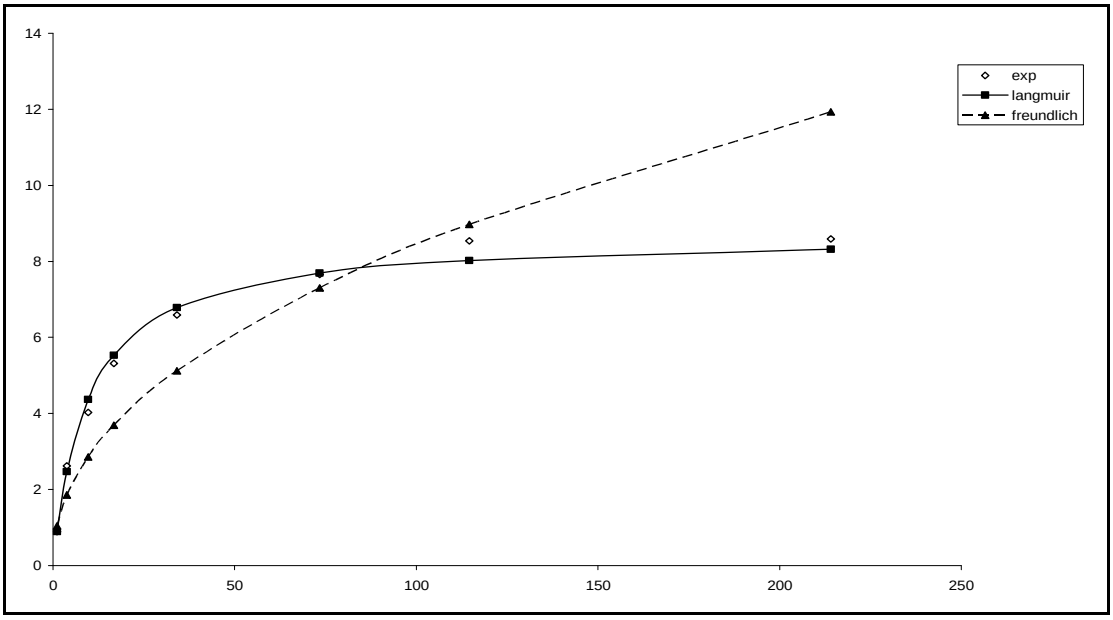

Figure 6.42. Equilibrium isotherm data for ammonium uptake onto clinoptilolite in the presence of calcium ions fitted to the Langmuir and the Freundlich uptake models.

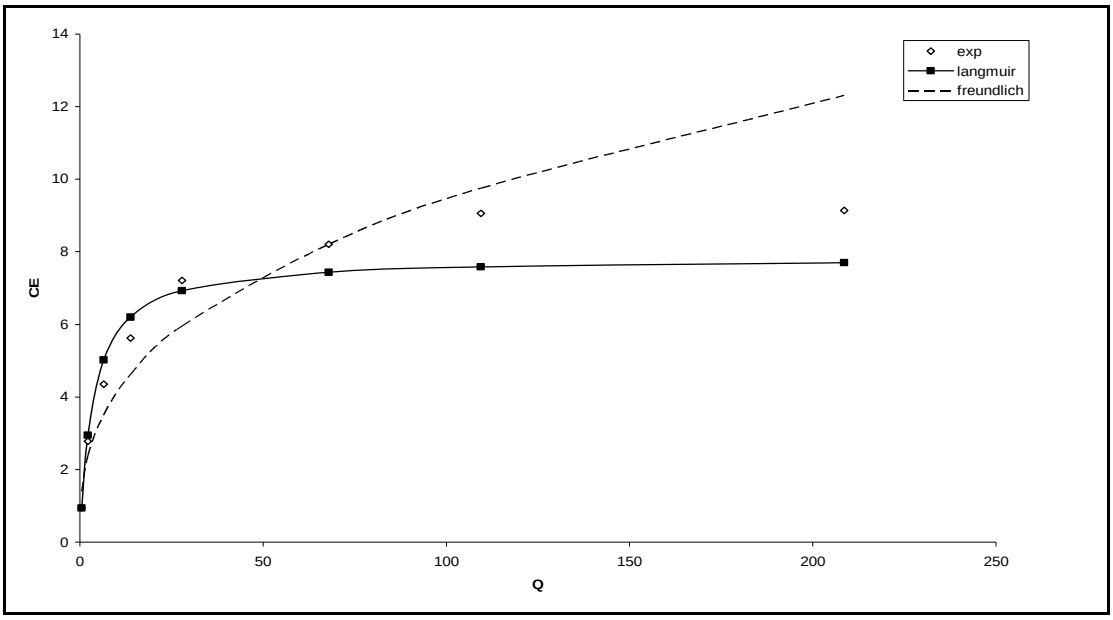

Figure 6.43. Equilibrium isotherm data for ammonium uptake onto clinoptilolite in the presence of potassium ions fitted to the Langmuir and the Freundlich uptake models.

The equilibrium isotherms obtained from the batch studies were shown in Figure 6.40-6.43, together with the corresponding Langmuir and Freundlich model values. These model parameters were tabulated in Table 6.19.

Table 6.19. Langmuir and Freundlich Model Parameters

Model	Langmuir			Freundlich		
Parameter	R^2	Q_m	k	R^2	K_L	1/n
NH_4^+	0.9975	9.03	0.076	0.9088	1.792	0.2529
NH_4^+-K^+	0.9962	7.84	0.273	0.9345	1.6963	0.4016
NH_4^+-Mg^{+2}	0.9992	8.76	0.1298	0.8901	1.466	0.3913
NH_4^+-Ca^{+2}	0.9661	8.695	0.104	0.897	1.294	0.4114

Langmuir model provided excellent correlation of the experimental data yielding correlation coefficient values of R^2>0.995 compared to results for the Freundlich model where R^2≈0.90. From the plateau of the isotherms maximum exchange capacities were determined as 9.03, 8.76, 8.695 and 7.84 mg NH_4^+/gr for NH_4^+, NH_4^+-Mg^{+2}, NH_4^+-$Ca^{+2}$and NH_4^+-K^+, respectively. As a consequence of this result, the ammonium capacity of Gördes clinoptilolite was approximately 0.51meq/gr for pure ammonium chloride solution.

6.9. Ammonium Ion Removal from Domestic Wastewater Effluent

In this part of the experiment, the samples were collected after Parshall Flumes (preliminary treated) and prior to Oxidation Ditch Tank (primary treated) at the plant. The average initial ammonium concentration was measured as 40 mg/lt. Batch experiments were conducted by using undiluted samples and diluted samples. Figure 6.44 and 6.45 show the change in ammonium concentration versus time for two treated samples. At the end of the shaking period, 40 mg/lt initial ammonium concentration decreased to 6.2 mg/lt , 30 mg/lt initial ammonium concentration decreased to 4.2 mg/lt, 20 mg/lt initial ammonium concentration decreased to 3.4 mg/lt, 10 mg/lt initial ammonium concentration decreased to 0.91 mg/lt , 5 mg/lt initial ammonium concentration decreased to 0.4 mg/lt for preliminary treated effluent. Similar results were obtained with the primary treated wastewater effluent.

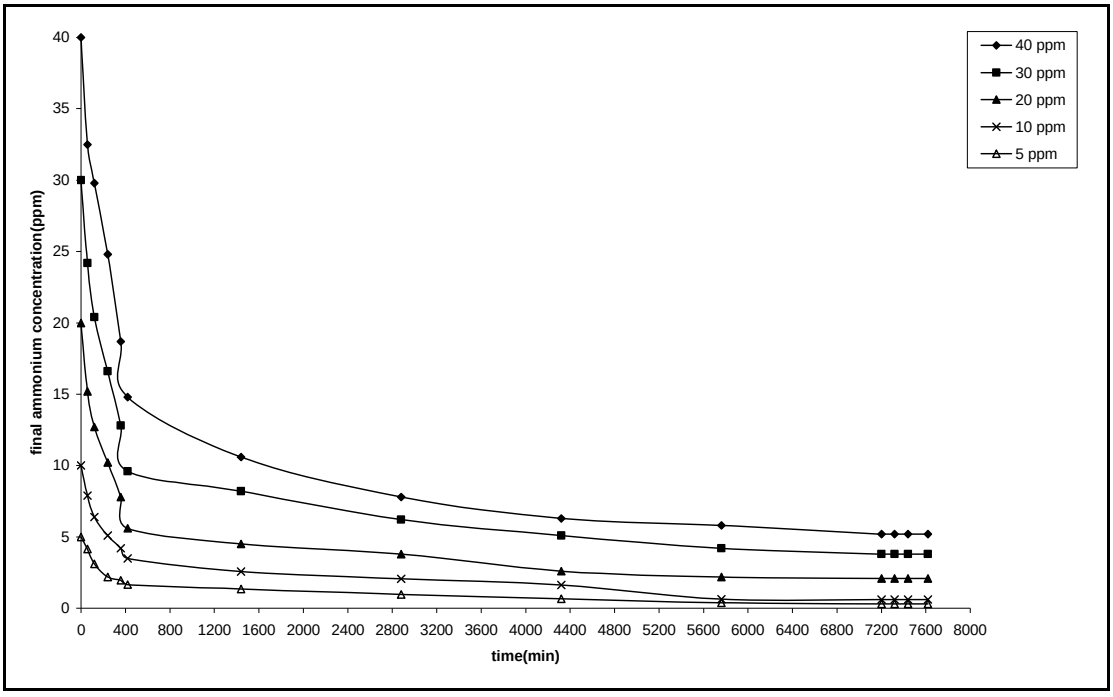

Figure 6.44. Change in NH_4^+ concentration with time for preliminary treated domestic wastewater samples, 1% solid: solution ratio, particle size=2.0-0.85 mm, pH<7.0, shaking rate= 170 rpm.

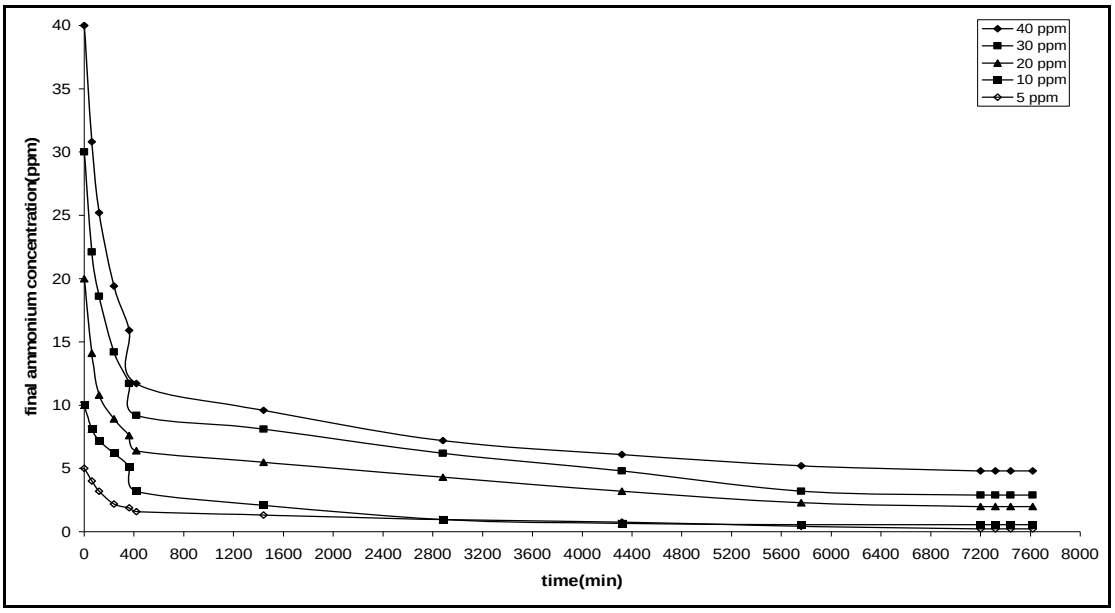

Figure 6.45. Change in NH_4^+ concentration with time for primary treated domestic wastewater samples, 1% solid: solution ratio, particle size=2.0-0.85 mm, pH<7.0, shaking rate= 170 rpm.

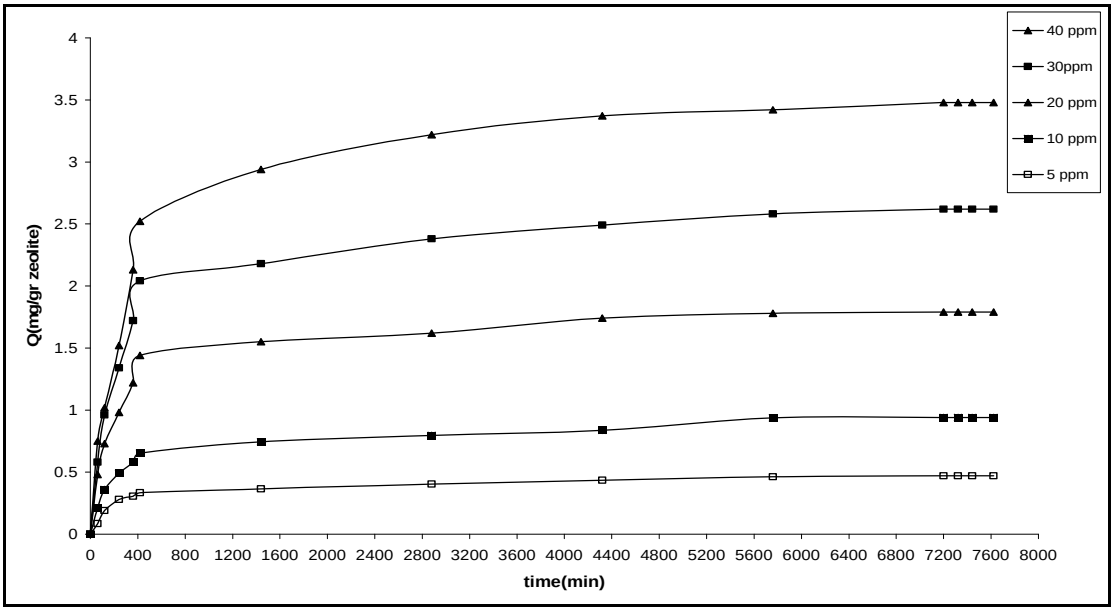

Figure 6.46. The kinetic curves of ammonium uptake for preliminary treated effluent, particle size =2.0-0.85 mm, pH<7.0, shaking rate= 170 rpm.

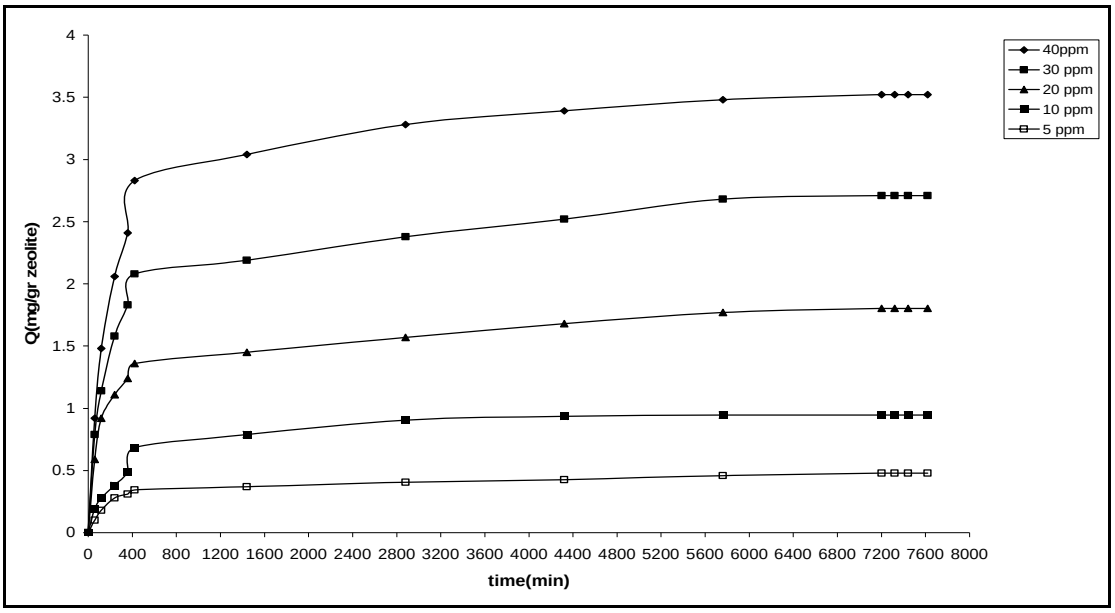

Figure 6.47. The kinetic curves of ammonium uptake for primary treated effluent, particle size =2.0-0.85 mm, pH<7.0, shaking rate= 170 rpm.

For wastewater effluent samples ammonium ion removal capacity with increasing initial concentration as was the case for the NH_4Cl solutions with and without competing cations. The percent NH_4^+ ion removal decreases with increasing initial ammonium concentration.

When comparing the removal of NH_4^+ ion from wastewater effluent and from NH_4Cl, the percent removal and the uptake capacity were lower for wastewater than for NH_4Cl for same solid: solution ratio and the same initial concentration. Experimental data of the synthetic and treated wastewater were tabulated in Table 6.21 and 6.22. Figure 6.48 shows the comparison of ammonium ion removal capacity for wastewater and ammonium chloride solution. For instance, the ammonium uptake capacity is 3.35 mg/gr and 3.4 mg/gr for preliminary and primary treated wastewater sample for 40 mg/lt initial ammonium concentration. And also, ammonium removal capacity is 3.59 mg/gr for pure ammonium chloride solution. It is expected that in domestic wastewater, where the complexity of the system is high, several matter could influence the removal of specific target cations. In the preliminary treatment, only large objects are removed from the wastewater which causes the maintenance and operational problem. Organic matter and suspended solid exist in the wastewater effluent. Two possible reasons exits why ammonium exchanges capacity of preliminary and primary treated samples lower than ammonium exchange capacity of pure ammonium chloride solutions. First reason

could be explained with small suspended solid could block the pores of clinoptilolite, hence inhibiting access of ammonium ions to many of the internal fixed exchange sites. Another reason was the presence of organic matter might influence the surface charge density of mobile ions within the clinoptilolite, which in turn would influence uptake and selectivity.

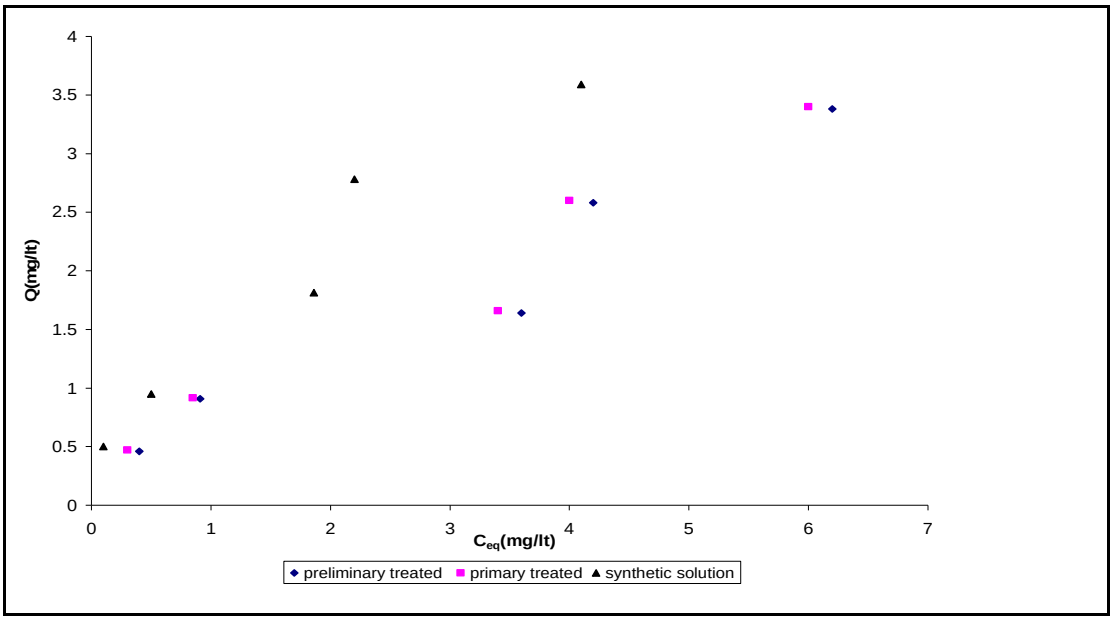

Figure 6.48. Comparison of ammonium uptake capacity data for synthetic solution and preliminary& primary treated wastewater effluents.

BOD, COD, NH_4^+, Mg^{+2}, Ca^{+2} and K^+ values of the preliminary and primary treated samples before and after ion exchange process were tabulated in Table 6.20 and 6.21. After the ion exchange experiments, COD and BOD values of domestic wastewater samples were reduced in the presence of clinoptilolite. Our experimental results show that 50% and 60% COD and BOD removal was obtained with the clinoptilolite.

Table 6.20. Preliminary and Primary Treated Samples Values

Values	Preliminary Treated Sample	Primary Treated Sample
BOD	300-500	270-450
COD	150-250	150-250
NH_4^+	40	40
Mg^{+2}	35	35
Ca^{+2}	33	33
K^+	27	27

Table 6.22. Equilibirum values for Synthetic Solution (%1 solid:solution ratio, 2-0.85 mm, pH of the solution < 7.0, shaking rate: 170 rpm)

	Initial NH_4^+ Concentration	Synthetic Solution				
		5	10	20	30	40
Equilibrium Values	NH_4^+	0.1	0.5	1.86	2.2	4.1
	Mg^{+2}	0.4	0.62	1.22	1.87	2.28
	Ca^{+2}	1.54	3.35	4.85	6.42	8.72
	K^+	2.94	3.45	5.96	8.65	10.8

Table 6.23. Equilibirum values for preliminary and primary treated samples (%1 solid:solution ratio, 2-0.85 mm, pH of the solution < 7.0, shaking rate: 170 rpm)

	Initial NH_4^+	Preliminary Treated Sample					Primary Treated Sample				
	Concentration	5	10	20	30	40	5	10	20	30	40
Equilibrium values	BOD	170	175	180	185	200	135	140	145	150	150
	COD	95	95	100	100	100	95	100	100	100	100
	NH_4^+	0.4	0.91	3.6	4.2	6.2	0.3	0.85	3.4	4	6
	Mg^{+2}	0.62	0.80	1.32	2.12	4.24	0.51	0.92	1.65	2.2	4.3
	Ca^{+2}	1.14	3.45	5.62	8.17	9.74	1.32	3.72	5.87	8.4	9.9
	K^+	2.84	4.84	6.82	9.36	11.6	2.94	4.51	7.2	9.86	12.01

For wastewater effluents, the higher NH_4^+ ion concentrations show the 84.5-86 % removal. And also, lower NH_4^+ ion concentrations show the 90-92 % removal. The generally accepted limit for free ammonium for receiving water is between 0.5 to 1 mg/lt. Our experimental results show that, ion exchange with clinoptilolite was applicable to reduce the ammonium concentration to acceptable levels before discharging. As a comprehended from the results, Gördes clinoptilolite was used as an ion exchange material for wastewater treatment and water reuse application. Also, exhausted clinoptilolite could de used as slow release fertilizer.

CHAPTER 7

CONCLUSION

In this study, the use of Gördes natural zeolite for removing NH_4^+ ion from wastewater effluent and from NH_4Cl solution was investigated under various conditions. The solid:solution ratio, initial concentration of the solution, presence of competing cation, particle size of the clinoptilolite, pH of the solution were selected as experimental parameters.

The obtained experimental results show that NH_4^+ uptake capacity decreases with increasing solid:solution ratio. Also, % NH_4^+ removal increases with increasing the solid:solution ratio. The increase in efficiency is expected result because of increasing the solid: solution contact surface. Highest amount of ammonium removal per gram zeolite was found in the solution having 1% solid: solution ratio.

The particle size of the clinoptilolite did not affect the NH_4^+ uptake capacity and % NH_4^+ removal. Total surface area of the clinoptilolite takes into account both external surface area of the particle and its internal surface area. The internal surface area is due to the pores and channels of the clinoptilolite. When reducing the particle size, the external surface area is considerably but not the internal surface area. Our experimental results show that the external surface area of clinoptilolite has an insignificant role in cation retention and that the internal sites are responsible for the cation exchange.

The initial concentration of the solution shows the significant effect on the ammonium exchange process. The obtained experimental results show that, ammonium uptake capacity increases with increasing initial ammonium ion concentration in the solution. The initial ammonium concentration provides the necessary driving force to overcome all mass-transfer resistances of ammonium between the aqueous and solid phases. Hence, higher initial ammonium concentration will have a beneficial effect on the uptake capacity. % NH_4^+ removal decreases with initial concentration of the solution. It would be expected that there would be some relationship between C_0 and the percentage of removed ammonium ion from solution since ion exchange of any cation by a cation exchanger is a function of the concentration of the cation in the solution.

Effective diffusion coefficients were calculated found from the experimentally determined uptake curves. It is noted that, effective diffusion coefficients slightly

change with different initial NH_4^+ ion concentration and particle size. The effective diffusion coefficient values were found as 2-4*10^{-12} m^2/s.

Our experimental results show that, the presence of competing cation was highly critical for the ammonium exchange process. Ammonium uptake capacity in the presence of potassium ion is less than in the presence of magnesium, and that in the presence of calcium ion. The effect of competing cation on the ammonium uptake capacity was explained with the free energies of hydration of the competing ions. Mg^{+2} with the largest hydration energy prefers the solution phase where it may satisfy its hydration requirements, and K^+ with the least hydration energy, prefers the zeolite phase. For this reason, magnesium ion had the least effect on the ammonium uptake capacity. The percentages of ammonium removal values in the presence of competing cation were lower than pure ammonium chloride solution. As comprehended from the results; potassium ion had the largest effect on the percentage of ammonium removal. Maximum removal percentage values were observed for the pure ammonium chloride solution.

Experimental results show that the ammonium uptake capacity is slightly reduced at pH values lower than 6. The slightly lower ammonium uptake capacities results obtained under low pH conditions may be due to the H^+-NH_4^+ competition for the exchange sites in the zeolite surface. Our experimental results show that optimum pH value was 7 for ammonium removal by zeolite.

In this study, a balance of equivalent of cations was constructed between the major exchangeable cations released to the solution phase and equivalent of change of ammonium ion in solution with and without competing cations. The differences found from NH_4^+ equivalent change and exchange cation equivalent change indicated 14 to 34% of NH_4^+ ions were adsorbed by physical adsorption and remaining was exchanged by cation.

Equilibrium data obtained have been found to fit both the Langmuir and Freundlich Model. Langmuir model provided excellent correlation of the experimental data yielding correlation coefficient values of R^2>0.995 compared to results for the Freundlich model where R^2≈0.90. From the plateau of the isotherms maximum exchange capacities were determined as 9.03, 8.76, 8.695 and 7.84 mg NH_4^+/gr for NH_4^+, NH_4^+-Mg^{+2}, NH_4^+-$Ca^{+2}$and NH_4^+-K^+, respectively. As a consequence of these results, the ammonium capacity of Gördes clinoptilolite was approximately 0.51meq/gr for pure ammonium chloride solution.

When comparing the removal of NH_4^+ ion from wastewater effluent and from NH_4Cl, the percent removal and the uptake capacity were lower for wastewater than for NH_4Cl for same solid: solution ratio and the same initial concentration. It is expected that in domestic wastewater, where the complexity of the system is high, several matter could influence the removal of specific target cations. In the preliminary treatment, only large objects are removed from the wastewater which cause the maintance and operational problem. Organic matter and suspended solid exist in the wastewater effluent. Two possible reasons exits why ammonium exchanges capacity of preliminary and primary treated samples lower than ammonium exchange capacity of pure ammonium chloride solutions. First reason could be explained with small suspended solid could block the pores of clinoptilolite, hence inhibiting access of ammonium ions to many of the internal fixed exchange sites. Another reason was the presence of organic matter might influnce the surface charge density of mobile ions within the clinoptilolite, which in turn would influence uptake and selectivity.

Experimental results show that the COD and BOD values of domestic wastewater samples were reduced in the presence of clinoptilolite. After ion exchange experiments, 50% and 60% COD and BOD removal was obtained with the clinoptilolite.

The SEM examination of used clinoptilolite exchange with domestic wastewater sample data indicates the inclusion of bacteriological debris. Giardia Intestinalis, which is the special microorganism found in wastewater, adhere to the surface of the clinoptilolite-rich minerals. As a comprehended from the results, clinoptilolite may be used for the removal of the microbiological constituents from wastewater effluents.

The generally accepted limit for free ammonium for receiving water is between 0.5 to 1 mg/lt. Our experimental results show that, ion exchange with clinoptilolite was applicable to reduce the ammonium concentration to acceptable levels before discharging. As a comprehended from the results, Gördes clinoptilolite was used as an ion exchange material for wastewater treatment and water reuse application. Also, exhausted clinoptilolite could be used as slow release fertilizer.

REFERENCES

Ackley, M., and Yang, R.T., "Diffusion in Ion Exchanged Clinoptilolites", *AlChE Journal*, 37 (11), 1991, pp. 1645-1656.

Ackley, M., Giese, R.F., Yang R.T., "Clinoptilolite: Untapped Potential for Kinetic Gas Separations", *Zeolites*, 12, 1992, pp. 780-788.

Ackley, M., and Yang, R.T., "Adsorption Characteristics of High-Exchange Clinoptilolites", *Industrial Engineering Chemistry Research*, 30, 1991, pp. 2523-2530.

Alsoy, S., "Natural Zeolites in Wastewater Treatment", M.Sc.Thesis, Izmir, 1993.

Blanchard, G., Maunaye, M., Martin, G., "Removal of Heavy Metals from Waters by Means of Natural Zeolites", *Water Research*, 18(12), 1984, pp. 1501-1507.

Booker, N.A., Cooney, E.L., Priestley, A.J., "Ammonia Removal from Sewage Using Natural Australian Zeolite", *Water Science and Technology*, 34(9), 1996, pp. 17-24.

Booker, N.A., Cooney, E.L., "Ammonia Removal from Wastewater Using Natural Australian Zeolite: I. Characterization of the Zeolite", *Separation Science and Technology*, 34 (12), 1999, pp. 2307-2327.

Booker, N.A., Cooney, E.L., "Ammonia Removal from Wastewater Using Natural Australian Zeolite: II.Pilot-Scale Study Using Continuous Packed Column Process", *Separation Science and Technology*, 34 (14), 1999, pp. 2741-2760.

Breck, D.W., Zeolite Molecular Sieves Structure, Chemistry and Use, Wiley-Interscience, New York, 1974.

Ciambelli, P., Corbo, P., Porcelli, C., Rimoli, A., "Ammonia Removal from Wastewater by Natural Zeolites. I. Ammonium Ion Exchange Properties of an Italian Phillipsite Tuff", *Zeolites*, 5, 1985, pp. 184-187.

Cincotti, A., Lai, N., Orru, R., "Sardinian Natural Clinoptilolites for Heavy Metals and Ammonium Removal: Experimental and Modeling", *Chemical Engineering Journal*, 84, 2001, pp. 275-282.

Çulfaz M., Yağız M., "Ion Exchange Properties of Natural Clinoptilolite: Lead-Sodium and Cadmium-Sodium Equilibria," *Separation and Purification Technology*, 00 (2003) 1-13.

Demir, A., Günay, A., Debik, E., "Ammonium Removal from Aqueous Solution by Ion Exchange Using Packed Bed Natural Zeolite", *Water SA*, 28(3), 2002, pp.329-335.

Dryden, H.T., Weatherley, L.R., "Aquaculture Water Treatment by Ion Exchange: Continuous Ammonium Ion Removal with Clinoptilolite", *Aquaculture Engineering*, 8 (2), 1989, pp. 109-126.

Dwairi, I.M., "Evaluation of Jordanian Zeolite Tuff as a Controlled Release Fertilizer for NH_4^+", *Environmental Geology*, 34(1), 1998, pp.1-4.

Dyer, A., Enamy, H., Towsend, R.P., "The Plotting and Interpretation of Ion Exchange Isotherms in Zeolite Systems", *Separation Science and Technology*, 16(2), 1981, pp. 173-181.

Dyer A., White K.J., "Cation Diffusion in the Natural Zeolite Clinoptilolite," *Thermochimica Acta*, 340-341 (1999) 341-348.

Green, M., Mels, A., Lahav, O., Tarre, S., "Biological-Ion Exchange Process for Ammonium Removal from Secondary Effluent", *Water Science and Technology*, 34(1-2), 1996, pp. 449-458.

Haralambous, A., Maliou, E., Malamis, M., "The Use of Zeolite for Ammonium Uptake", Water Science and Technology, 25 (1), 1992, pp. 139-145.

Helfferich, F., Ion Exchange, McGraw-Hill, New York, 1962.

Hlavay, J., Vigh, G.Y., Olaszi, V., Inczudy, J., "Investigations on Natural Hungarian Zeolite for Ammonia Removal", *Water Research*, 16(4), 1982, pp. 417-420.

Hedström, A., "Ion Exchange of Ammonium in Zeolites: A Literature Review", *Journal of Environmental Engineering*, 127(8), 2001, pp. 673-681.

Inglezakis, V.J., Grigoropoulou, H.P., "Applicability of Simplified Models for the Estimation of Ion Exchange Diffusion Coefficients in Zeolites", *Journal of Colloid and Interface Science,* 234, 2001, pp. 434-441.

Inglezakis, V.J., Handjiandreou, K.J, "Pretreatment of Natural Clinoptilolite in a Laboratory–Scale Ion Exchange Packed Bed", *Water Resource*, 35(9), 2001, pp. 2161-2166.

Inglezakis V.J., Loizidou M.D., Grigoropoulou H.P., "Equilibrium and Kinetic Ion Exchange Studies of Pb^{2+}, Cr^{3+}, Fe^{3+} and Cu^{2+} on Natural Clinoptilolite," *Water Research,* 00 (2001) 1-10.

Inglezakis V.J., Loizidou M.D., Grigoropoulou H.P., "Ion Exchange of Pb^{2+}, Cu^{2+}, Fe^{3+}, and Cr^{3+} on Natural Clinoptilolite: Selectivity Determination and Influence of Acidity on Metal Uptake," *Journal of Colloid and Interface Science*, 261 (2003) 49-54.

Inglezakis V.J., Zorpas A.A., Loizidou M.D., Grigoropoulou H.P., "Simultaneous Removal of Metals Cu^{2+}, Fe^{3+} And Cr^{3+} with Anions SO_4^{2-} and HPO_4^{2-} Using Clinoptilolite," *Microporous and Mesoporous Materials*, 61 (2003) 167-171.

Iznaga I.R., Gomez A., Fuentes G., Aguilar A., Ballan J., "Natural Clinoptilolite as an Exchanger of Ni^{2+}, NH_4^+ Ions Under Hydrothermal Conditions and High Ammonia Concentration," *Microporous and Mesoporous Materials*, 53 (2002) 71-80.

Jama, M.A., Yücel, H., "Equilibrium Studies of Sodium-Ammonium, Potassium-Ammonium and Calcium-Ammonium Exchanges on Clinoptilolite Zeolite", *Separation Science and Technology*, 24(15), 1990, pp. 1393-1415.

Jorgensen, S.E., "Ammonium Removal by Use of Clinoptilolite", *Water Research*, 10, 1976, pp. 213-224.

Jung, J.Y, Pak, D., Shin, H.S., "Ammonium Exchange and Bioregeneration of Bio-Flocculated Zeolite in Sequence Batch Reactor", *Biotechnology Letters,* 21, 1999, pp. 289-292.

Kallo, D., "Wastewater Purification in Hungary Using Natural Zeolites", Natural Zeolites 93: Occurrence, Properties, Use, Ming, D.W., and Mumpton, F.A., International Committee on Natural Zeolites, New York, 1995, pp. 341-350.

Kesraoui-Ouki, S., Cheeseman, C.R., Perry, R., "Natural Zeolite Utilisation in Pollution Control: A Review of Application to Metals' Effluents", *Journal of Chemical Technology & Biotechnology*, 59, 1994, pp. 121-126.

Klieve, J.R., Semmens, M.J., "An Evaluation of Pretreated Natural Zeolites for Ammonium Removal", *Water Research*, 14, 1979, pp. 161-168

Komarowski, S., Yu, Q., "Ammonium Ion Removal from Wastewater Using Natural Australian Zeolite: Batch Equilibrium and Kinetic Studies", *Water Science and Technology*, 34(9), 1996, pp. 17-24.

Koon, J.H., Kaufman, W.J., "Ammonia Removal from Municipal Wastewaters by Ion Exchange", *J.Wat. Pollut. Control Fed.,*47 (3), 1975, pp. 448-464.

Krivacsy, Z., Hlavay, J., "A Simple Method for the Determination of Clinoptilolite in Natural Zeolite Rocks", *Zeolites,* 15(6), 1995, pp. 551-555.

Lahav, O., Green, M., "Ammonium Removal Using Ion Exchange and Biological Regeneration", *Water Research*, 32(7), 1998, pp. 2019-2028.

Langella, A., Pansini, M., Cappelletti, P., " NH_4^+, Cu^{+2}, Zn^{+2}, Cd^{+2} and Pb^{+2} exchange for Na^+ in a sedimentary clinoptilolite, North Sardinia, Italy", *Microporous and Mesoporous Material*, 37, 2000, pp. 337-343.

Liberti, L., "Nutrient Removal and Recovery from Wastewater by Ion Exchange", *Water Research*, 15(3), 1981, pp. 337-342.

Liberti, L., Helfferich, F., G., Mass Transfer and Kinetics of Ion Exchange, Martinus Nijhoff Publishers, 1983.

Lin, H.S., Wu, C.L., "Ammonia Removal from Aqueous Solution by Ion Exchange", *Ind.Eng.Chem.Res.* 35, 1996, pp. 553-558.

Metcalf and Eddy, Wastewater Engineering, McGraw Hill, New York, 1991.

Metropoulos, K., Maliou, E., "Comparative Studies between Synthetic and Natural Zeolites for Ammonium Uptake", *J. Environmental Science and Health*, 28(7), 1993, pp. 1507-1518.

Milan, Z., Sanchez, E., "Ammonia Removal from Anerobically Treated Piggery Manure by Ion Exchange in Columns Packed with Homoionic Zeolite", *Chemical Engineering Journal*, 66, 1997, pp. 65-71.

Rodriguez, G., Salvador, A.R., "Thermal and Cation Influence on IR Vibrations of Modified Natural Clinoptilolite", *Microporous and Mesoporous Material*, 20, 1998, pp. 269-281.

Rodney, M., "Biofilms: Microbial Life on Surfaces", *Emerg Infect Dis*, 8 (9), 2002, pp.1-14.

Ruthven D.M., Principles of Adsorption Processes ,John Wiley and Sons, 1984.

Ruthven D.M., Diffusion in Zeolites, John Wiley and Sons, 1992.

Semmens, M.J., Seyfarth, M., "The Selectivity of Clinoptilolite for Certain Heavy Metals", Natural Zeolites: Occurrence, Properties, Use, Sand, L.B., and Mumpton, F.A., Pergamon, New York, 1978, pp. 517-526.

Semmens, M., Klieve, J., Schnobrich, D., "Modeling Ammonium Exchange and Regeneration on Clinoptilolite", *Water Research*, 15(6), 1981, pp. 655-666.

Sherman, J.D., "Ion Exchange Separations with Molecular Sieve Zeolites", Adsorption and Ion Exchange Separations, AlChE Symposium Series No: 179, The American Institute of Chemical Engineers, 1978, pp. 98-116.

Şenatalar, A.E., Sirkecioğlu, A., "Removal of Ammonium Ion from Wastewaters by Bigadiç Clinoptilolite", *Turkish Journal of Engineering and Environmental Sciences*, 19, 1995, pp. 399-405.

Tanaka, H., Yamasaki, N., Muratani, M., Hino, R., "Structure and Formation Process of (K, Na)-Clinoptilolite", *Materials Research Bulletin*, 2189, 2003, pp.1-10.

Tarasevich, Y.I., Krysenko, D.A., Polyakov, V.E., "Selectivity of Low and High Silica Clinoptilolite with respect to Alkali and Alkaline Earth Metal Cations", *Colloid Journal*, 64(6), 2002, pp. 759-764

Tomazovic, B., Ceranic, T., "The Properties of the NH_4-Clinoptilolite: Part 1", *Zeolites*, 16, 1996, pp. 301-308.

Tomazovic, B., Ceranic, T., "The Properties of the NH_4-Clinoptilolite: Part 2", *Zeolites*, 16, 1996, pp. 309-312.

Top, A., "Cation Exchange (Ag^+, Zn^{+2}, Cu^{+2}) Behaviour of Natural Zeolite Mineral, Clinoptilolite", M.Sc.Thesis, Izmir, 2001.

Towsend, R.P, "Ion Exchange in Zeolites: Some Recent Developments in Theory and Practice", *Pure & Applied Chemistry*, 58 (10), 1986, pp. 1359-1366.

Tsitsishvili, G.V., Andronikashvili, T.G., Kirov, G.N, Filizova, L.D., Natural Zeolites, Ellis Horwood, New York, 1992.

Turan, M., Çelik, M.S., "Regenerability of Turkish Clinoptilolite for Use in Ammonia Removal from Drinking Water", *Water Science and Technology*, 34(9), 1996, pp. 17-24.

Ülkü, S., "Application of Natural Zeolite in Water Treatment", Türk-Alman Çevre Sempozyomu, Çevre 84, Umvelt 84, V. Deutch-Turkisches Symposium fur Umweltingeniurwesen.

Ülkü, S., Kaban Y., Ağace, M., Topçu, S., Türkan, S., Alkan N., "Porsuk Çayının Kirlilik Durumu ve Tabii Zeolit Yataklarının Su Tasfiyesinde Kullanılması", TÜBİTAK VII. Bilim Kongresi Bildiri Kitabı, Çevre Araştırma Grubu, Ankara, 1984, pp. 201-215.

Wilkin, R.T., Barnes, H.L., "Thermodynamics of Hydration of Na& K Clinoptilolite to 300 °C", *Physical Chemistry Minerals*, 26, 1999, pp. 468-476.

Yaşyerli, S., Ar, I., Doğu, G., Doğu, T., " Removal of Hydrogen Sulfide by Clinoptilolite in a Fixed Bed Adsorber", *Chemical Engineering and Processing*, 00 (2002) 1-8.

Yücel, H., and Çulfaz, A., "Yerel ve Doğal Klinoptilolit Zeolitin Fiziksel ve Kimyasal Özellikleri", *Doğa Bilim Dergisi*, 9(3), 1985, pp. 288-296.

Zamzow, M.J., and Murphy, J.E., "Removal of Metal Cations from Water Using Zeolites", *Seperation Science and Technology*, 27(14), 1992, pp. 1969-1984.

APPENDIX

A.1 Ammonium Selective Electrode

The ammonia selective electrode is the gas permeable hydrophobic membrane. It can be used to measure the ammonium ion after conversion to ammonia. Ammonium is converted to ammonia by raising pH to above 11 with strong base caustic solution. The ammonia-selective electrode method is applicable over the range of 0.03 to 1400 mg/L. ammonium in domestic and industrial wastewaters. In this system, all the measurements should be performed at constant temperature. 2 °C temperature changes give rise to a 1 % percent error in the experimental result. Dosimat Unit consists of glass cylinder, precision pump, piston and keyboard. By using precision pump, high accurate dispensing of the smallest volume is achieved. With the keyboard and manual setting of the dispensing rate, titrations can be performed easily. And also, this device can be used to dilute the standard ammonium chloride solution for preparing the synthetic solution and measure ion concentration by standard addition method. Standard addition method was used to determine the ammonium concentration in the solution. In the standard addition method, a linear relationship between voltage and log concentration is assumed. In this method, firstly initial voltage of the solution that was obtained from the batch experiment is measured. There are 5 small amount of addition of standard ammonium chloride solution. After each addition, the voltage of the solution is changed. And after required time for stable reading, voltage is measured. Next addition is done automatically. After 5 measurements, typical graph is obtained which shows the electrode voltage response as a function of the logarithm concentration. The sample concentration is calculated with the related equation 1.

$$C_{NH_4^+} = 10^{\left[\frac{U(0)-E(0)}{Slope}\right]}$$

where ;

U (0): initial voltage of the solution.

E (0): intercept of the plot

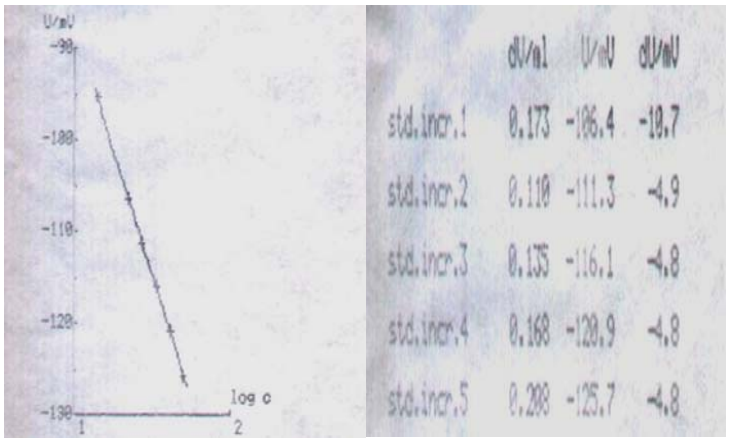

Figure A.1.1. The electrode voltage versus logarithm concentration plot result by using standard addition method.

The calibration curve for direct method was given in A.1.2. This calibration curve was useful for compare the direct and standard addition methods.

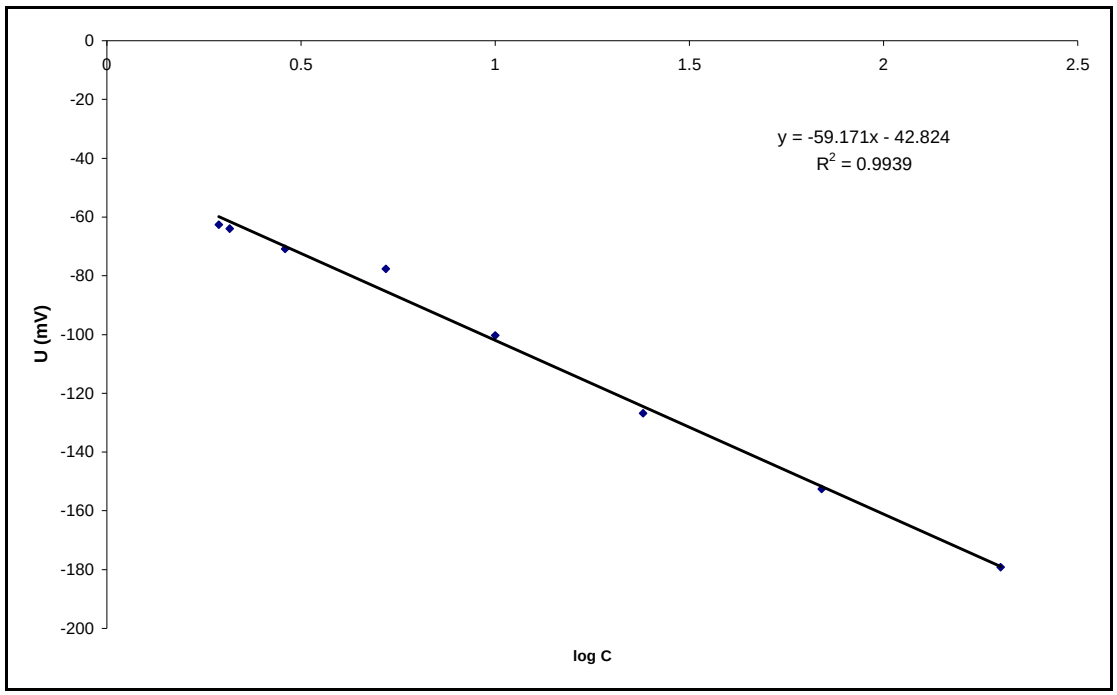

Figure A.1.2. Ammonium Ion Calibration Curve by using Direct Method

A.2 ICP Methods

Inductively Coupled Atomic Emission Spectroscopy (ICP-AES 96, Varian) was used to measure the competing cation concentration in the solution after equilibrium. In the ICP analyses, the nitric acid stock solution was prepared by mixing 110 ml of 65 wt% of HNO_3 with deionized water which adds up to 1 liter of solution. After this mixing with 1 lt deionized water, 10 wt% of HNO_3 solution was obtained. The sample solutions which was obtained from the batch experiment can be diluted by adding deionized water to the mixture of 10 ml of sample solution and 10 ml of 10 wt% of HNO_3 which adds up to 100 ml. The final solution contains 1 wt% of HNO_3 and hence the solution was diluted by ten fold. ICP standard solution was prepared by using 100 ml of 1000 ppm ICP multi-element standard solution. Then, this standard solution was diluted to 100 ppm by taking 10 ml of this standard solution, 10 ml of 10 wt% of HNO_3 and 80 ml of deionized water. After that, 100 ml of 100 ppm ICP standard solution was obtained. In the experiment, the dilution of the solutions was made by using the 100 ppm ICP standard solution. And also, the blank sample was prepared by using 10 ml of 10 wt% of HNO_3 and 90 ml of deionized water.

A.3. Materials Characterization

A.3.1 X-Ray Results:

The original clinoptilolite minerals were characterized using different instrumental techniques. Identification of the crystalline species present in the clinoptilolite-rich rocks was achieved by X-ray diffraction analysis. X-ray diffraction patterns were obtained with Philips X'Pert Pro diffractometer (CuKα radiation, 2θ=2-45°). X-ray diffactograms of the clinoptilolite sample was given in Figure A.3.1. The clinoptilolite mineral from Gördes is a mixture of the clinoptilolite, quartz and halloysite. The mineralogical features of the clinoptilolites samples were determined by using RIR factors (reference intensity ratio, Chung) based on an external standard method. According to this method, clinoptilolite sample has a purity of more than 64% clinoptilolite, quartz and halloysite being the major impurities. The clinoptilolite sample of the three major peaks was 9.93, 22.47 and 30.15, respectively.

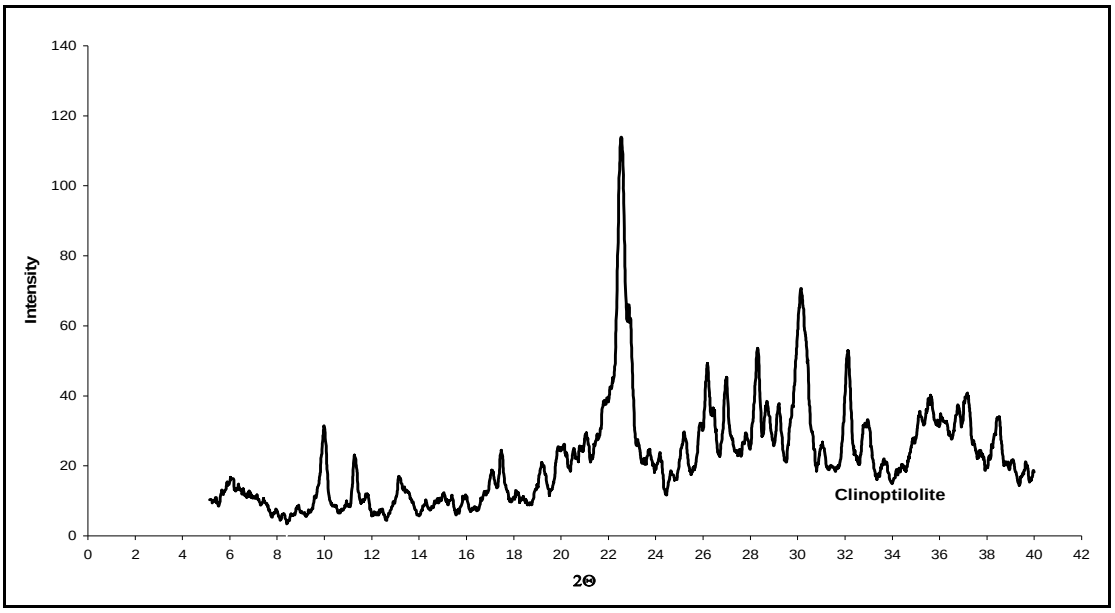

Figure A.3.1. X-ray diffraction patterns of Gördes clinoptilolite sample.

X-ray diffactograms of the clinoptilolite sample before and after ion exchange experiments were given in Figure A.3.2. The ammonium ion can make both ionic and hydrogen bond with the framework of zeolite, depending on the electrostatic characteristic of cationic sites (Tomazovic et al, 1996). According to model given by Koyama and Takeuchi, the position M (1) ammonium ion will be bonded predominantly by the hydrogen ion. In the M (2) position, ammonium ion can be connected by both ionic and hydrogen bond. The position M (3), ammonium ion is bonded only ionic bond due to the strong electrostatic field in this position. Finally, ammonium ion will be connected by hydrogen bond because of the absence of an electrostatic field. The presence of light NH_4^+ (I) ions on the cationic sites affected the intensity of maxima of the ammonium- clinoptilolite in the diffactograms of the samples (Figure A.3.2). The intensities are increased considerably in the presence of these cationic sites.

A.3.2. SEM/EDX Results

The crystalline morphology of clinoptilolite samples was investigated by using the Scanning Electron Microscopy (Philips, XL30). Electron microscopy reveals numerous details of the structure of the zeolitic rocks and allows a through a study of crystalline forms of microcrystals grown in voids. A scanning electron photomicrograph of the crystalline morphology of Gördes clinoptilolite was given in Figure A.3.3. These

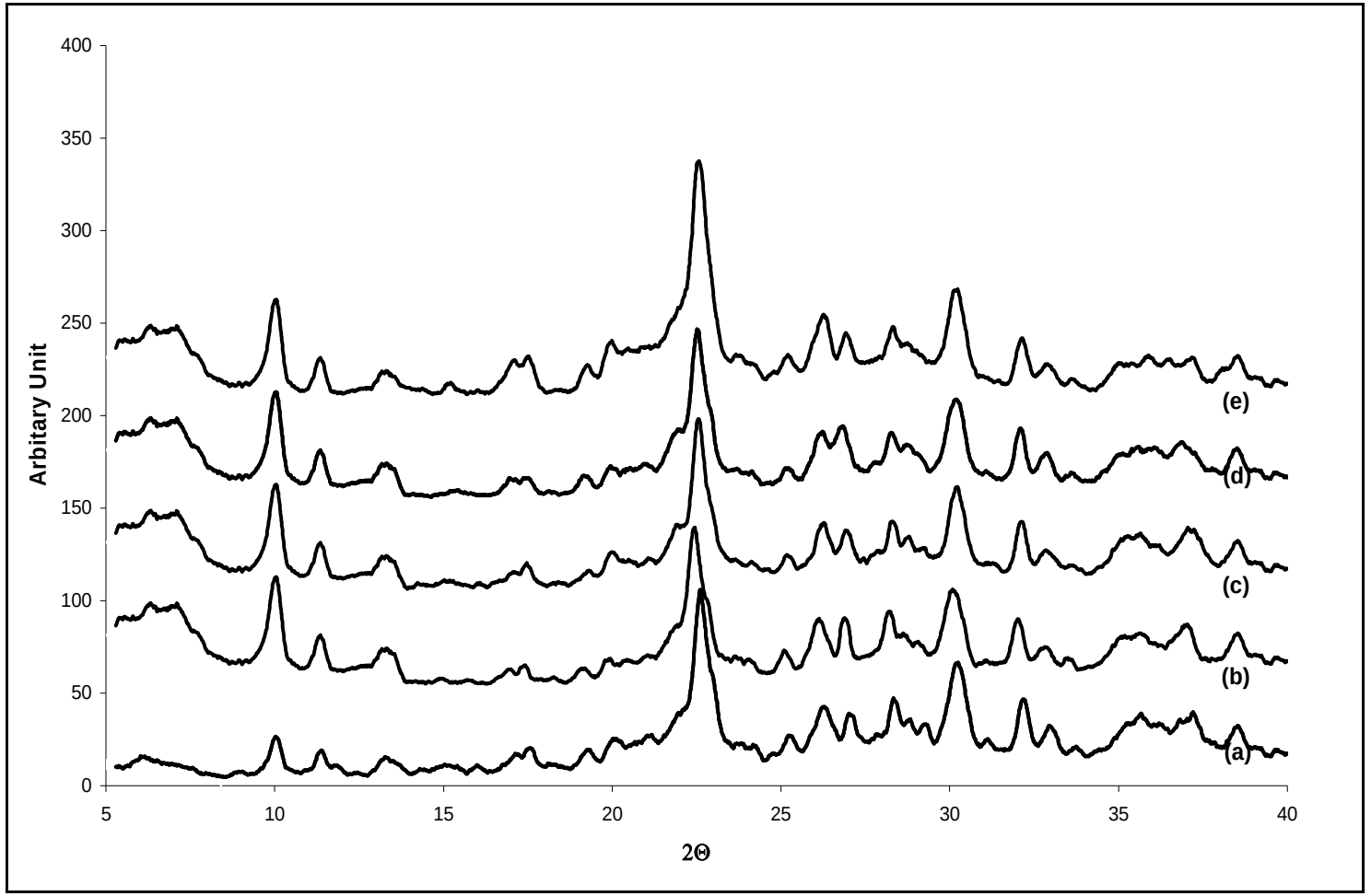

Figure A.3.2. X Ray difractograms for various clinoptilolite samples (a) Natural clinoptilolite(2-0.85 mm), (b)NH_4^+ exchange clinoptilolite, (c) NH_4^+-K^+ exchange76 clinoptilolite, (d) NH_4^+-Ca^{+2} exchange clinoptilolite, (e) NH_4^+-Mg^{+2} exchange clinoptilolite

crystals appear only in cavities in the raw material sample and it is characterized by thin platy crystals.

Figure A.3.3 shows the SEM images of the clinoptilolite rich mineral samples before and after the ion exchange process. This figure indicates that clinoptilolite crystal structure does not change after the ion exchange process. EDX results of the clinoptilolite samples before ion exchange process were tabulated in Table A.3.1. The main exchangeable cation (Na, Mg, K, Ca) are present in the structure of Gördes clinoptilolite. K and Ca are the major exchangeable cations in the structure.

Figure A.3.3 (e) and (f) shows SEM images of the clinoptilolite rich mineral samples after the ion exchange process with primary and secondary treated wastewater effluents. The SEM examination of used clinoptilolite sample data indicates the inclusion of bacteriological debris. Microbial flocs on the surface of the zeolite were seen in Figure A.3.3 (f). Also, Figure A.3.3 (e) indicates that, Giardia Intestinalis adhere to the surface of the clinoptilolite- rich minerals. As a comprehended from the results, clinoptilolite may be used for the removal of the microbiological constituents from wastewater effluents.

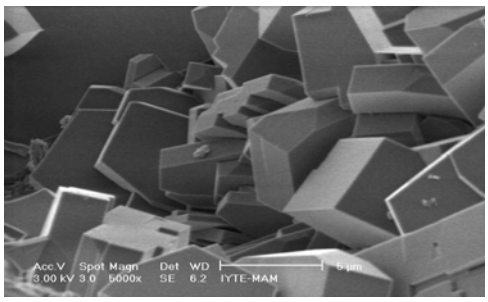

(a)

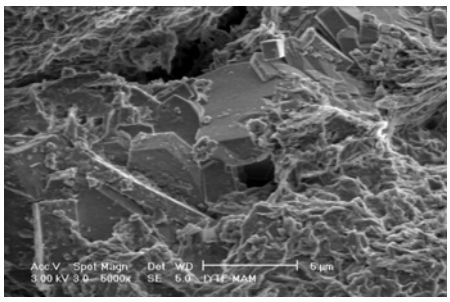

(b)

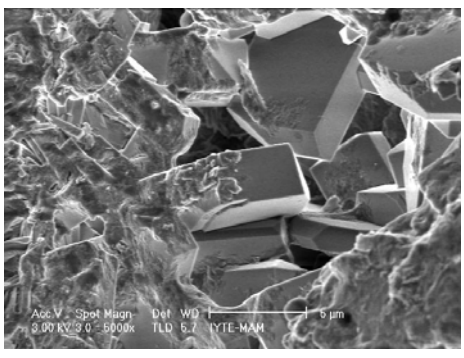

(c)

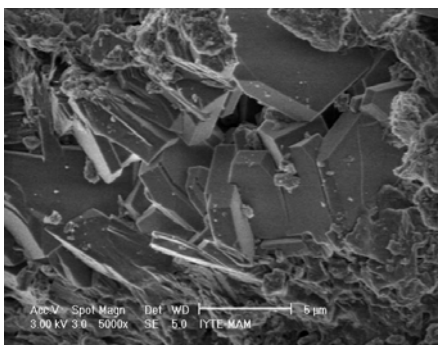

(d)

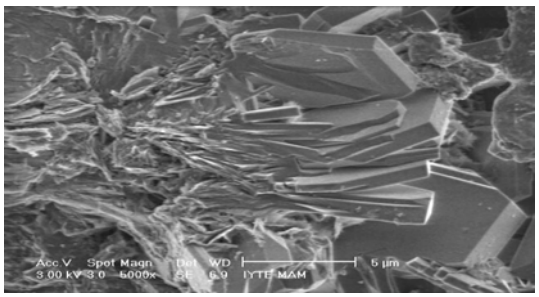

(e)

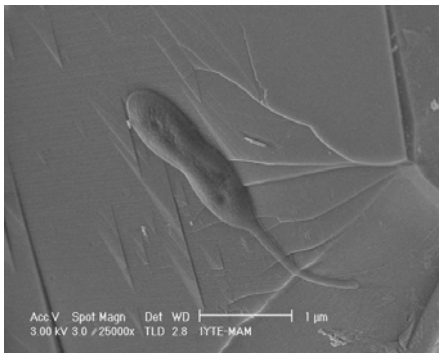

(f)

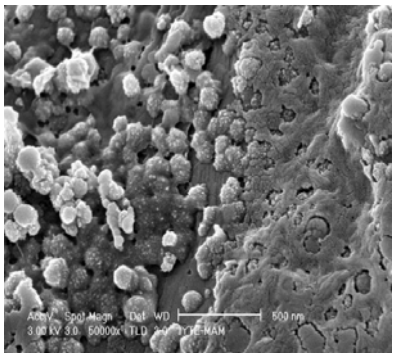

(g)

Figure A.3.3. (a) SEM image of the clinoptilolite samples (2-0.85), Magnification: 5000x (b) SEM image of the clinoptilolite after ion exchange process with 10 ppm pure ammonium chloride (2-0.85), Magnification: 5000x,(c) SEM image of the clinoptilolite after ion exchange process with 10 ppm ammonium chloride with competing cation Ca^{+2} (2-0.85), Magnification: 5000x,(d) SEM image of the clinoptilolite after ion exchange process with 10 ppm ammonium chloride with competing cation K^{+} (2-0.85), Magnification: 5000x,(e) SEM image of the clinoptilolite after ion exchange process with 10 ppm ammonium chloride with competing cation Mg^{+2} (2-0.85), Magnification: 5000x. (f), (g) SEM images of the clinoptilolite rich mineral samples after the ion exchange process with primary and secondary treated wastewater effluents.

Jung et al., (1999) investigated the roles of biofilm in the ammonium exchange and bioregeneration. Also, they studied ammonium exchange and bioregeneration of bio-flocculated zeolite in the biological nitrogen removal processes. Bio-flocculation was observed using the scanning electron microscope. SEM micrograhs of the biofilm on the zeolite surface were given in Figure A.3.4. Microorganisms grown on the surface of the zeolite were seen in Figure A.3.4 (C, D). Powdered zeolite of sizes smaller than 1 μm were branched and entrapped by microorganisms (Figure A.3.4-E, F).

Rodney et al., (2002) invesitigated the microbial life on different surfaces. Microorganisms attach to surfaces and develop biofilms. A biofilm is an assemblage of

microbial cells that is irreversibly associated (not removed by gentle rinsing) with a surface. Biofilms may form on a wide variety of surfaces, including living tissues, indwelling medical devices, industrial or potable water system piping, or natural aquatic systems. The variable nature of biofilms can be illustrated from scanning electron micrographs of biofilms from an industrial water system and a medical device, respectively (Figures A.3.5 a and b). The water system biofilm is highly complex, containing corrosion products, clay material, fresh water diatoms, and filamentous bacteria. The biofilm on the medical device, on the other hand, appears to be composed of a single, coccoid organism and the associated extracellular polymeric substance (EPS) matrix.

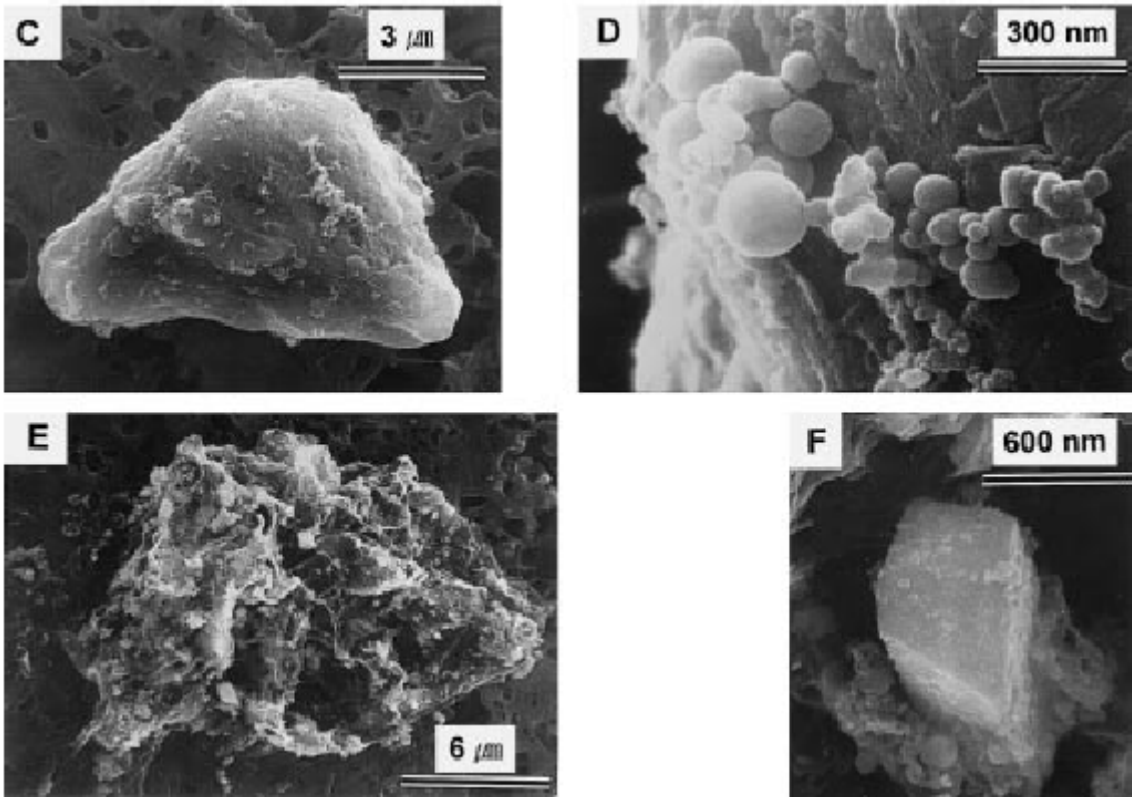

Figure A.3.4 SEM micrographs of the biofilms on the zeolite surface. (C-D) Attached microorganisms on the zeolite surface. (E-F) Entrapment of small particle zeolite in the microbial floc.(Jung et al., (1999)

From the literature results, we concluded that, microbial organisms were grown on the clinoptilolite surface. Our SEM micrographs show the good agreement with the literature SEM micrographs.

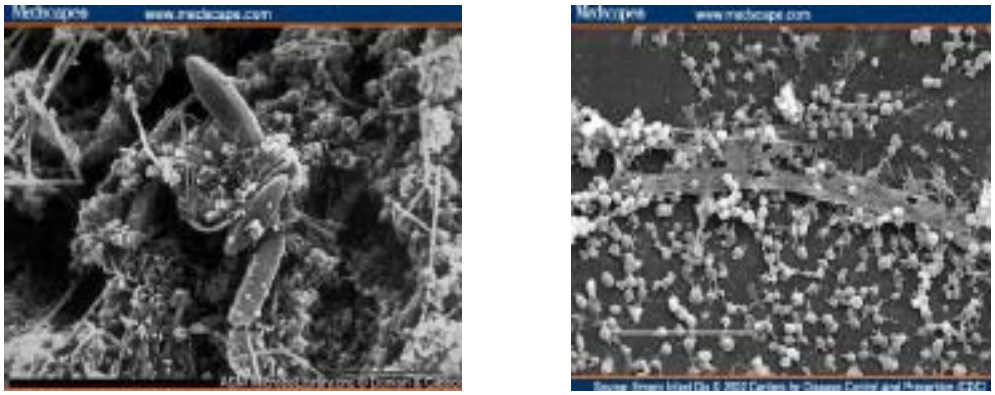

(a) (b)

Figure A.3.5 SEM micrographs of the biofilms on the different surface. (a)Biofilms from an industrial water system, (b) Biofilms on the medical device (Rodney et al., (2002))

Table A.3.1. Composition of the clinoptilolite (2-0.85 mm)

ELEMENT	Wt%
O	50.21
Na	0.944
Mg	1.15
Al	7.6
Si	34.83
K	3.39
Ca	1.87
TOTAL	100

A.3.3 FTIR Results

The IR absorption measurements were carried out using a Fourier Transform IR (FTIR) spectrophotometer (Shimdzu, 8201). FTIR spectra can be useful in obtaining crucial information about the structure, the channel size and the cation substitution (Si^{+4} by Al^{+3}), in the tetrahedral sites of zeolite minerals. The bands occurring in the FTIR spectra of zeolites can be characterized as follows :(Breck, 1974)

1. Bands due to the Si–O–Si and Si–O–Al vibrations, in the regions 1200–950/cm and 420–500/ cm. In the first region (1200–950/cm) the strongest vibration band appears. It is found in all zeolites due to the internal tetrahedron vibrations, and is assigned to a T–

O stretching mode. In the second region (420–500/cm) there is the next strongest band that is assigned to a T–O bending mode.

2. Bands due to presence of zeolite water. The three typical bands observed are the broad band, characteristic of hydrogen-bonded OH to oxygen ions at about 3440/cm, the sharp band typical of isolated OH stretching vibration at 3619/cm, and the usual bending vibration of water at 1640/cm.

3. Bands due to pseudo-lattice vibrations found in the region 500–800/cm. These vibrations are insensitive to the nature of the channel cations, as well as to the Si/Al ratio.

The FTIR spectra in the wave number range from 400 to 4000/cm were obtained with the use of the KBr pellet technique. Typical pellet contains 1-2 %wt sample in KBr and was prepared by 0.004 mgr zeolite powder with 0.2 mgr of KBr. The clinoptilolite minerals were kept in desiccator for several weeks and IR spectrums were taken. An IR spectrum of original clinoptilolite sample was represented in Figure A.3.6. Vibrations bands of the sample were shown in Table A.3.2.

Table A.3.2. Assignment of Vibrations Bands for the Gördes Clinoptilolite

Vibration modes	Wave Number (cm^{-1})
	Original Gördes Sample
Internal tetrahedra bending	468
External tetrahedra bending	607
External tetrahedra sym. stretching	796
External tetrahedra asym. stretching	1056
Internal tetrahedra asym. stretching	1215
O-H bending	1640

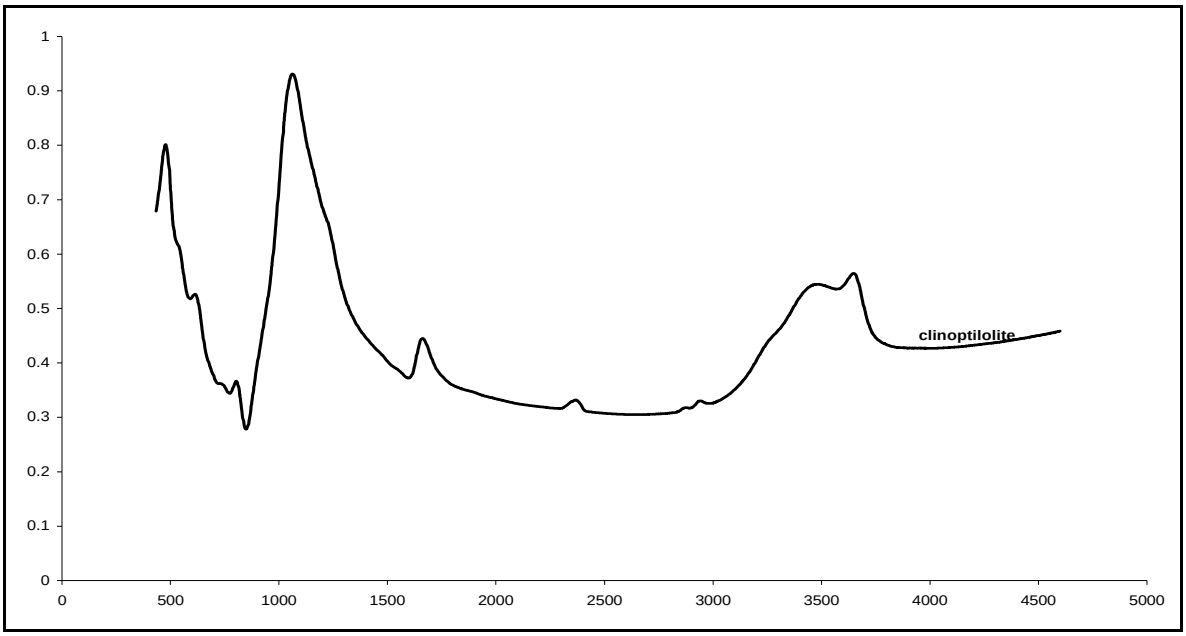

Figure A.3.6 IR spectra of Original Gördes Clinoptilolite sample

Figure A.3.7 shows the Infrared spectra of the ammonium exchange clinoptilolite. As stated in the literature, ammonium ion has band at 1484-1390 cm^{-1} (NH_4 deformation). According to the Figure A.3.5, ammonium can be seen on IR band near 1400 cm^{-1}. From this result, ammonium exchange with exchangeable cation of the clinoptilolite.

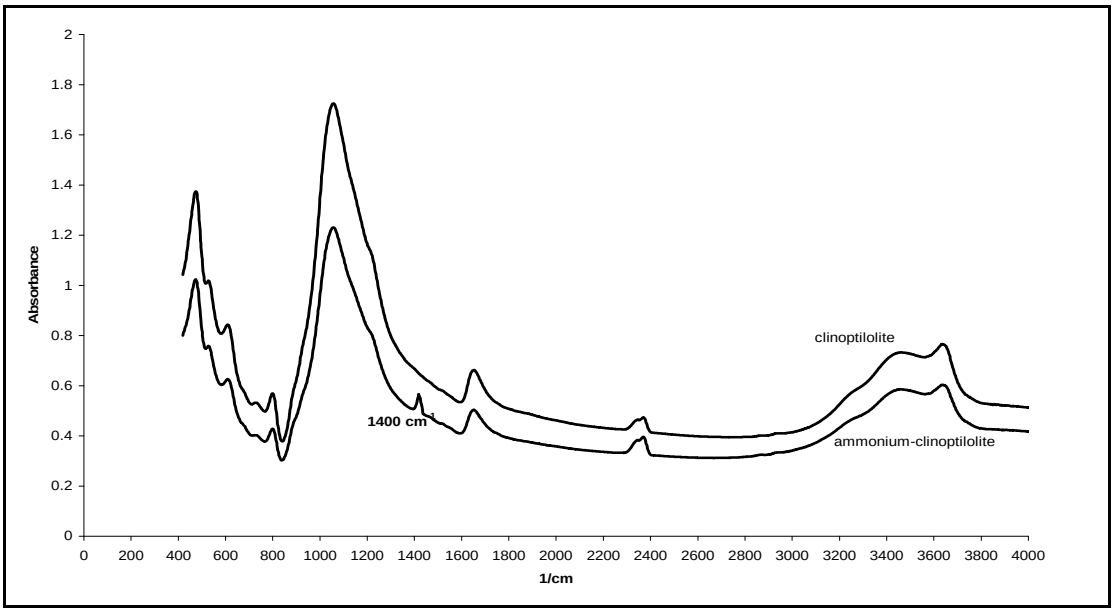

Figure A.3.7 Infrared spectra of the Ammonium Exchange Clinoptilolite.

A.3.4 TGA-DTA-DSC Results:

Differential Scanning Analysis (DSC), Thermogravimetric Analysis (TGA) and Differential Thermal Analysis give information about the dehydration properties of zeolites. Thermal behaviour of original clinoptilolite rich samples were established by DSC (DSC 50, Shimadzu), DTA (DTA 50, Shimadzu), TGA (51/52 H, Shimadzu). The zeolite samples was heated in a dry N_2 stream up to 1000 °C at a heating rate of 10 °C/min. TGA curves of the clinoptilolite sample was given in Figure A.3.8. In TGA method, water content of the clinoptilolite was examined by using the procedure outlined Knowlton and White. Based on their study "external" water released up to 85 °C, "loosely bound" water is lost rapidly up to 185 °C. After 285 °C the clinoptilolite started to loose its "tightly bound" water. After 700 °C there is no noticeable weight loss takes place in the structure. The percent of lost of "external" water, "loosely and tightly bound water" was given in Table A.3.3. External water, loosely bound and tightly bound water content in sample were about % 2.21, %5.54 and 0.89%, respectively.

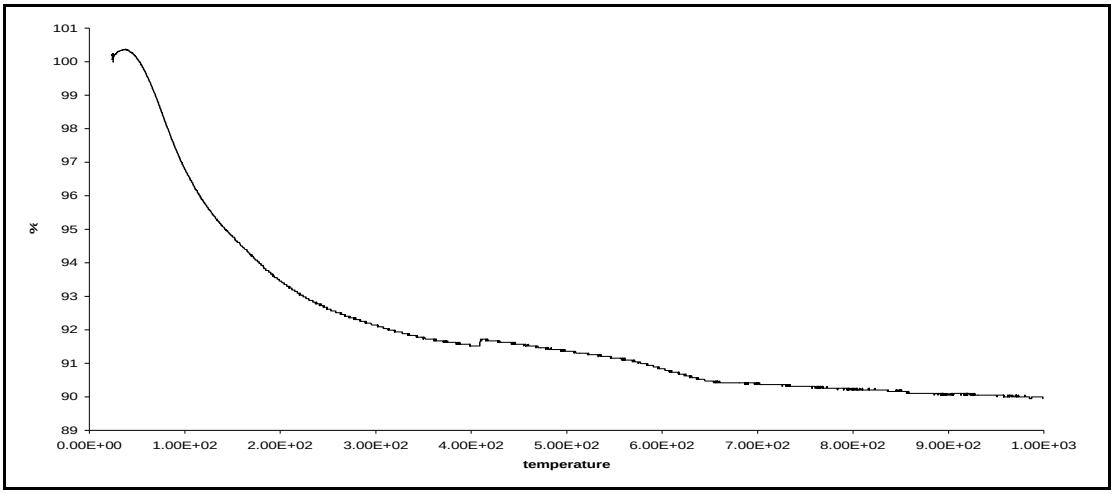

Figure A.3.8. TGA curve of the clinoptilolite rich mineral from Gördes Region

Table A.3.3 % Weight losses of original clinoptilolite mineral

Natural Zeolite	< 85 °C	85-285 °C	285-500 °C	> 500 °C	Total
Gördes	2.21	5.54	0.89	1.42	10.06

In DTA curves, low temperature endotherm represents the loss of water while the high temperature endotherm represents conversion of the zeolite to another

amorphous or crystalline phase. The high temperature exotherm represents the loss of structure. DTA curve of the clinoptilolite sample was given in Figure A.3.9. The DTA patter of sample indicated that clinoptilolite was stable toward dehydration. The sample has broad endotherm, which is the characteristic of natural zeolites. At higher temperatures second endotherm exhibits but it was not certain as the main endotherm indicates the conversion of zeolite to another amorphous or crystalline phase. On the DTA curve, Gördes region shows broad endotherm at 97.8 °C.

DSC curve for clinoptilolite samples was given in Figure A.3.10. In the DSC curve of the Gördes clinoptilolite sample broad endotherm was observed in 74.59 °C

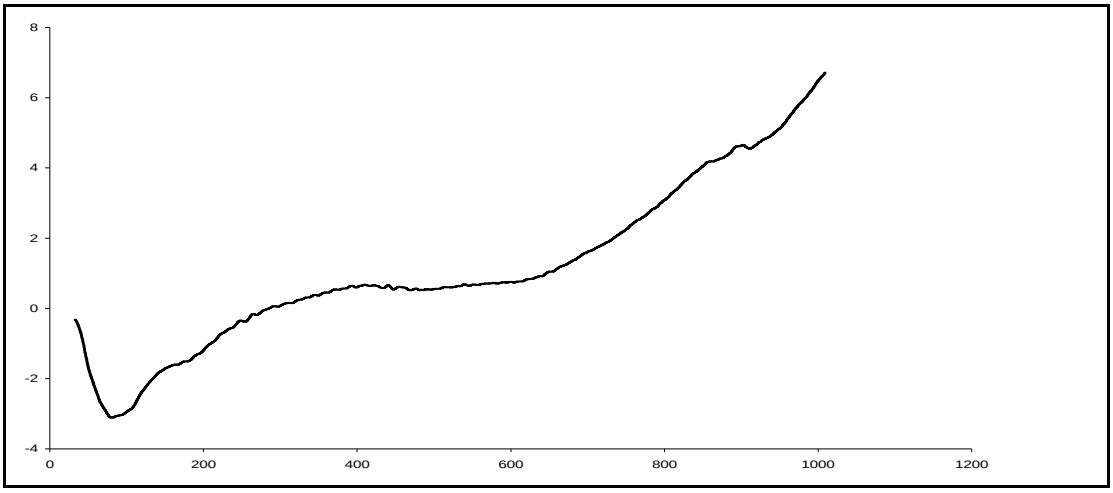

Figure A.3.9 DTA curve of clinoptilolite from Gördes Region

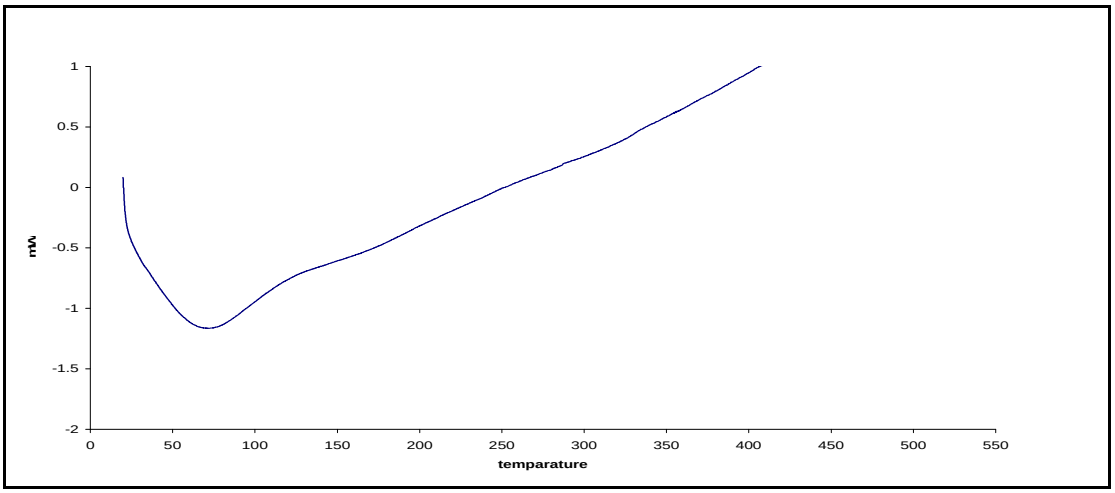

Figure A.3.10 DSC curve of the Gördes clinoptilolite sample

A.3.5 Adsorption Analysis

Adsorption related properties of clinoptilolite sample were determined. Adsorption Isotherms of clinoptilolite sample by N_2 at 77 K was given in Figure A.3.11. Surface area of the sample was determined from BET and Langmuir Models.

According to the IUPAC classification, clinoptilolite samples were shown the characteristic Type IV isotherm. The Type IV isotherm, whose region is closely related to the Type II isotherm, tends to level off at high relative pressures. It exhibits a hysteresis loop, the lower branch of which represents measurements obtained by progressive addition of gas of the adsorbent, and the upper branch by progressive withdrawal. The hysteresis loop is usually associated with the filling and emptying of the mesopores by capillary condensation. The summarized data for N2 adsorption of clinoptilolite were given in Table A.3.4.

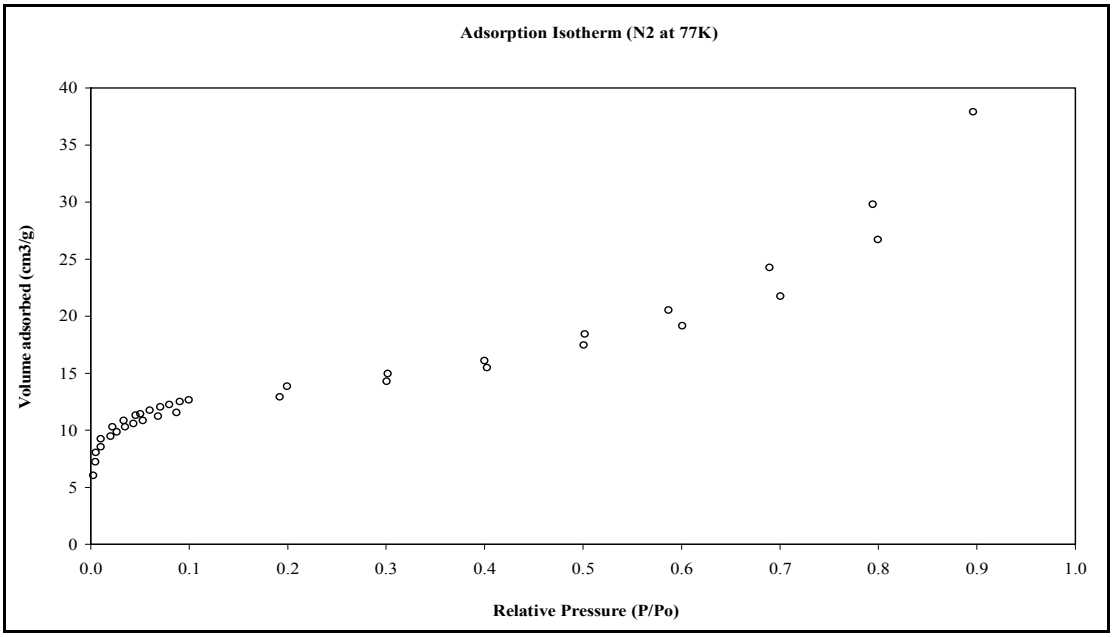

Figure A.3.11 N2 Adsorption Isotherm of Gördes Clinoptilolite

Table A.3.4 Summary of adsorption and desorption measurements for the clinoptilolite

Single Point Surface Area at P/P_o = 0.30167021	45.4675 m^2/g
BET Surface Area	45.5362 m^2/g
Langmuir Surface Area	65.1663 m^2/g
Micropore Area	17.3945 m^2/g
Micropore Volume	0.009144 cm^3/g
Median Pore Diameter *(H – K Method)*	9.2182 Å
Micropore Surface Area (Astakhov) *(D-A Method)*	64.017235 m^2/g

A.4 Design of Experiment

Factorial designs are widely used in experiments involving several factors where it is necessary to study the joint effect of the factors on a response. There are several special cases of the general factorial design that are important because they are widely used in research work. The most important of these special cases is *k* factors, each at only two levels. These levels may be quantitative, such as two values of temperature, pressure or time; or the may be qualitative, such as two machines, two operators, the "high" or "low" levels of a factor.

The 2^k design is particularly useful in the stages of the experimental work, when there are likely to be many factors to be investigated. In this study, 2^4 factorial design can be used, which suppose that four factors A, B, C and D. The four factors are given as follows:

(A) Concentration of solution
(B) Grain size of the zeolite particle
(C) Solid: Solution ratio
(D) Competing cation

To calculate the 2^4 factorial designs, Design of Expert 6.0.10 computer program is used. For this reason, the factors and level can be identified at two levels (low and high level). In order to be able to construct design matrix, 16 runs were preformed. In each case, ANOVA model was selected to compute ammonium concentration response data. As it can be seen from the ANOVA results (Table A.4.2), the model F value 3137, the model is significant. Values of Prob>F less than 0.05 indicates model terms are significant. In this case, A, C, D, AC, AD are significant model terms as can be seen from the ANOVA table.

The analysis of the experimental data by constructing a normal probability plot of effect estimates. The normal probabilities of these effects were shown in Figure A.4.1, A.4.3 and A.4.5. After interpreting the normal probability results, main effects were computed. The percent of contribution, sum of squares, degrees of freedom and probability result were given in Table A.4.3, A.4.5 and A.4.7. The main effects of A, C and D and the interaction effects AC, AD were plotted in Figure A.4.2., A.4.4. and A.4.6.

Table A.4.1. Summary Design Matrix for Ammonium Concentration

Factor	Name	Units	Type	Low Actual	High Actual
A	Concentration	mg/lt	numeric	10	50
B	Grain Size	mm	numeric	2-0.85	2.8-2.0
C	Solid: Solution ratio	gr/gr	numeric	1/100	1/20
D	Competing Cation	type	categorical	pure	Ca^{+2},Mg^{+2},K^{+}

In the half normal probability plot, the effects that lie along the line are negligible. The large effects are far from the line, which is defined as the main effects. The important effects that emerge from this analysis are the main effects of A, C and D and the AC, AD interactions. These interactions are the key to solving the problem. According to the interaction graph, AD interaction that the concentration effects is very small when the competing cation is at high level and very large when the competing cation is at low level (pure), with the best results obtained with pure solution and high concentration. AC interaction shows that solid: solution ratio has little effect at low concentration. At higher concentration this effect has positive significant effect on the ammonium response data. Therefore, the best ammonium response data would appear to be obtained when A is at high level and C and D are at the low level.

A.4.1 Calcium Competing Cation

Table A.4.2. Design-Expert Output for Ammonium Concentration ANOVA for Selected Factorial Model Analysis

Source of variation	Sum of squares	Degrees of Freedom	F	**Prob > F**
Model	*171.85*	*5*	*3137.1*	< 0.0001 significant
A	*114.97*	*1*	*10493.8*	< 0.0001 significant
C	*22.68*	*1*	*2070.2*	< 0.0001 significant
D	*12.73*	*1*	*1161.6*	< 0.0001 significant
AC	*16.10*	*1*	*1469.5*	< 0.0001 significant
AD	*5.37*	*1*	*490.2*	< 0.0001 significant
Residual	0.11	10		
Cor Total	171.96			

Table A.4.3. Factors Effect Estimates and Sum of Squares for 2^4 Factorial Designs

Model Term	Effect Estimate	Sum of Squares	Percent Contribution %
A	5.36	114.92	66.85
B	0.073	0.021	0.012
C	-2.38	22.68	13.19
D	-1.784	12.72	7.40
AB	0.049	0.009	0.005
AC	-2.00	16.10	9.362
AD	1.655	5.371	3.123
BC	-0.018	0.001	0.0008
BD	0.00375	5.62E-05	3.21E-05
CD	0.0737	0.0217	0.012
ABC	-0.018	0.0014	0.0008
ABD	0.0037	5.62E-05	3.21E-05
ACD	0.104	0.04	0.025
BCD	-0.003	0.006	0.003
ABCD	-0.004	0.004	0.003

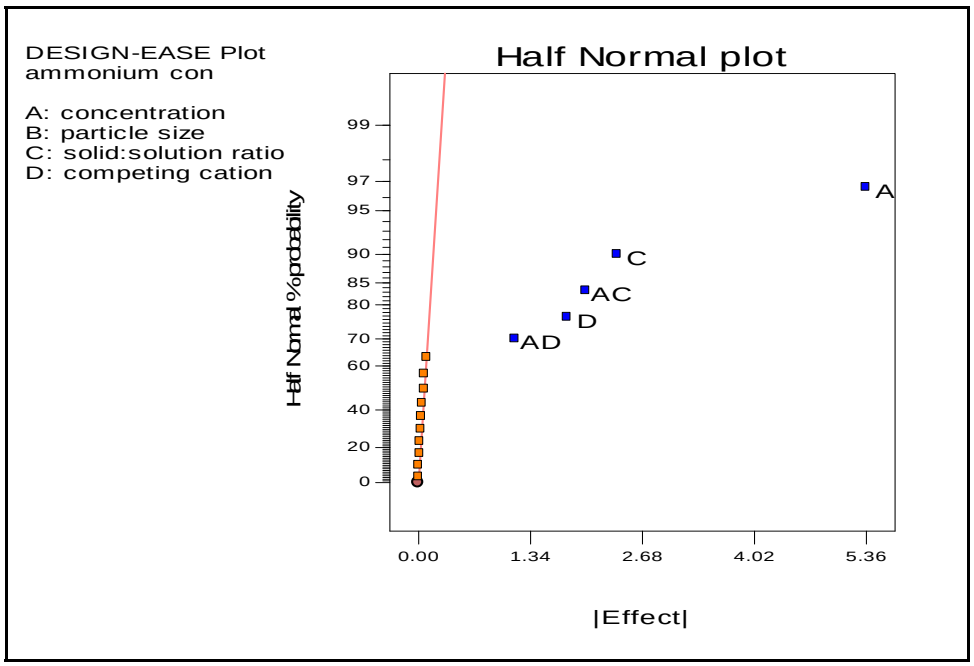

Figure A.4.1. Half normal probability plot of effects for ammonium concentration

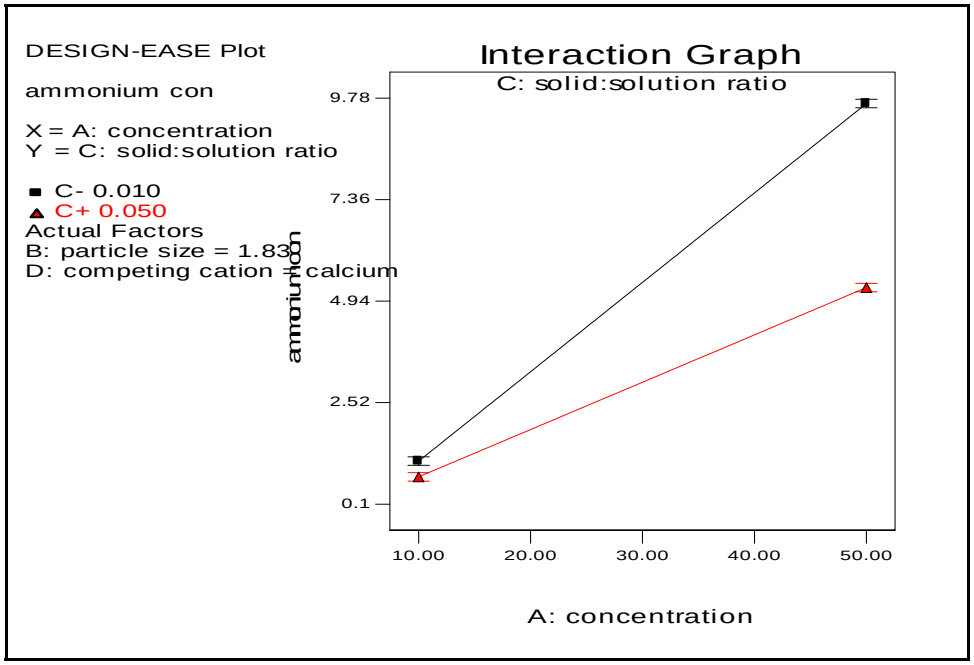

(a) Concentration- Solid: Solution Ratio Interaction

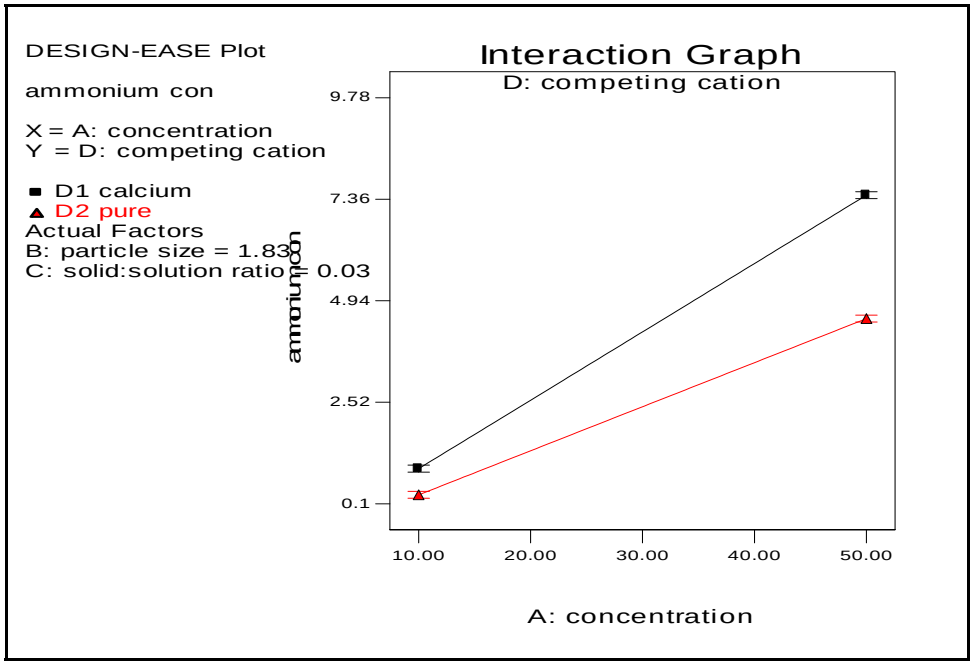

(b)Concentration-Competing Cation Interaction

Figure A.4.2. Interaction plots for ammonium concentration, (a)AC interaction, (c) AD interaction

A.4.2. Potassium Competing Cation

Table A.4.4. Design-Expert Output for Ammonium Concentration ANOVA for Selected Factorial Model Analysis

Source of variation	Sum of squares	Degrees of Freedom	F	**Prob > F**
Model	*221.94*	*5*	*1048.61*	< 0.0001 significant
A	*150.25*	*1*	*3549.3*	< 0.0001 significant
C	*16.42*	*1*	*387.96*	< 0.0001 significant
D	*22.97*	*1*	*542.58*	< 0.0001 significant
AC	*17.08*	*1*	*403.43*	< 0.0001 significant
AD	*15.23*	*1*	*359.77*	< 0.0001 significant
Residual	0.42	10		
Cor Total	222.37			

Table A.4.5. Factors Effect Estimates and Sum of Squares for 2^4 Factorial Designs

Model Term	Effect Estimate	Sum of Squares	Percent Contribution %
A	6.128	150.3	67.56
B	0.053	0.011	0.005
C	-2.023	16.42	7.385
D	-2.39	22.96	10.32
AB	0.024	0.002	0.001
AC	-2.06	17.08	7.68
AD	-1.95	15.22	6.85
BC	-0.021	0.0018	0.0008
BD	-0.00125	6.22E-06	2.81E-06
CD	-0.256	0.262	0.118
ABC	-0.021	0.0018	0.0008
ABD	0.0037	5.62E-05	2.52E-05
ACD	0.189	0.142	0.065
BCD	-0.011	0.005	0.0002
ABCD	-0.006	0.0001	7.02E-05

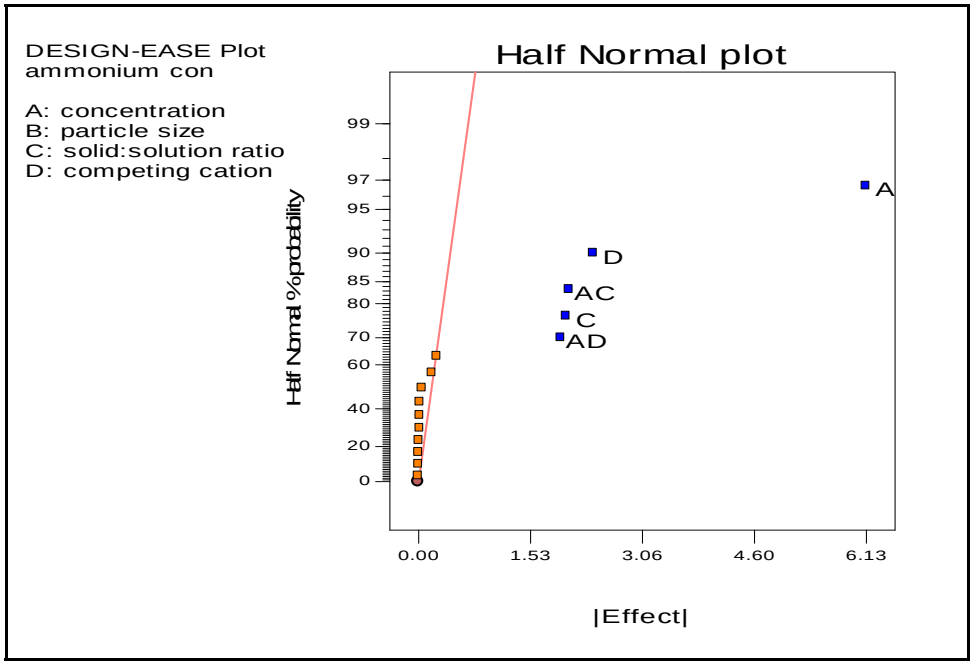

Figure A.4.3. Half normal probability plot of effects for ammonium concentration

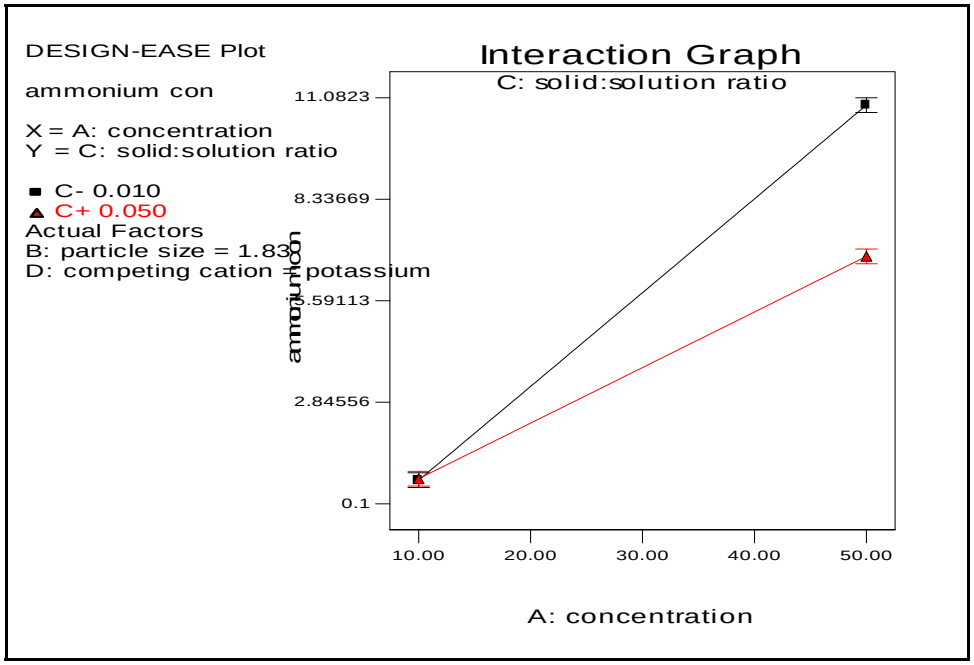

(a) Concentration- Solid: Solution Ratio Interaction

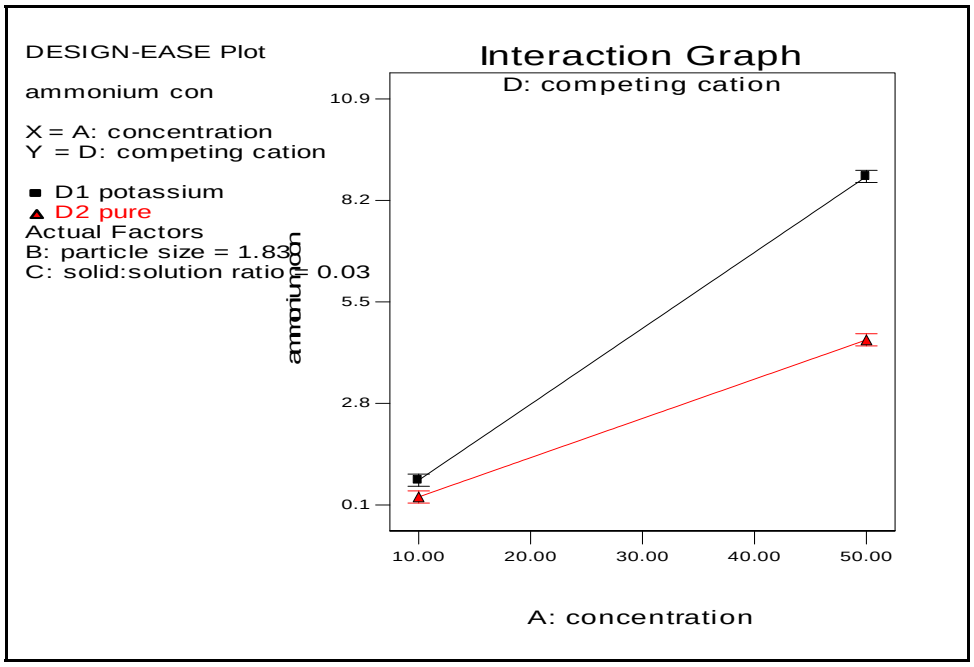

(c) Concentration- Competing Cation Interaction

Figure A.4.4. Interaction plots for ammonium concentration (a) AC interaction, (c) AD interaction

A.4.3. Magnesium Competing Cation

Table A.4.6. Design-Expert Output for Ammonium Concentration ANOVA for Selected Factorial Model Analysis

Source of variation	Sum of squares	Degrees of Freedom	F	**Prob > F**
Model	*119.01*	*5*	*8873.2*	< 0.0001 significant
A	*81.09*	*1*	*30229.3*	< 0.0001 significant
C	*20.93*	*1*	*7802.7*	< 0.0001 significant
D	*2.21*	*1*	*822.08*	< 0.0001 significant
AC	*14.36*	*1*	*5354.74*	< 0.0001 significant
AD	*0.42*	*1*	*157.5*	< 0.0001 significant
Residual	0.027	10		
Cor Total	119.04			

Table A.4.7. Factors Effect Estimates and Sum of Squares for 2^4 Factorial Designs

Model Term	Effect Estimate	Sum of Squares	Percent Contribution %
A	4.502	81.1	68.12
B	0.06	0.014	0.012
C	-2.288	20.93	17.85
D	-0.742	2.205	1.85
AB	0.027	0.003	0.002
AC	-1.90	14.36	12.07
AD	-0.325	0.422	0.354
BC	-0.022	0.002	0.0017
BD	-0.0175	0.0012	0.001
CD	0.005	0.001	8.41E-05
ABC	-0.021	0.0016	0.0013
ABD	-0.01	0.0004	0.0003
ACD	-0.0175	0.0012	0.001
BCD	-0.02	0.0016	0.0013
ABCD	-0.0175	0.0012	0.00102

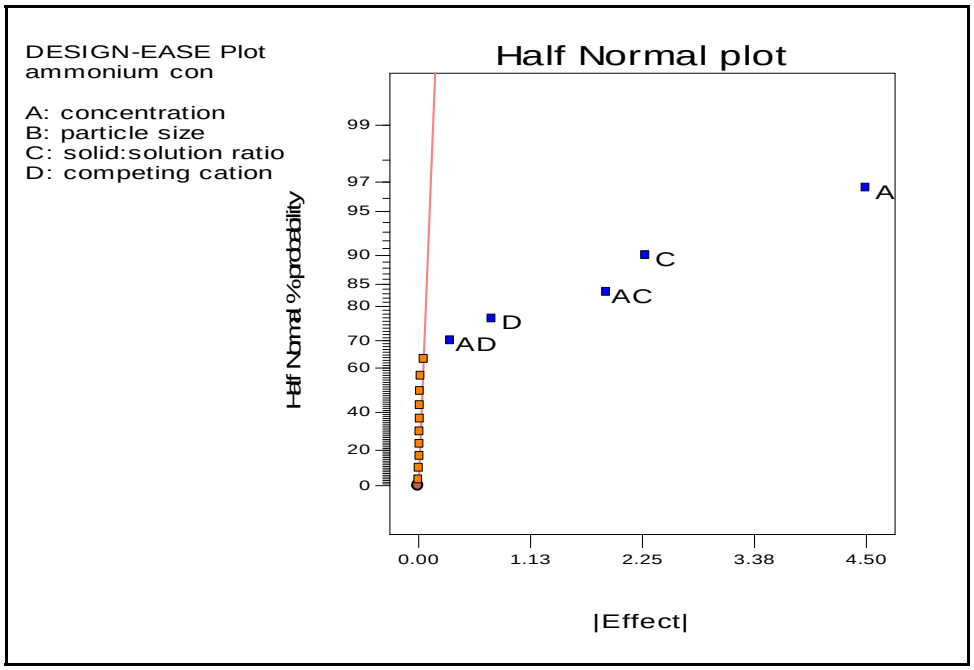

Figure A.4.5. Half normal probability plot of effects for ammonium concentration

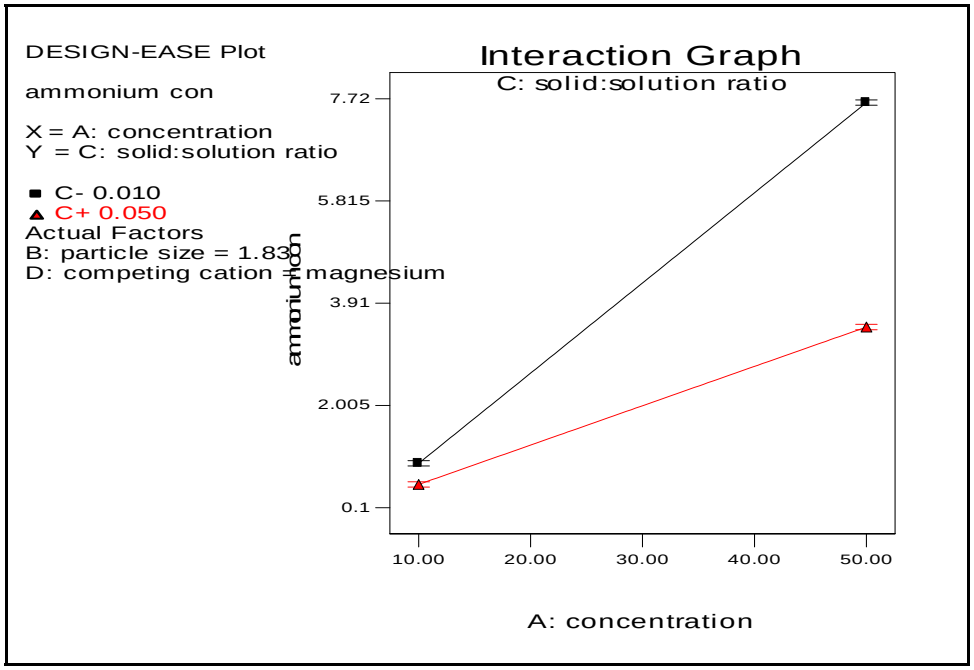

(a)Concentration- Solid: Solution Ratio Interaction

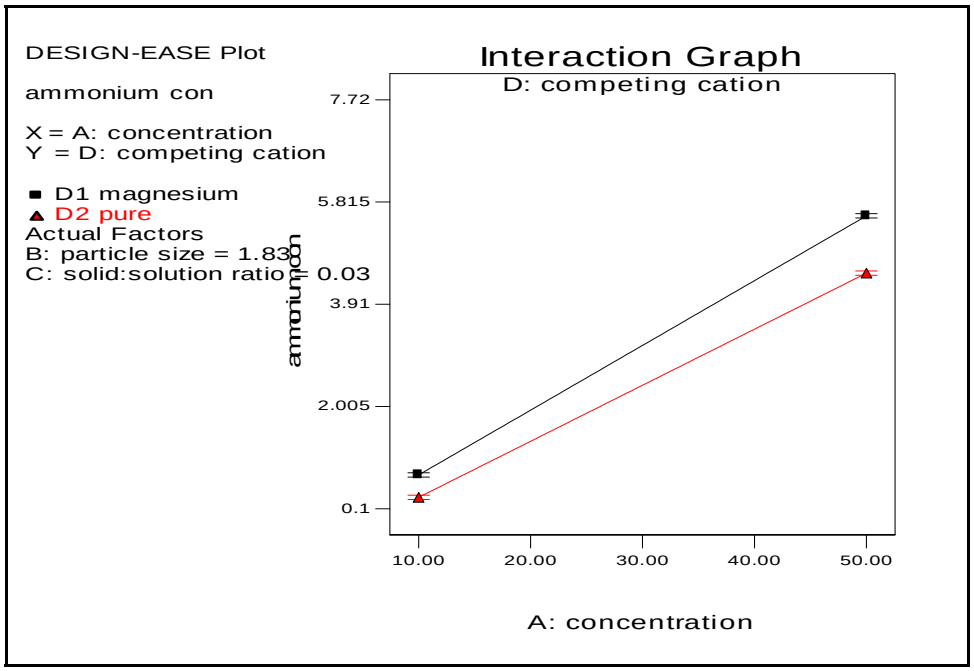

(c) Concentration- Competing Cation Interaction

Figure A.4.6. Interaction plots for ammonium concentration, (a)AC interaction, (b) AD interaction